Adsorption of Ethanol - Water Mixtures on High Silica Zeolites

by

Andrew Paul Franks.

A Thesis submitted for the Degree of Doctor of Philosophy of the University of London and for the Diploma of Imperial College.

Physical Chemistry Laboratories
Imperial College
London SW7 2AY.

November 1986.

Abstract.

The adsorption of ethanol-water mixtures on a silicalite-1 sample, HSIL, at 20, 30 and 40°C has been studied. Detailed composite isotherms have been determined experimentally. Heats of immersion of this silicalite-1 sample in pure ethanol, pure water and in three mixtures of the pure components have been measured calorimetrically. These heats of immersion have been compared with those obtained from a thermodynamic analysis of the composite isotherms. The analysis was carried out using the method of Everett[52], Schay[53] and Sircar[54]. The analysis was found to fail in this case. This failure is due in part to the nature of the system studied and in part to large errors introduced into the calculations.

Composite isotherms at 30°C for a second silicalite-1 sample, HSILB, calcined at several temperatures, have also been obtained. It has been proposed[26] that calcination at high temperatures removes silanol groups present in the zeolite which can act as active sites for adsorption. In this study, no change in the HSILB 30°C composite isotherm was seen for samples calcined at 550, 670 and 800°C.

The composite isotherms for two ZSM5 samples of different silicon:aluminium ratio have also been determined. These isotherms showed no significant differences from those obtained above, indicating that the presence of small amounts of aluminium in the zeolite do not greatly affect the composite isotherm.

The composite isotherm of ethanol - water mixtures on activated carbon at low concentrations of ethanol has also been determined experimentally.

'Single component' isotherm calculations and various other theoretical treatments have been carried out on the HSIL 20, 30 and 40^{o}C composite isotherms; on the 30^{o}C composite isotherm for the HSILB sample calcined at 550^{o}C; and on the composite isotherms for the two ZSM5 samples.

It has been found that the structure of the ethanol-water liquid mixture strongly influences the shape of the composite isotherm in the low ethanol concentration region.

Also, at intermediate concentrations of ethanol, the presence of ethanol in the adsorbent is thought to provide adsorption sites for water, thus increasing the concentration of water in the adsorbed phase.

The presence of aluminium in the zeolite considerably affects the shape of the 'single component' isotherms, more water being adsorbed than in the case of the silicalite-1 samples, especially at intermediate concentrations of ethanol.

TO GOD, MY WIFE AND MY FAMILY.

Acknowledgements.

In producing this thesis, I would like to thank the following: my supervisor Dr.L.V.C.Rees of Imperial College, Drs. F.R.Fitch, C.W.Roberts and A.E.Comyns of Laporte Inorganics. I would also like to thank Laporte Inorganics for the provision of zeolite samples and analyses and for their support of this project through a C.A.S.E. studentship; and thanks to all members of the Research Group Coffee Club, past and present (especially Mr.S.Patel and Dr.P.Graham) for their friendship, support and for many profitable discussions. Finally, thanks are due to my wife for her patience, encouragement and love.

Contents. Page

Chapter 1. Introduction.

1.1. Zeolites.[1,2,3]

Zeolites are crystalline hydrated aluminosilicate minerals. Structural studies (using X-ray and neutron diffraction, for example) have shown that zeolites are tectosilicates. That is, they have framework structures based on infinitely extending 3-dimensional networks of SiO_4 and AlO_4 units joined by sharing every one of their tetrahedral oxygen atoms. Zeolites may be considered as framework silicates in which SiO_4 tetrahedra have been isomorphously replaced by AlO_4 tetrahedra. The extent to which this replacement may occur is governed by Lowenstein's rule[4] which states that two aluminium atoms cannot be joined by the same oxygen atom.

The presence of AlO_4 tetrahedra also results in a net negative charge on the lattice, which is balanced by the presence of suitable cations, usually those of group I or II elements.

Zeolites may then be represented by the following empirical formula :

$$M_{2/n}O.Al_2O_3xSiO_2yH_2O$$

Where M is a cation of valency n, $x \geq 2$ remembering Lowenstein's rule and y is a function of the framework porosity. A zeolite may be designated by an abbreviated form, such as MX, for example, where M is the balancing cation and X is the zeolite type.

The porosity of a zeolite is a result of the presence of highly regular systems of cavities and channels in the crystal, in which water (or other) molecules and cations may reside. Such species are usually mobile and this gives rise to the phenomenon of ion

exchange, where one cationic species present in a zeolite may be replaced to a greater or lesser extent by another, by contacting the zeolite with a solution containing the counter ion.

The presence of a channel-cavity system also gives rise to interesting adsorption properties. The water usually adsorbed in a zeolite may be driven off on heating (a process called 'activation'), to permit the adsorption of other species.

Zeolites occur naturally and can also be synthesised. Synthesis is hydrothermal[5] and usually uses sodium silicates or colloidal silicas formed into gels with sodium aluminate additions. Synthesis may also take place in the presence of an organic molecule, often a base. In some cases, these species are thought to have a structure directing effect. Where this is so, the organic species is designated a 'template' molecule.

There are approximately 40 recorded zeolite structures, although the possible number is infinite. Zeolites can be obtained which are isostructural but contain different proportions of silicon and aluminium. These proportions are usually expressed in terms of the silicon to aluminium ratio, Si/Al.

Zeolites are commonly classified by identification of certain recurring structural subunits. These subunits are specific arrangements of tetrahedral atoms (see Figure 1.).

Classification by such a method gives rise to nine (possibly ten) zeolite groups[1,2].

Members of one such group are known as the pentasils. Zeolites belonging to this group have structures containing a large number of 5-membered rings of tetrahedral atoms (see Figure 1.).

Figure 1 . Common Secondary Building Units in Zeolites.[3]

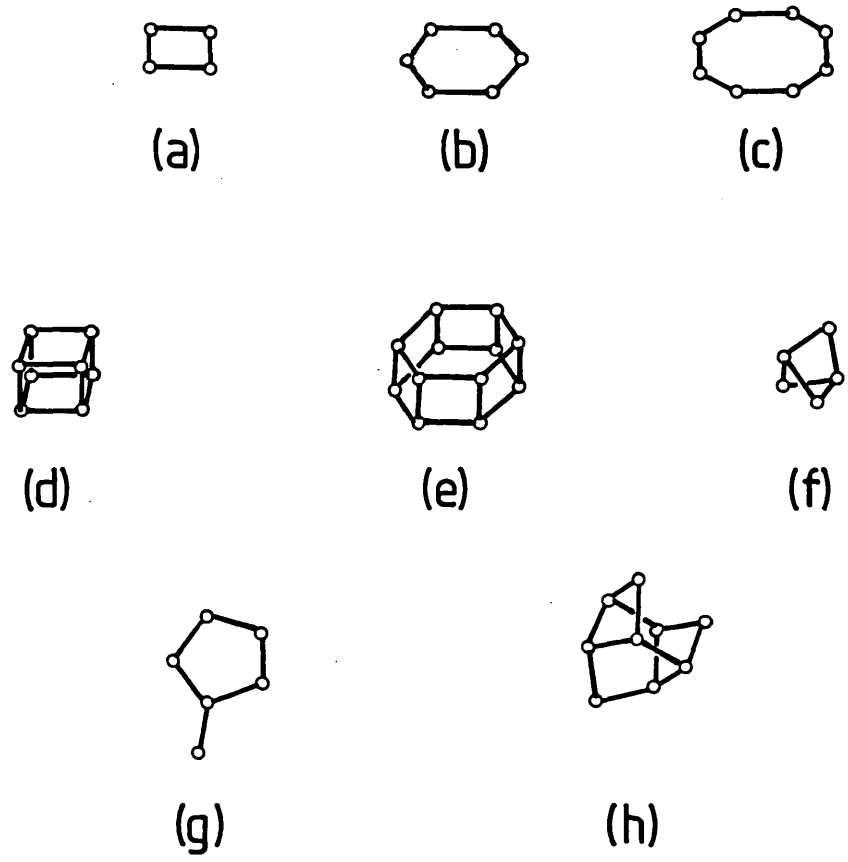

Circles denote tetrahedral atoms. Straight lines do not represent bonds.

KEY:

(a) Single 4-ring, S4R; (b) Single 6-ring, S6R; (c) Single 8-ring, S8R; (d) Double 4-ring, D4R; (e) Double 6-ring, D6R; (f) $T_5 O_{10}$ 4-1 ; (g) $T_8 O_{16}$ 5-1; (h) $T_{10} O_{20}$ 4-4-1 .

Representative of the pentasils is the zeolite designated ZSM5. The structural subunit from which ZSM5 is built is shown in Figure 3a below. Diagrams of the ZSM5 structure are shown in Figures 2 and 3b [6-8]. As may be seen from the diagrams, the structure consists of straight channels running parallel to the [010] direction, having openings made of 10-membered rings of approximately 0.54x0.56nm diameter; and sinusoidal channels running parallel to the [100] direction having 10-ring openings of approximately 0.51x0.54nm diameter.

ZSM5 is synthesised from reaction mixtures containing many different templates,or no template at all. Tetrapropylammonium bromide[9,10] is the template giving the widest possible range of final zeolite compositions. The organic molecules in the reaction mixture become included in the zeolite structure during its formation. These occluded species are then driven off by calcination, in which the as-synthesised zeolite is heated to temperatures in excess of 500^{o}C.

ZSM5 has been produced with Si/Al ratios from about 20 to greater than 10 000. ZSM5 zeolites then, even in their least siliceous forms, are high silica zeolites. A 'pure silica' analogue of ZSM5, containing virtually no aluminium, was synthesised by Flanigen et al.[7] and is commonly known as silicalite-1.

Zeolites find a wide range of applications, of which catalysis is the most important. Catalytic properties of zeolites vary according to structure and the type of balancing cation present. Catalysis may be shape selective, depending on

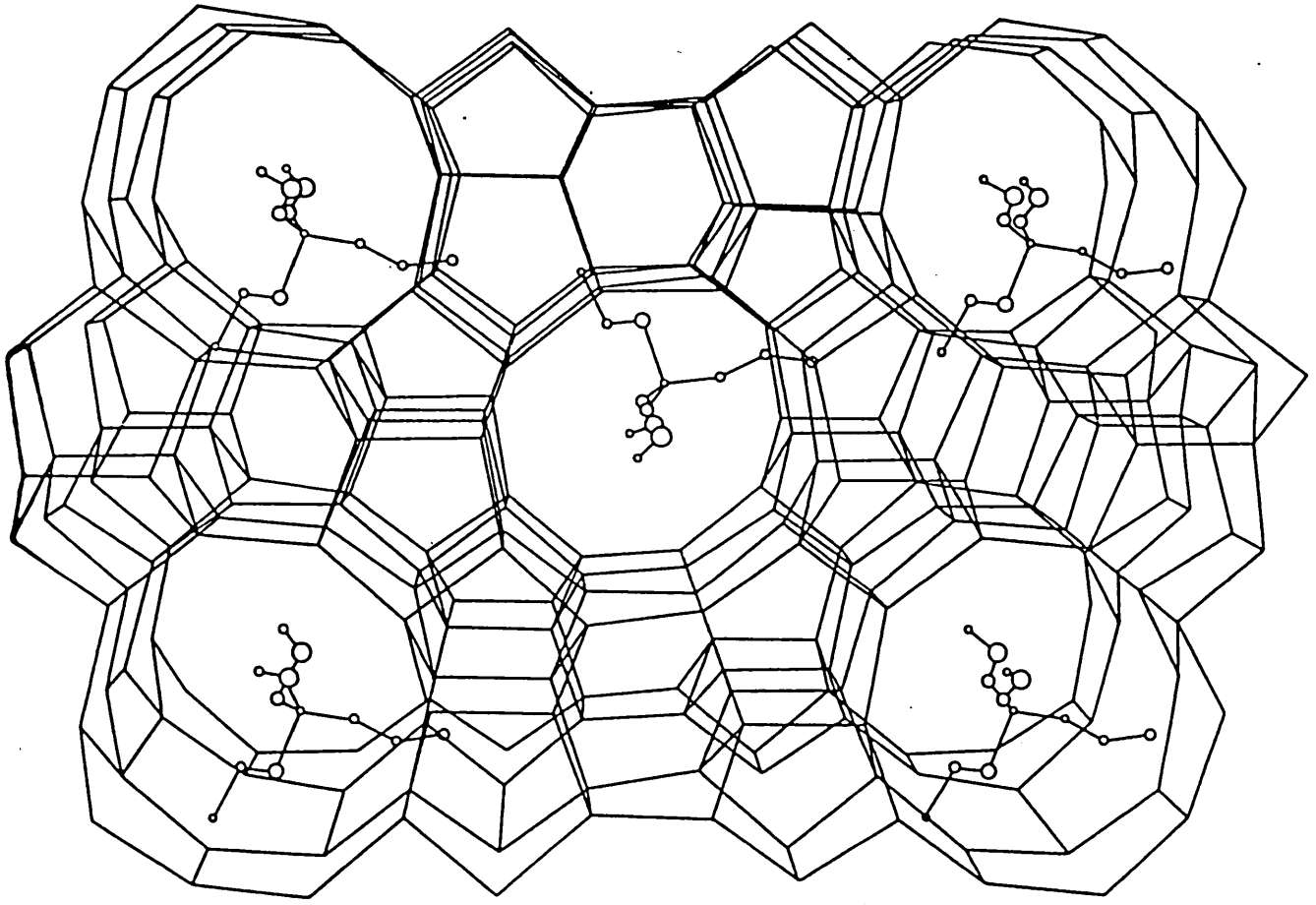

Figure 2. ZSM5 Framework Structure Viewed along the 010 Axis, Showing Occluded Tetrapropylammonium Ions.

Figure 3a . Secondary Building Unit of Pentasil Zeolites.

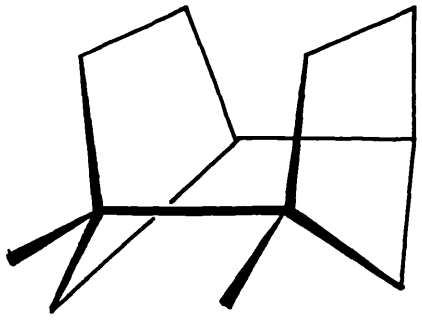

Figure 3b . Idealised Internal Channel Structure of ZSM5 and Silicalite-1.

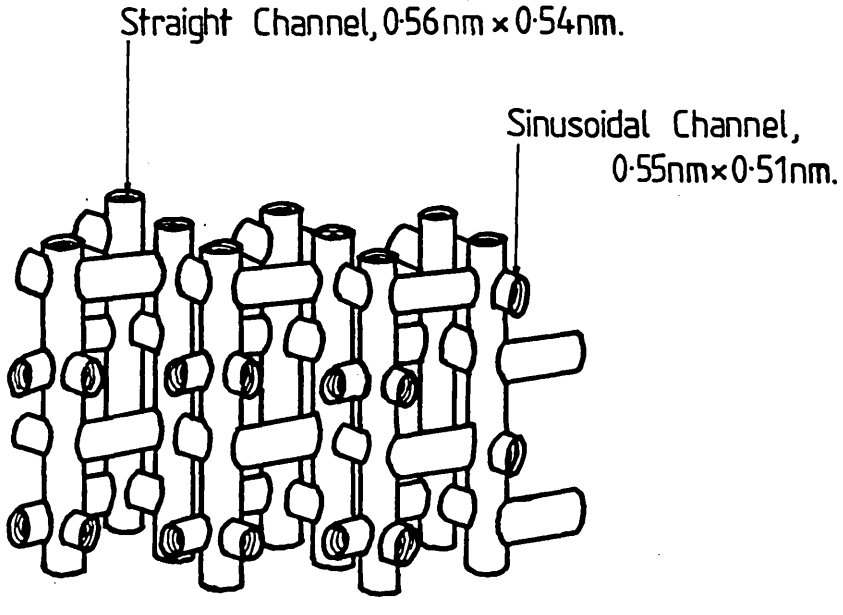

the shape of the reactant, transition-state, or product . ZSM5 is used as a catalyst in the conversion of methanol to gasoline and in the interconversion of aromatic compounds[11-14].

Other uses are as builders in detergents,in radioactive waste storage, in agriculture and as selective adsorbents for gas or liquid mixtures.

1.2. Adsorption from Solution on Zeolites.

Adsorption from solution by zeolites is of particular interest in this study and therefore a discussion of the relevant factors is presented, with special reference to ethanol/water/zeolite systems. Factors affecting adsorption from solution by zeolites may include :

(i)Zeolite-adsorbate interactions. Zeolites may be described as being of a higher or lower polarity. A 'polar' zeolite is one with a high aluminium content (i.e.- a low Si/Al ratio) and therefore with a higher residual charge on the framework. A less polar zeolite is then one with a higher Si/Al ratio. A polar zeolite will selectively adsorb the more polar component of a mixture[15-17] due to the stronger zeolite - adsorbate interaction. Conversely, a less polar zeolite will preferentially adsorb the less polar component of a mixture.

The Si/Al ratio of a zeolite may be adjusted after synthesis by dealumination of the zeolite. Methods of dealumination include EDTA extraction[18], steaming[19], silicon tetrachloride treatment[20] and use of ammonium hexafluorosilicate[21].

ZSM5 and silicalite-1 have been shown to be hydrophobic[7] by virtue of their high Si/Al ratios. The hydrophobicity of these

adsorbents may be explained in the following way: These highly siliceous zeolites possess relatively few adsorption sites (such as silanol groups or charged ionic species) with which a water molecule is able to interact through its dipoles. In addition, the small size of the molecule means that any Van der Waals interaction with the surface will be small. Hence there is essentially no means by which water may be adsorbed, other than at the external surface where 'dangling' silanol groups may be present, or at the relatively few number of internal silanol groups. It is more energetically favourable for a water molecule to remain in solution in its hydrogen bonded state.It may be expected, then, that ZSM5 or silicalite-1 would selectively adsorb ethanol from an aqueous solution. Hence silicalite-1 and ZSM5 zeolites were used in this study.

The presence of aluminium in the lattice provides centres of charge separation at which water molecules may be adsorbed.

The thermal pretreatment of the zeolite (i.e.- activation or calcination) may also have some effect on the zeolite's adsorption properties. In some cases, the structure may be altered by such treatments[7]. As mentioned earlier, heating drives off any water or other molecules adsorbed in the channel system, thus increasing the potential adsorption capacity for other species.

Chemical pretreatments of zeolites include production of surface hydroxyl groups (by ion exchange with ammonium ions followed by heating[22,23]) and further modification of such groups by silylation. Altering the nature of the surface by such

procedures alters the zeolite - adsorbate interactions.

Varying the cation present in the zeolite also changes the zeolite - adsorbate interactions. The presence of a cation provides a site with high, localised charge density, especially in the case of multivalent cations. Here, where fewer cations are required to balance the lattice charge, the cations are spread further apart throughout the framework, resulting in a greater charge separation. Hence the type of balancing cation present may greatly affect the strength of interaction of the adsorbent with polar species, for example.Large ions may block or restrict movement of molecules into all or part of the channel system.

Different types of zeolite - adsorbate interaction may occur within a given zeolite. If this is the case, the zeolite adsorbent is said to be heterogeneous. Possible sources of heterogeneity in zeolites include :

- Differences between adsorption on the external and internal surfaces of the zeolite. The external surface of a zeolite may possess a large number of `dangling' silanol groups. These can act as sites for the adsorption of polar molecules, interaction taking place through hydrogen bonding.

However, the internal surface area of the zeolite is several orders of magnitude greater than that of the external surface. Hence any `external' adsorption effects are likely to be masked by internal adsorption effects.

- Certain regions of the channel - cavity structure may interact more favourably with adsorbed molecules due to steric effects. In ZSM5, for example, molecules may preferentially adsorb in either the channel intersections, or in the sinusoidal channels, or in

the linear channels, depending on the molecule's size and shape.

- Heterogeneity may not arise from the zeolite itself, but from impurities which are precipitated with the zeolite on synthesis. Such impurities may be crystalline or amorphous and will probably have quite different adsorption properties to that of the zeolite.

- High silica ZSM5 zeolites have been shown [24-26] to contain large numbers of (internal) silanol groups that are part of the framework but not associated with the aluminium atoms. Solid state ^{29}Si n.m.r. spectroscopy[26] indicates that as many as 18% of the framework silicon atoms have associated OH groups. As mentioned earlier, such silanol groups could provide active sites for adsorption.

Heterogeneity, where present, may give rise to unusual adsorption phenomena.

(ii) Steric effects. The size of the openings to the interior channel - cavity system of a zeolite may be such that one component of a mixture is too large to enter. Other, smaller, components will then be adsorbed exclusively. This is the phenomenon known as molecular sieving[27-31]. In less extreme cases, molecules approaching the size of the channel opening will be less readily adsorbed than smaller species, because of steric hindrance. Bulkier molecules may also find themselves restricted to only a part of the channel system for similar reasons.

However, in the case of ethanol and water with a ZSM5 as adsorbent, the channel openings are wide enough to admit both

species without significant hindrance.

(iii)Solute - solvent interactions. The thermodynamic stability of a species in the liquid phase will also effect the extent to which it is adsorbed. Such stability depends chiefly on the strength and nature of the solute - solvent interactions.

The detailed structure of ethanol - water solutions is not well known. Indeed, the structure of liquid water is still very much under debate[32]. However, investigation of the bulk thermodynamic properties[33], proton n.m.r.[34] and picosecond fluorescence anisotropy spectroscopy[35] studies of ethanol - water mixtures covering a wide range of concentrations have offered some insight into the solution structure. These studies indicate that at very low ethanol concentrations ($x \lesssim 0.08$, where x is the mole fraction of ethanol in solution) the presence of ethanol promotes hydrogen bonding association among water molecules. The structure of the solution may be thought of as consisting of 'ice-like' hydrogen bonded water molecules, surrounded by less highly structured regions of ethanol and water molecules. At intermediate ethanol concentrations ($0.25<x<0.75$), the water clusters appear to become increasingly disrupted, as ethanol molecules become included in the water clusters. At higher ethanol concentration ($x>0.8$) the water molecules seem either to coordinate or be incorporated into the linear hydrogen bonded aggregates peculiar to ethanol. These structures are adversely effected by increasing temperature.

Precisely what influence these interactions will have on adsorption is difficult to assess, except to indicate that where one species is included to a greater extent than the other in

some hydrogen bonded structure, that species will be less favourably adsorbed.

(iv) Adsorbate - adsorbate interactions. Changes in the arrangement of molecules within the zeolite cavities at certain levels of adsorption may occur. It has been proposed that such rearrangement is responsible for peculiarities in the vapour - phase adsorption isotherms of xylenes on ZSM5[36].

In the case of the adsorption of ethanol and water on ZSM5 zeolites, it is conceivable that some hydrogen bonded structure may arise within the zeolite cavities and result in unusual adsorption properties.

1.3. Ethanol as a Fuel or Fuel Additive.[37]

There has been much interest in recent years in alternative energy sources. One such alternative under investigation is the use of ethanol as a fuel or as an additive to petroleum fuels. Ethanol is readily produced by well-known fermentations. However, these procedures have not proved economical enough to permit the use of ethanol in fuels. A major problem is the high cost of distilling the ethanol off from the fermentation liquor. Fermentation liquors are generally only 6-9%(w/v) ethanol since higher concentrations prove toxic to the fermenting organism. Various attempts to solve this problem have been made, including: (i)Increasing the efficiency of the fermentation process, producing ethanol at higher concentrations using mutant yeast strains.

(ii)Using less energetically expensive methods of separating the ethanol from the fermentation liquor, such as :

- azeotropic distillation with benzene
- adsorption of the excess water using materials such as zeolite 3A
- reverse osmosis
- solvent extraction
- liquid carbon dioxide extraction
- selective adsorption of ethanol using zeolites, polymers, or other materials.

With regard to the last of these possibilities, detailed knowledge of the ethanol-water-adsorbent system would prove valuable. It was partly for this reason that this study was inducted.

The aim of this study was to investigate closely the adsorption of ethanol from ethanol-water mixtures by solid adsorbents. Adsorbents investigated include silicalite-1, ZSM5 zeolites and activated carbon.

Various theoretical treatments of the adsorption isotherms produced were also carried out, in order to obtain a better understanding of these systems.

Chapter 2. Theory.

2.1. Adsorption at the Solid-Liquid Interface.[38-40]

Extent of adsorption of a species from solution at a solid surface may be defined in terms of its specific surface excess, $n_2^{\sigma(n)}$,

$$n_2^{\sigma(n)} = \frac{n_0 \Delta x}{m} \qquad -(1)$$

Where n_0 = Total number of moles of substance initially in contact with the adsorbent.

$$\Delta x = x_2^{1,0} - x_2^1$$

and x_2^1 = final mole fraction of component 2 in the liquid phase.

$x_2^{1,0}$ = initial mole fraction of component 2 in the liquid phase.

m = mass of adsorbent used (g).

All of the quantities on the right hand side of equation (1) are known or may be determined experimentally.

Adsorption isotherms take the form of composite isotherms, where the specific surface excess is plotted against the equilibrium mole fraction in solution of component 2, for a given temperature.

The specific surface excess expresses the increased (or decreased) concentration of a species at the surface, above the concentration in the bulk liquid.

The change in concentration of a species during an adsorption experiment is brought about by the transfer of n_1^s moles of component 1 and n_2^s moles of component 2 onto the surface of unit weight of solid. At equilibrium, n_1 moles of component 1 and n_2

moles of component 2 remain in the liquid phase, giving a concentration of x_2^1 with respect to component 2[38,39].

Then, the total number of moles of substance in the system,

$$n_0 = n_1 + n_2 + n_1^s m + n_2^s m \quad -(2)$$

Then,

$$x_2^{1,0} = \frac{n_2 + n_2^s m}{n_0} \quad -(3)$$

and

$$x_2^1 = \frac{n_2}{n_1 + n_2} \quad -(4)$$

Combining (2),(3) and (4) :

$$\Delta x = \frac{n_2 + n_2^s m}{n_0} - \frac{n_2}{n_1 + n_2} \quad -(5)$$

$$\Delta x = \frac{(n_2+n_2^s m)(n_1+n_2)-n_2 n_0}{n_0(n_1+n_2)}$$

Hence,

$$\Delta x = \frac{m(n_2^s n_1 - n_1^s n_2)}{n_0(n_1+n_2)} \quad -(6)$$

At equilibrium, the mole fraction of component 1 in solution is:

$$x_1^1 = (1-x_2^1) = \frac{n_1}{n_1+n_2} \quad -(7)$$

Then, from (6) and (7),

$$\frac{n_0 \Delta x}{m} = n_2^s(1-x_2^1) - n_1^s x_2^1 \quad -(8)$$

Rewriting the specific surface excess in this way enables a better understanding of the shapes of composite isotherms to be obtained. There are three main types of composite isotherm (although a more detailed classification has been made[38]), shown in Figure 4. The first type of isotherm shown is known as a 'U' shaped isotherm. It indicates selectivity for component 2 over the whole concentration range, the specific surface excess being positive at all concentrations and the curve having its peak at $x_2^1 < 0.5$. The second type of isotherm is known as an 'S' shaped isotherm. It indicates that the adsorbent is selective for component 2 over part of the concentration range and selective for component 1 over the rest (note - a positive adsorption of component 1 shows as a negative adsorption of component 2).

The third type of isotherm is linear and represents the special case of molecular sieving, where component 2 is adsorbed to the exclusion of component 1.

The shapes of these isotherms are perhaps more easily understood with reference to equation (8).

For a 'U' shaped isotherm n_2^s must be large with respect to n_1^s. That is, much more of component 2 is adsorbed over component 1.

For an 'S' shape, the magnitudes of n_1^s and n_2^s may be comparable, or one may be slightly greater than the other.

Also, the specific surface excess must be zero at $x_2^1 = 0$ and at $x_2^1 = 1$.

2. . Calculation of 'Single Component' Isotherms.

Single component isotherms are plots of the amount of a species

Figure 4. Typical Composite Isotherms.

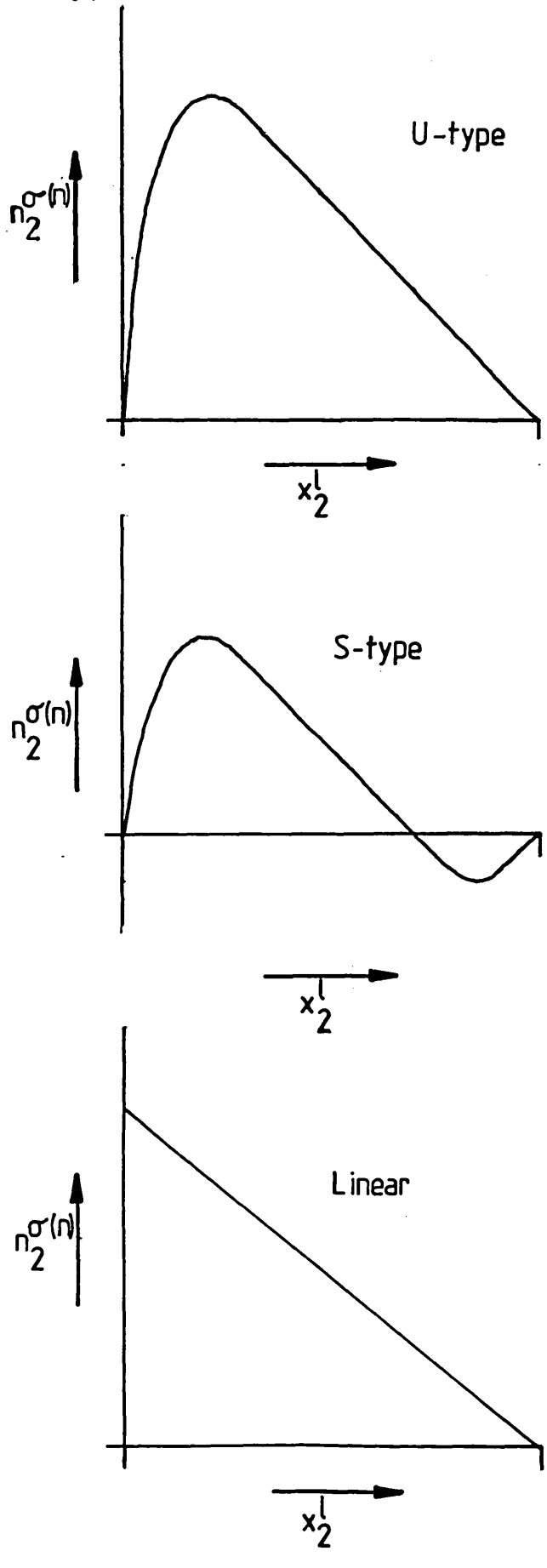

adsorbed against the equilibrium liquid phase concentration of that species, at a given temperature. They usually take the form shown in Figure 5. Unlike composite isotherms, such isotherms are not obtainable directly by experiment. However, numerous methods of calculating the single component isotherms from the composite isotherm have been proposed. Some methods rely on equations originally applied to gas phase adsorption such as the Freundlich[41] equation or Langmuir[42] equation. Use of these equations in application to adsorption from the liquid phase is difficult to justify, especially in the case of the Freundlich equation. Use of the Langmuir equation is usually only suitable for solutions at low concentrations.

Another way of obtaining `single-component' isotherms[43-45] is to assume that the adsorbed layer is monomolecular and that the adsorbing surface is completely covered at all concentrations. That is, that both components completely wet the surface and that the influence of the surface is not effective beyond the first monolayer. However, the term `monolayer' is somewhat ambiguous when applied to a zeolite.

Similar in principle to the monolayer treatment is the pore-filling method[46,47], where it is assumed that, instead of constant area coverage, constant filling of the pore volume of a porous adsorbent occurs. In the case of a zeolite, there are difficulties in finding the actual volume of the zeolites' internal space occupied by the adsorbates. In practice, however, the mathematical treatment is essentially the same as that in the monolayer method.

Figure 5 Typical Single Component Isotherms. Mole Fraction of Component i in the Surface Phase (x_i^s) against Mole Fraction of Component 2 in the Liquid.

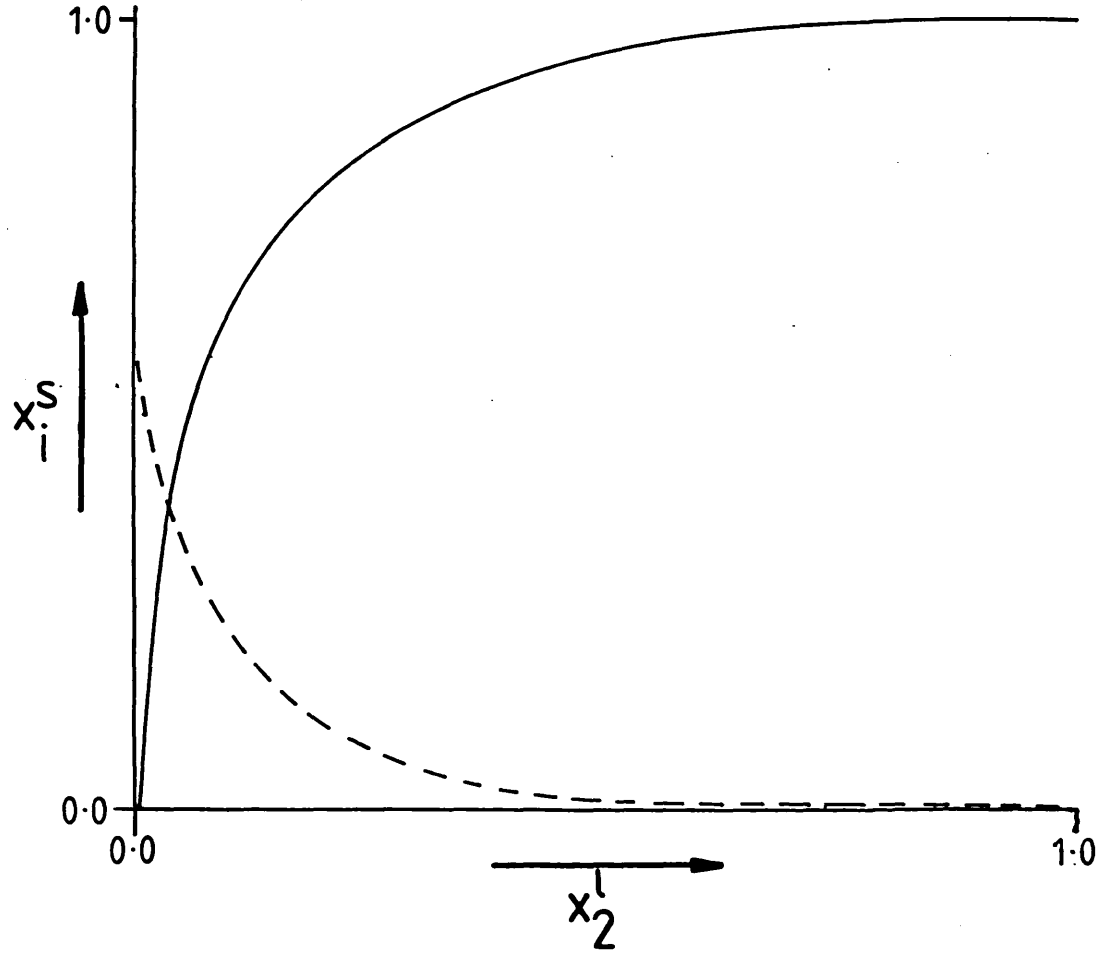

——— Component 2

– – – – – – Component 1

Using the pore-filling assumption, then:

$$n_1^s V_1 + n_2^s V_2 = V \qquad -(9)$$

Where V_i = the partial molar volume of component i in the adsorbed phase.

V= pore volume of the adsorbent occupied.

Equation (9) may be written:

$$\frac{n_1^s}{n_{1(m)}^s} + \frac{n_2^s}{n_{2(m)}^s} = 1 \qquad -(10)$$

Where $n_{i(m)}^s$ =number of moles of component i required to completely fill the pore volume of unit weight of adsorbent.

(In the monolayer treatment, (9) becomes:

$$n_1^s A_1 + n_2^s A_2 = A$$

Where A_i = area occupied by one mole of component i on the surface,

from which (10) is derived. The $n_{i(m)}^s$ values then represent the number of moles of component i required to cover the surface area of unit mass of adsorbent to form a monolayer).

The $n_{i(m)}^s$ values may be calculated from vapour phase adsorption data or from thermogravimetric analysis results.

Hence, rearranging (10) :

$$n_1^s = \left[1 - \frac{n_2^s}{n_{2(m)}^s} \right] n_{1(m)}^s \qquad -(11)$$

Therefore, (8) may be written :

$$\frac{n_0 \Delta x}{m} = (1-x_2^1)n_2^s - x_2^1\left[1 - \frac{n_2^s}{n_{2(m)}^s}\right] n_{1(m)}^s$$

or,

$$n_2^s = \frac{n_2^{o(n)} + x_2^1 n_{1(m)}^s}{[\,1-x_2^1 + (n_{1(m)}^s x_2^1 / n_{2(m)}^s)\,]} \qquad -(12)$$

All of the terms on the right hand side of equation (12) are known, so that n_2^s is known. n_1^s may then be calculated from equation (11). Then,

$$x_2^s = \frac{n_1^s}{n_1^s + n_2^s}$$

and, $-(13)$

$$x_1^s = 1 - x_2^s$$

Where x_i^s = mole fraction of i in the adsorbed phase.

Single component isotherms are then plots of x_2^s against x_2^1 or x_1^s against x_1^1. It is important to remember that interpretation of these isotherms must be done carefully, since their shape depends on the assumptions made in calculating them.

2.3. Linear Isotherm Sections.

Schay and Nagy[48] and Szekrenyesy[49] observed that on many porous adsorbents, composite isotherms exhibited a long, linear decreasing section over a wide concentration range (see Figure 6). It was suggested that the composition of the adsorbed phase is constant in this region. This can be seen by writing equation (8) as :

Figure 6. Diagram Showing Linear Composite Isotherm Section.

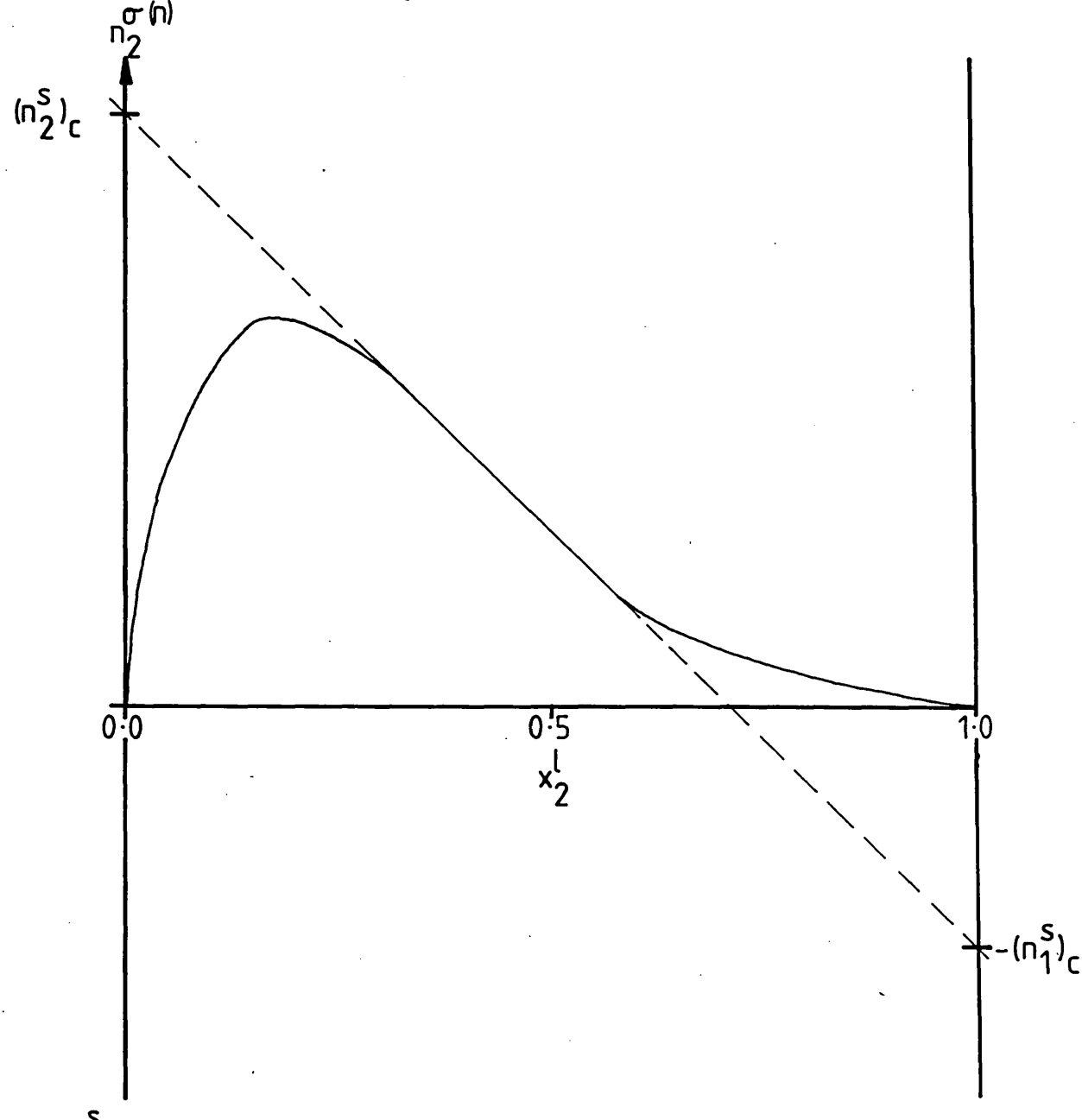

$(n_i^s)_c$ = Number of Moles of Component i in Surface Phase in Linear Region.

$$\frac{n_0 \Delta x}{m} = n_2^s - (n_1^s + n_2^s)x_2^1$$

If n_1^s and n_2^s are constant, then this equation becomes that of a straight line. Extrapolation of this line to $x_2^1=0$ and $x_2^1=1$ gives the values of $(n_1^s)_c$ and $(n_2^s)_c$ respectively, which define the composition of the adsorbed phase in this region.

In the monolayer treatment, from the monolayer values, Schay and Nagy calulated the mean thickness of the adsorbed layer, t:

$$t = \frac{(n_1^s)_c}{n_{1(m)}^s} + \frac{(n_2^s)_c}{n_{2(m)}^s} \qquad -(14)$$

They found that $t \approx 1$ for a number of porous adsorbents.

Kipling et al.[50] pointed out that the existence of an adsorbed layer of constant composition is only one possible condition for the linearity of composite isotherms. By using a virial equation to represent the single component isotherms, they identified three specific cases which satisfied the conditions for linearity.

Single component isotherms are given by:

$$n_1^s = a_1 + b_1(1-x_2^1) + c_1(1-x_2^1)^2 + d_1(1-x_2^1)^3 + \ldots \qquad -(15)$$

$$n_2^s = a_2 + b_2 x_2^1 + c_2(x_2^1)^2 + d_2(x_2^1)^3 + \ldots$$

Terms of order>2 are negligible for most systems.

The first case satisfying linearity is then when $b_1=b_2=0$. Then, $n_1^s=a_1$ and $n_2^s=a_2$; ie- the Schay and Nagy condition. However, this condition must obey a certain thermodynamic criterion. The chemical potentials of component 2 in the liquid and adsorbed

phase are given by:

$$\mu_2^s = (\mu_2^s)^0 + RT\ln(\gamma_2^s x_2^s)$$

$$\mu_2^l = (\mu_2^l)^0 + RT\ln(\gamma_2^l x_2^l) \qquad -(16)$$

μ_2 and $(\mu_2)^0$ are the chemical potentials of 2 in the mixture and standard state respectively. Superscript l denotes liquid phase and superscript s denotes surface phase. γ 's are the corresponding activity coefficients.

At equilibrium,

$$\mu_2^s = \mu_2^l$$

Therefore, the composition of the adsorbed phase will only be constant if changes in $\gamma_2^s x_2^s$ are exactly compensated for by changes in $\gamma_2^l x_2^l$. This is unlikely to occur in reality.

The second case is when $b_1 = b_2 = b$. Then,

$$n_2^s = a_2 + bx$$

$$n_1^s = a_1 + b - bx$$

These equations represent a pair of parallel straight lines, which, when added to give the composite isotherm, give another straight line.

The third case is when b_1 and b_2 are both small. Here, the composite isotherm will approximate to a straight line. Kipling et al. suggest that this is likely to occur in systems which are far from ideal and that most of the systems investigated by Schay and Nagy are of this type.

In this study, should any linear isotherm portions be observed, it may prove interesting to apply these analyses.

2.4. Thermodynamics of Adsorption.

In interpreting the thermodynamic properties of real systems it has proved convenient to establish an 'ideal' reference behaviour against which deviations from ideality may be measured[51].

Consider a solid surface in contact with a solution, and the equilibrium:

$$(1)^1 + (2)^s \rightleftharpoons (1)^s + (2)^1 \qquad -(17)$$

Where superscript 1 denotes a species in the liquid phase and superscript s denotes a species in the surface phase, then:

$$K = \frac{x_2^s x_1^1}{x_1^s x_2^1} \qquad -(18)$$

K is the equilibrium constant for (17) above , for an ideal system (these K values may be calculated if x_1^s and x_2^s are known from single component isotherm calculations). K is also known as the 'separation factor' and is used as a measure of the adsorbent selectivity. A high K value indicates a high selectivity by an adsorbent for component 2.

Since

$$x_1^1 = 1 - x_2^1 \quad \text{and} \quad x_1^s = 1 - x_2^s$$

Then,

$$x_2^s = \frac{Kx_2^1}{[1 + x_2^1(K-1)]}$$

If it is now assumed that the two components have the same molecular area, then:

$$n_1^s + n_2^s = n^s$$

Where n^s = total number of moles of substance in the adsorbed phase.

Then,

$$x_2^s = \frac{n_2^s}{n^s}$$

and

$$n_2^s = \frac{Kn^s x_2^1}{[1 + x_2^1(K-1)]}$$

Hence, from (8)

$$\frac{n_0 \Delta x}{m} = \frac{n^s x_1^1 x_2^1 (K-1)}{1 + x_2^1(K-1)}$$

The applicability of this equation to a set of experimental results may be tested by using it in its linear form:

$$\frac{x_1^1 x_2^1}{n^{\sigma(n)}} = \frac{1}{n^s}\left[x_2^1 + \frac{1}{(K-1)} \right] \qquad -(19)$$

An expression for the heat of immersion of the solid in the solution for a perfect system may also be obtained. In the initial state, where there are n^0 moles of solution and n^a moles of adsorbent separate from it, then the initial enthalpy is:

$$H_i = n_1^0 h_1^1 + n_2^0 h_2^1 + n^a h^a$$

$$H = n^0(x_1^{1,0} h_1^1 + x_2^{1,0} h_2^1) + n^a h^a$$

Where n_i^0 = initial number of moles of component i in solution and h_i^1 = molar enthalpy of pure component i

h^a = molar enthalpy of adsorbent

While, after immersion and establishment of equilibrium:

$$H_f = n_1 h_1^l + n_2 h_2^l + n_1^s h_1^s + n_2^s h_2^s + n^a h^a$$

$$H_f = n^l(x_1^l h_1^l + x_2^l h_2^l) + n^s(x_1^s h_1^s + x_2^s h_2^s) + n^a h^a$$

The enthalpy change is therefore :

$$\Delta H = n^0\{(x_1^l - x_1^{l,0})h_1^l + (x_2^l - x_2^{l,0})h_2^l\} + n^s(x_1^s h_1^s - x_1^l h_1^l + x_2^s h_2^s - x_2^l h_2^l)$$

But remembering

$$x_2^l = \frac{n_2}{n^l} = \frac{(n_2^0 - n_2^s)}{n^l}$$

Therefore,

$$\Delta x = x_2^{l,0} - x_2^l = \frac{n^s}{n^l}(x_2^s - x_2^{l,0})$$

or

$$\Delta x = \frac{n^s}{n^0}(x_2^s - x_2^l)$$

Hence,

$$\Delta H = x_1^s \Delta H_1^0 + x_2^s \Delta H_2^0$$

Where

$$\Delta H_1^0 = n^s \Delta_a h_1 \quad \text{and} \quad \Delta H_2^0 = n^s \Delta_a h_2$$

Then, from (19),

$$\Delta H - (x_1^l \Delta H_1^0 + x_2^l \Delta H_2^0) = \frac{n_2^{\sigma(n)}}{n^s}(\Delta H_1^0 - \Delta H_2^0)$$

The applicability of this treatment may first be tested using equation (19), before using (20) to relate heat of immersion and equilibrium adsorption data.

Where the system under investigation deviates significantly from ideality, a more detailed treatment becomes necessary. Such

an analysis is presented below and is a combination of those proposed by Everett[51,52], Schay[53] and Sircar et al.[54].

ε is defined as the excess Gibbs free energy of the surface due to adsorption and

$$\Delta\varepsilon = \varepsilon^{*} - \varepsilon \qquad -(21)$$

Where ε^{*} = Excess Gibbs free energy of the standard state

ε = Excess Gibbs free energy of the final state

$\Delta\varepsilon$ = Change in excess Gibbs free energy in going from the standard to the final state.

That is , $\Delta\varepsilon$ is defined with reference to a standard state.

It will be convenient to express ε in terms of the excess Gibbs free energy per unit mass of adsorbent:

$$\dot{\Delta\varepsilon} = \Delta\varepsilon/m = \dot{\varepsilon}^{*} - \dot{\varepsilon} \qquad -(22)$$

The explicit expression for the surface excess energy is[29]:

$$G^{s} = TS^{s} - pV^{s} - \dot{\Delta\varepsilon}m + m\Sigma_i \mu_i n_i^{\sigma(n)} \qquad -(23)$$

The complementary differential relations are:

$$dG^{s} = TdS^{s} - pdV^{s} - \dot{\Delta\varepsilon}dm + m\Sigma_i \mu_i dn_i^{\sigma(n)} \qquad -(24)$$

and

$$S^{s}dT - V^{s}dp - md\dot{\Delta\varepsilon} + m\Sigma_i n_i^{\sigma(n)} d\mu_i = 0 \qquad -(25)$$

Then, for a binary mixture at constant temperature and pressure,

$$d\dot{\Delta\varepsilon} = \frac{n_2^{\sigma(n)}}{x_1^{1}} d\mu_2^{1} \qquad -(26)$$

But, remembering (16),

$$d\mu_2^{1} = RTd\ln\gamma_2^{1}x_2^{1} \qquad -(27)$$

Substituting (27) in (26) and integrating gives:

$$\dot{\Delta\varepsilon} - \dot{\Delta\varepsilon}_2^* = RT\int_{x_1^1}^{n_2^{\sigma(n)}} d\ln\gamma_2^1 x_2^1$$

or

$$\dot{\Delta\varepsilon} - \dot{\Delta\varepsilon}_2^* = RT\int_{x_1^1 x_2^1 \gamma_2^1}^{n_2^{\sigma(n)}} d\gamma_2^1 x_2^1 \quad -(28)$$

Where $\hat{\Delta\varepsilon}_2^*$ = change in ε in going from standard state to immersion of adsorbent in pure component 2, in $J.g^{-1}$.

The integrand on the right hand side of equation (28) may be calculated if activity coefficient data are available (Professor Everett at the University of Bristol has kindly made available to us activity coefficient data for ethanol-water mixtures over a range of temperatures). The plotted curve of the integrand against $x_2^1\gamma_2^1$ may then be integrated numerically to give values of $\hat{\Delta\varepsilon} - \hat{\Delta\varepsilon}_2^*$. Integration over the entire concentration range gives $\hat{\Delta\varepsilon}_1^* - \hat{\Delta\varepsilon}_2^*$.

Then,

$$\frac{\partial}{\partial(1/T)}\left[\frac{\Delta\varepsilon - \dot{\Delta\varepsilon}_2^*}{T}\right]_{x_2^1} = \dot{\Delta_w h} - \dot{\Delta_w h}_2^* \quad -(29)$$

Where $\hat{\Delta_w h}$ = enthalpy of immersion of solid in equilibrium solution per unit mass of solid ($J.g^{-1}$)

$\hat{\Delta_w h}_2$ = enthalpy of immersion of solid in pure component 2 per unit mass of solid.

The corresponding entropy values are given by:

$$\dot{\Delta_w s} - \dot{\Delta_w s}_2^* = (1/T)[(\dot{\Delta_w h} - \dot{\Delta_w h}_2^*) - (\dot{\Delta\varepsilon} - \dot{\Delta\varepsilon}_2^*)] \quad -(30)$$

In equation (31), the values of $\hat{\Delta_w h}$ and $\hat{\Delta_w h}_2$ may be determined directly by calorimetry. Calorimetric data therefore provide a

useful check on this analysis. Unfortunately, very few studies have been carried out against which this treatment may be checked, since it requires equilibrium adsorption data of detail and quality in combination with calorimetric data.

In this study, the integrand in equation (28) is calculated from a smooth curve drawn through isotherm data obtained experimentally, fitted using cubic splines on a computer. Cubic splines are also used to fit the $n_2^{\sigma(n)}/(x_1^1 x_2^1 \gamma_2^1)$ against $\gamma_2^1 x_2^1$ curve. The area beneath this curve is then integrated numerically by computer. Computer programs are listed in Appendix 1.

The integrals from curves at several temperatures are then used to find $\hat{\Delta h}$ values from equation (29). The results of these calculations are then compared with calorimetric data.

Analyses of this type have been succesful in application such systems as Graphon with mixtures of benzene and cyclohexane, benzene and heptane, and cyclohexane and heptane [55]; and Graphon with mixtures of benzene with n-pentane, iso-pentane and n-butyl benzene[56]; for example.

Chapter 3. Previous Work.

A survey of work carried out on the adsorption of ethanol from aqueous solution is presented.

In 1981 Milestone and Bibby[57] presented a study of the concentration of alcohols by adsorption on silicalite. The adsorption of several different alcohols, including ethanol, was studied. Gas chromatography was used to analyse the solutions before and after equilibration with silicalite. 'Single component' isotherms over the range 0-2%(w/v) alcohol in water were presented. ethanol was shown to be adsorbed preferentially over water. The 'single component' isotherms were calculated by assuming that no water was adsorbed on the silicalite, an assumption later shown to be erroneous[58]. Furthermore, these data would be unsuitable for the thermodynamic analysis intended in this study, mainly because of the narrow concentration range studied.

Thermogravimetric analysis of the ethanol-water-silicalite system indicated the presence of water on the adsorbent, which the authors ascribe to adsorption of water at surface hydroxyl groups.

Milestone and Bibby studied the adsorption of alcohols from aqueous solution on ZSM5 zeolites[59]. For ethanol, the amount adsorbed increased with increasing aluminium content. However, it was not shown whether the amount of water adsorbed increased similarly. This increase was dependent on the type of balancing cation present. For the alkali metal ion forms, the amount of alcohol adsorbed decreased as the cation size increased, the effect being particularly pronounced for Cs^+.

Thermal desorption studies showed that the adsorbed ethanol was retained by the zeolites up to temperatures of ≈250^{o}C, at which point catalytic reaction of the alcohol was observed to begin. This makes it improbable that ZSM5 zeolites will be used for alcohol concentration,unless alternative desorption methods are used, but does raise another interesting possibility. Costa et al.[60] have carried out studies on the conversion of ethanol to gasoline using ZSM5 zeolites as catalysts. Their results indicate that such a conversion is indeed possible. A situation may be envisaged where a suitable ZSM5 is used to selectively adsorb ethanol from a fermentation liquor and, after separation from the liquor, the ethanol - loaded zeolite is heated to produce gasoline catalytically. Such a process remains speculative at present.

Recently, Klein[61] and co-workers[62] studied the adsorption of ethanol-water vapours on silicalite-1 and from these results heats of adsorption were calculated. These heats were 69.7 kJ.mol^{-1} for ethanol and 39.8 kJ.mol^{-1} for water. Calorimetry was also used to provide a value of the heat of adsorption of ethanol, by measuring the heat of immersion of silicalite in a dilute aqueous solution, and then correcting the result by the known heat of vaporisation. The value so obtained was 61.5 kJ.mol^{-1}. Again it was assumed that only alcohol was adsorbed. Calorimetry experiments showed no detectable heat of immersion in liquid water, hence the value of the heat of vaporisation, 39.8 kJ.mol^{-1}, was assigned.

A Langmuir model was used to fit the 'single component'

isotherm. This model was then used to predict a solution isotherm. A poor fit with the experimental data of Chriswell[63] and Milestone and Bibby[57] was achieved.

Farhadpour and co-workers[58] determined composite isotherms for the ethanol/water/silicalite system. Liquid phase diffusion results were also presented. The practicality of using silicalite to produce ethanol from fermentation systems was discussed. Gas chromatography was used to analyse the solutions. Unfortunately, the isotherm data presented are unsuitable for the intended thermodynamic analysis since they do not cover a sufficiently wide concentration range and are not of the required accuracy.

Messow, Quitzsch and Herden[64] studied calorimetrically the heats of immersion of ZSM5 zeolites and silicalite in 1-alkenes, n-alkanes and 1-alcohols at 30°C. The heat of immersion of silicalite-1 in ethanol was found to be 54.0J.g^{-1}.

Ake[65] obtained 'single component' adsorption isotherms for ethanol and water on silicalite, and proposed a process by which ethanol could be extracted from water using silicalite as adsorbent.

Bui et al.[65] compared the adsorption characteristics of silicalite, ZSM5 and activated carbon with ethanol, water and glucose as observed in the 'single component' isotherms. The adsorption of ethanol on silicalite and ZSM5 was found to be nearly independent of ethanol concentration in the range 2-8%(w/v) and independent of temperature in the range 30-60°C, with equilibrium being achieved rapidly. No measurable adsorption of glucose on silicalite was found.

The adsorption of ethanol and glucose on activated carbon was

found to be significantly greater than that on silicalite, increasing with concentration of adsorbate in the liquid phase and decreasing with temperature. Silicalite was chosen as being the most suitable adsorbent for ethanol from fermentation broths on the basis of selectivity and rates of adsorption and desorption.

In addition, a number of patents have been published which deal with the selective adsorption of ethanol from aqueous solution.

Dessau et al.[67] described the recovery of ethanol from fermentation mixtures by sorption on zeolites. The zeolite used was either ZSM5, ZSM11, ZSM12, ZSM23, ZSM35 or ZSM48. The zeolites had Si/Al>35.

Nai et al.[68] report the use of a ZSM5 in the hydrogen form, containing virtually no aluminium, in selectively adsorbing ethanol from a fermentation mixture with essentially no adsorption of water.

Garg et al.[69] used alumina, silicalite or ultrahydrophobic zeolite Y for the adsorption of ethanol from a wet vapour mixture stripped from the fermentation broth with an inert gas.

Groszek[70] described the use of high silica zeolites in a process for separating ethanol from dilute aqueous solutions.

Other adsorbents used in this application include activated carbon and crosslinked polymers.

Kulprathipanja[71] and Akhmadeev et al.[72] report the use of activated carbon in processes for separating ethanol from water. In the case of the former, the ethanol produced is said to be pure enough to be blended directly into a motor fuel.

The various polymers used in the extraction of ethanol include divinyl benzene crosslinked polystyrene[73], crosslinked polyvinylpyridine[74] and aminated PVC[75].

To summarise, although the ethanol-water-zeolite system is of interest commercially, very little detailed examination has been carried out. Adsorption isotherms, where given, cover only restricted ranges of ethanol concentration and rely on relatively few experimental points. Certainly, isotherm data obtained to date are unsuitable for the proposed thermodynamic analysis. A more detailed examination of these systems is required, which may prove of interest commercially and add to the present knowledge of liquid phase adsorption in general and particularly adsorption on zeolites.

Chapter 4. Experimental.

4.1. Samples and Materials Used.

Zeolite 3A Pellets: supplied by Laporte Inorganics and activated in air at 350°C overnight before use.

Ethanol: supplied by James Burroughs Fine Alcohols Division as 'Absolute Alcohol 100'. This was stored over activated zeolite 3A before use.

Water: distilled water was used in all ethanol - water mixtures and in washing glassware.

Activated Carbon: supplied by B.D.H. Chemicals Ltd. .

Other Adsorbents: the followng materials were supplied by Laporte Inorganics. The samples were characterised by X-ray powder diffraction (X.R.D.), X-ray fluorescence spectroscopy (X.R.F.) and by scanning electron microscopy (S.E.M.). The instruments used were: for X.R.D. a Pye-Unicam 1710 diffractometer, for X.R.F. a Pye-Unicam 1400 spectrometer, and for S.E.M. a Camscan Series 4 scanning electron microscope.

Silicalite-1 HSIL. The sample HSIL was calcined in air at 550°C before use. X.R.D. showed the expected ZSM5 structure. S.E.M. showed crystal size to be in the range 1-5μm . X.R.F. analysis gave the following:

Oxide	Wt.%
Al_2O_3	0.01
SiO_2	99.5
K_2O	<0.01
BaO	0.01
CaO	0.01
TiO_2	0.04
SrO	<0.01
MgO	0.07
Total	99.7

This indicates that Si/Al>2000. Note that X.R.F. analysis does

not give an accurate measure of Si/Al ratio.

Silicalite-1 HSILB. Experiments were carried out on this sample after calcination at 550, 670 and 800°C. X.R.D. showed the ZSM5 type structure. S.E.M. showed crystal sizes to be in the range 15-25 μm . X.R.F. analysis gave the following results:

Oxide	Wt.%
Al_2O_3	<0.01
SiO_2	98.9
K_2O	<0.01
BaO	<0.01
CaO	<0.01
TiO_2	0.01
Fe_2O_3	<0.01
SrO	<0.01
MgO	<0.01
Na_2O	<0.01
Total :	98.9

Indicating that Si/Al>2000.

ZSM5 Sample NaZSM5/1. Experiments were carried out on this sample after calcination at 550°C. X.R.D. showed the ZSM5 structure. Crystal sizes in the range 0.5-5μm were revealed by S.E.M. . X.R.F. analysis results were:

Oxide	Wt.%
Al_2O_3	1.03
SiO_2	97.7
K_2O	<0.01
BaO	0.01
CaO	<0.01
TiO2	0.05
Fe_2O_3	0.06
SrO	<0.01
Na_2O	0.72
Total :	99.6

Which gives Si/Al≈ 67.

ZSM5 Sample NaZSM5/2. NaZSM5/2 was calcined at 550°C before use. X.R.D. showed the ZSM5 type structure. S.E.M. gave crystal sizes of 0.5-4.0μm. X.R.F. gave the following:

Oxide	Wt.%
Al_2O_3	1.93
SiO_2	95.9
K_2O	<0.01
BaO	<0.01
CaO	<0.01
TiO_2	0.02
SrO	<0.01
MgO	0.11
Na_2O	1.13
Total	:99.1

Which gives Si/Al≈35.

4.2. Thermogravimetric Analysis Experimental.

The adsorption capacities of the zeolite samples for ethanol and water were determined by thermogravimetric analysis.

Samples were prepared by activating the zeolite at 350°C in air in a furnace overnight. The activated sample was then left in a desiccator containing some of the desired liquid for 3-5 days to equilibrate. Experiments were then carried out using approximately 5 mg of the saturated sample on a Stanton-Redcroft TG762 thermogravimetric balance. Run conditions were as follows :

Initial temperature ≈ 23°C

Heating rate = 20°Cmin^{-1}

Final temperature = 500°C

carried out under flowing dry nitrogen.

From the weight loss of the sample, the number of moles of adsorbate required to saturate one gram of the unsaturated sample was calculated.

Let the initial weight of the saturated sample be M (g) and the loss of weight on heating be m (g). Then, M (g) of the saturated sample contains m (g) of adsorbate. Therefore (M-m) (g) of the unsaturated sample will adsorb m (g) of adsorbate. So, 1g of the unsaturated sample will adsorb m/(M-m) (g) or m/[(M-m)A] moles of the adsorbate, where A is the molar mass of the adsorbate (mol.g^{-1}). The expression for the adsorption capacity of the adsorbent is then :

$$n_i^{s,0} = \frac{m}{A_i(M-m)}$$

Where $n_i^{s,0}$ = sample saturation adsorption capacity (mol.g^{-1})

From the weight loss with temperature readings, the differential weight loss with temperature was calculated, using :

$$\left[\frac{dW}{dT}\right]_{T_2} = \frac{w_1 - w_2}{T_2 - T_1}$$

Where T_1 = Initial (lower) temperature (K)

T_2 = Final (higher) temperature (K)

w_1 = Weight loss at temperature T_1 (mg)

w_2 = Weight loss at temperature T_2 (mg)

$(dW/dT)_{T2}$ = Rate of weight loss with temperature at temperature T_2 $(mg.K^{-1})$

Thermogravimetric studies were carried out on the samples HSIL, HSILB, NaZSM5/1, NaZSM5/2 and activated carbon, saturated with ethanol and with water. The activated carbon samples were activated at a temperature of 100°C overnight prior to use.

Repetition of experiments showed that the $n_i^{s,0}$ results were reproducible to within 2%.

4.3. Calorimetry Experimental.

4.3.1. Basic Principle and Method of Calculation of Results.

In the majority of calorimetry experiments, the heat evolved or absorbed in a reaction is observed as a change in temperature of the calorimetry vessel. By means of a comparison experiment, in which a precisely known amount of electrical energy is supplied to the calorimeter vessel, the amount of heat necessary to cause an identical temperature rise is determined.

In the calorimeter used (an LKB 8721-1 immersion calorimeter) the temperature of the calorimeter vessel is measured accurately as a function of time by means of thermistor which forms one arm of a Wheatstone bridge. A second arm consists of a variable resistor which is used to balance the bridge and so give a value of the thermistor resistance. The remaining two arms of the bridge are formed by standard 2kΩ resistors.

During the calibration experiment, a known amount of heat is provided by a heater of measured resistance in the calorimeter vessel (see Fig. 7 , diagram of calorimeter vessel).

To carry out the 'reaction' experiment, the sample, contained in a small sealed glass bulb, is first positioned between the stirrer blades. Here the sample is held in place beneath the surface of the desired solution. At the appropriate time, the bulb is broken by forcing it down on to the the spike fixed to the base of the vessel.

In order to obtain an accurate value of the change in thermistor resistance (ΔR, Ω) during the course of an experiment it is necessary to observe the small temperature

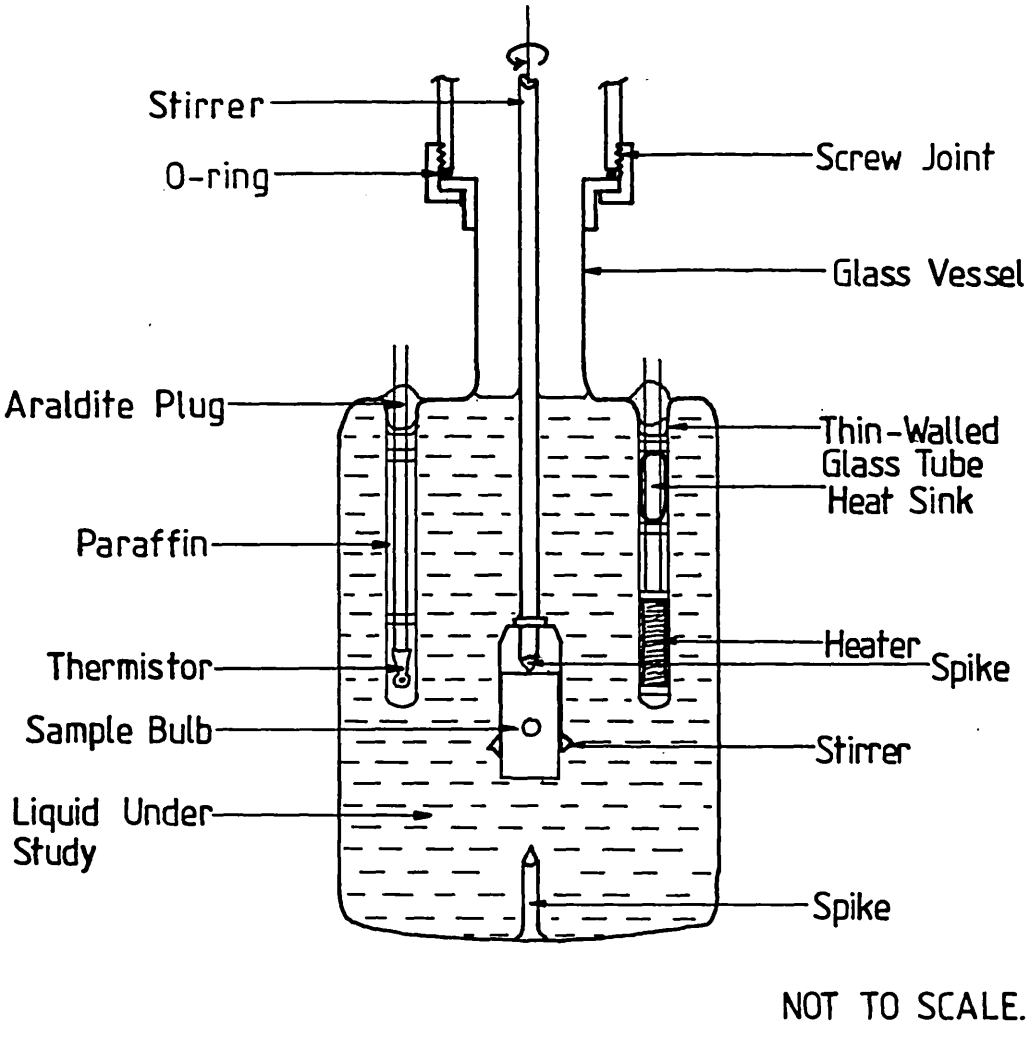

Figure 7. Diagram of Calorimeter Vessel.

gradients present both before and after the experiment.

Results may be calculated from the resistance-time plot, either manually or by computer. A calibration experiment gives rise to a near linear resistance-time plot, whereas a 'reaction' experiment gives rise to an exponential curve. Methods of calculating ΔR therefore differ slightly for each type of experiment. A typical resistance-time graph for a 'reaction' experiment is shown in Figure 8.

As may be seen from Fig.8 , ΔR is calculated by extrapolating the line fitted to the linear region of the main 'reaction' period to its intercepts with the lines fitted to the fore- and after- period measurements. The intercept with the fore-period line gives the initial thermistor resistance R_i (Ω), the intercept with the after-period line giving the final thermistor resistance R_f (Ω). Then,

$$\Delta R = R_i - R_f$$

Generally, calculations then proceed as follows:

Thermistor resistance and temperature are related by:

$$R = Ae^{B/T} \qquad -(31)$$

Where A and B are constants and

R=Thermistor resistance (Ω).

T=Temperature (K).

Then,

$$\frac{dR}{dT} = \frac{-A.B.e^{B/T}}{T^2}$$

or,

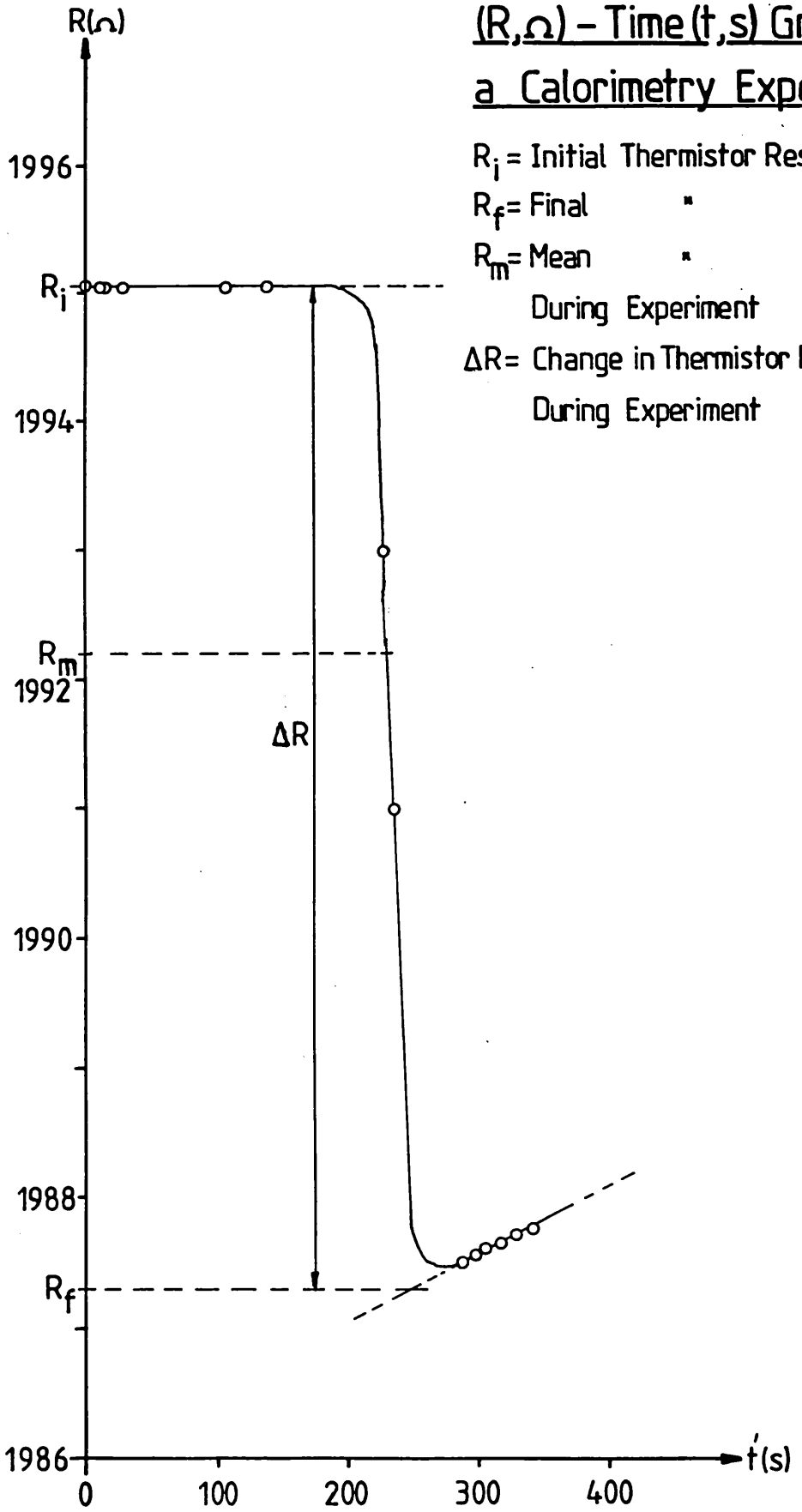

Figure 8 .Typical Resistance (R,Ω) – Time (t,s) Graph for a Calorimetry Experiment.

R_i = Initial Thermistor Resistance

R_f = Final " "

R_m = Mean " "
During Experiment

ΔR = Change in Thermistor Resistance
During Experiment

$$\frac{dR}{dT} = \frac{-B.R}{T^2}$$

then,

$$\frac{\Delta R}{\Delta T} = \frac{-B.R_m}{T_m^2}$$

Where subscript m indicates a mean value. Hence,

$$\Delta T = \frac{-T_m^2}{B} \frac{\Delta R}{R_m}$$

However, during a series of calorimetry experiments T_m^2 is nearly constant, so,

$$\Delta T \alpha \frac{\Delta R}{R_m} \qquad -(32)$$

For a calibration experiment,

$$R_m = 0.5\Delta R + R_i \qquad -(33)$$

Where R_i is the initial thermistor resistance. However, for a 'reaction' experiment,

$$R_m \approx (1-1/e)\Delta R + R_i$$

or,

$$R_m \approx 0.63\Delta R + R_i \qquad -(34)$$

since the resistance-time curve is exponential in shape.

From the calibraton experiment, a calibration constant, ϵ, may be obtained from:

$$\epsilon = \frac{Q_{calib}}{(\Delta R/R_m)_{calib}} \qquad -(35)$$

Where Q_{calib} = Quantity of heat used in calibration experiment, in Joules.

and $(\Delta R/R_m)_{calib}$ = $\Delta R/R_m$ value from calibration experiment.

Also,

$$Q_{calib} = R_h I^2 t' \quad -(36)$$

Where R_h = Measured calibration heater resistance (Ω).

I = Heater current (A)

t'= Heating time (s).

Then, having performed a 'reaction' experiment, the heat released during the reaction is obtained from:

$$Q_{react} = \epsilon(\Delta R/R_m)_{react} \quad -(37)$$

In this study, it was desirable to express the heat evolved in terms of Joules per gram of adsorbent used :

$$-\Delta H = \frac{Q_{react}}{m} \quad -(38)$$

Where ΔH = enthalpy of reaction ($J.g^{-1}$).

m = Mass of adsorbent used (g).

Corrections may have to be made to the results obtained from calorimetry experiments to account for such phenomena as heat of stirring, heat of bulb breaking and heat of vaporisation (produced when liquid vapour saturates gas contained in the sample bulb, on bulb breaking).

In the case of this study, instrument design has reduced the heat of stirring to a negligible quantity. Bulb breaking experiments have been carried out, using bulbs containing only air and no sample, to determine the magnitude of the latter two corrections mentioned above. These experiments were carried out in water and in ethanol. In both cases the heats produced were not measurable. This indicates that these corrections are negligibly small.

It was also assumed that the volume of the calorimeter vessel

was so great that the change in the mole fraction of ethanol in solution on immersion of the adsorbent was negligibly small.

4.3.2. Summary of Experimental Procedure.

'Reaction' Experiment:

(i)The zeolite samples to be used were activated in air at 350^{0}C overnight,before introduction into the sample bulb under dry conditions in a glove bag.

(ii)The filled, sealed sample bulb was then introduced into the calorimeter vessel containing the required solution.

(iii)The vessel was left to reach the desired temperature in a thermostatic bath overnight.

(iv)The small temperature gradient present was measured for several minutes.

(v)The bulb was broken and the change in thermistor resistance with time recorded.

(vi)The small temperature gradient present after the run was measured again for several minutes.

(vii)ΔR was calculated from the results by computer and R_m from equation (34). Hence $(\Delta R/R_m)_{react}$ was obtained.

Then the calibration experiment was performed :

(i)The calibration heater resistance, R_h, was measured.

(ii)The desired calibration heating current and heater resistance were set.

(iii)The initial temperature gradient was measured, as in the 'reaction' experiment.

(iv)Calibration heating was begun and the thermistor resistance

recorded as a function of time throughout heating.

(v)The small temperature gradient present after heating was measured , as in the 'reaction' experiment.

(vi)By computer and from equation (33), $(\Delta R/R_m)_{calib}$ was calculated. Then from equation (37) Q was calculated, and ΔH calculated from equation (38).

4.3.3. Experiments Performed.

Initially, the heat of solution of potassium chloride in water at $30^{o}C$ was determined, in order to check the accuracy of the instrument. Comparison of our result with the value given in the C.R.C. handbook gave agreement to within 1-2%.

Heats of immersion at $30^{o}C$ of the silicalite sample HSIL in pure ethanol, pure water, and in solutions where the mole fractions of ethanol present were 0.0138, 0.0560, and 0.3821 were determined.

Solutions were made up by weighing the required amounts of ethanol and water into a volumetric flask. Experiments were performed two or more times in each case to check the reproducibility of the results.

4.4. Isotherm Experimental.

4.4.1. Methods of Detecting Alcohols in Water.

A study by Pirzada et al.[76] compared three methods of analysing ethanol-water mixtures. The methods examined were gas chromatography, spectrophotometry and measurement of specific gravity. Of these, gas chromatography was found to be the most suitable.

One further method of analysis has been investigated by ourselves, that of refractive index measurement. The refractive index of nine ethanol-water solutions of different concentrations was determined and a calibration curve plotted from the results. This curve is shown in Figure 9 . The curve shows a peak followed by a relatively flat region. These features would give rise to ambiguous results when analysing solutions of unknown ethanol concentration. Therefore, gas chromatography, using a system very similar to that of Pirzada et al., was selected as the method of analysis of ethanol-water mixtures. The gas chromatograph used was a Pye Unicam 4500 fitted with a thermal conductivity detector, DP88 computing integrator, chart recorder and a 2.1m x 4mm glass analytical column packed with 'Porapak T'. Helium was used as carrier gas. The chromatograph was calibrated with a large number of ethanol solutions of known concentrations. The quantity used to measure the mole fraction of ethanol in a given solution was the 'area fraction' of ethanol in the chromatogram, f_{EtOH}, defined as follows :

$$f_{EtOH} = \frac{\text{Area under ethanol peak}}{\text{Area under ethanol peak} + \text{Area under water peak}}$$

Figure 9. Calibration Curve for Refractive Index Measurement, Refractive Index against Mole Fraction of Ethanol in Solution (x).

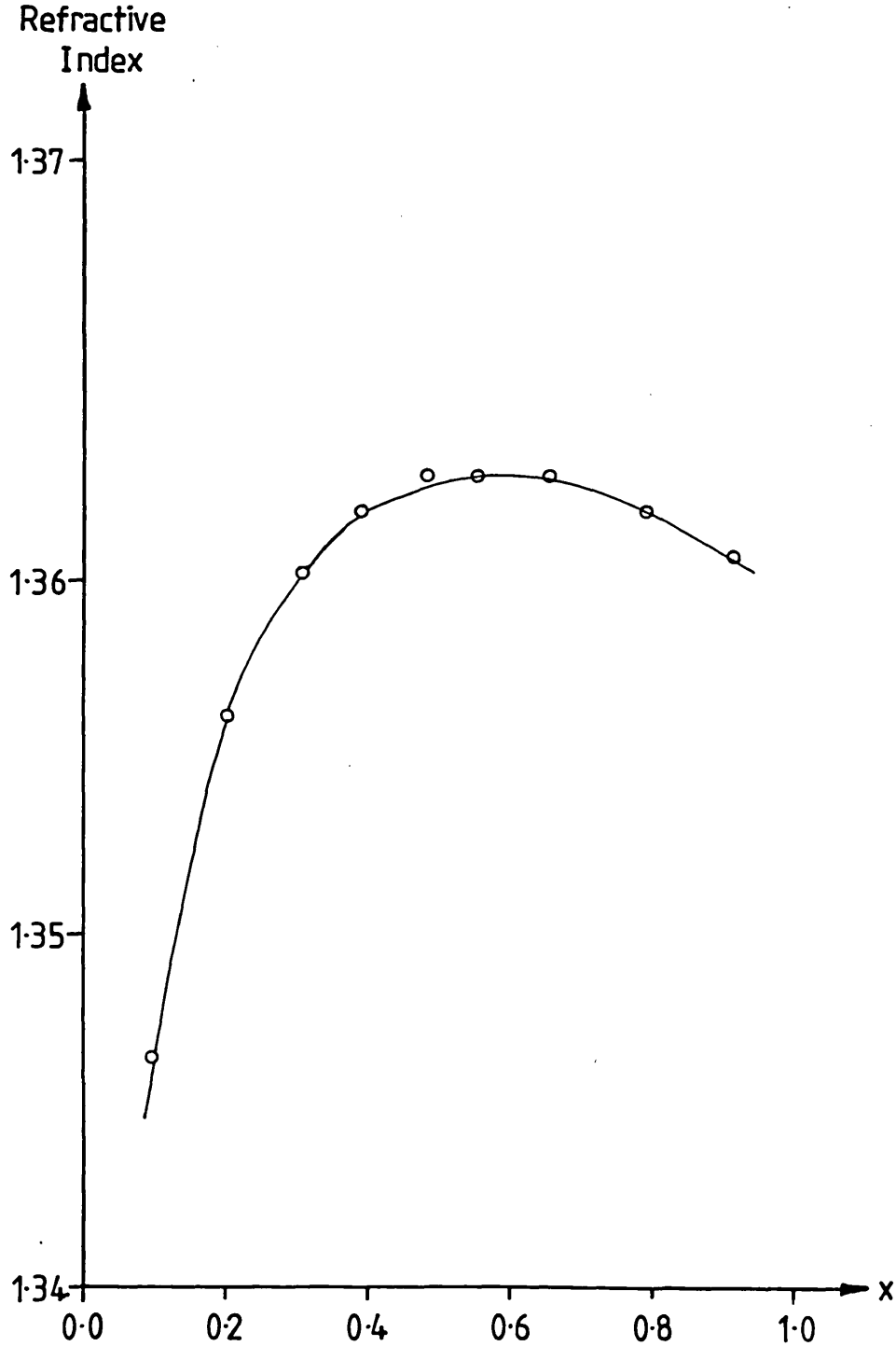

This was found to be an accurate and reproducible measure of ethanol mole fraction in a given solution.

The calibration curve obtained (a plot of f_{EtOH} against mole fraction of ethanol in the solution) was fitted and stored on computer . The mole fraction of ethanol in an unknown solution was then read, again by computer, from this curve.

4.4.2. Experimental Method.

The basic method involved activation of the calcined zeolite at 350^{o}C in air overnight. The zeolite was then left to cool in a desiccator (containing zeolite 3A as desiccant), before adding to pre-weighed Quickfit conical flasks under dry conditions. The flasks were then stoppered and reweighed to determine the amounts of zeolite added. To each of the flasks approximately 10ml of an ethanol-water solution of known concentration was added. Each flask received a different solution. Once again the flasks were weighed, to find the weight of solution present. Solutions were made up by weighing the necessary amount of ethanol and water into a volumetric flask. Solutions were made and used on the same day.

The flasks, now containing adsorbent and solution, were then placed in a thermostatic shaker bath at the required temperature. The samples were left to equilibrate overnight, with vigorous shaking. Some of the final liquid was then removed and centrifuged to seperate off any suspended solid. The resulting solutions were then analysed by gas chromatography.

Initially, experiments were performed to determine the effect

of the following :

(i) Weight of Sample Used.

Experiments were carried out as outlined above,using different weights of zeolite equilibrated with solutions of the same ethanol concentration. It was found that using weights of zeolite of approximately 1g gave a large degree of scatter in the results (~30%). This was due to the fact that insufficient zeolite was present to cause a significant reduction in the concentration of ethanol. When weights of zeolite of 4-5g were used, the results were found to be highly reproducible. Using weights of zeolite of around 7g caused the zeolite-solution mixture to form a thick slurry from which it was impossible to remove any liquid for analysis. Sample weights of 4-5g were therefore used in our experiments (except in the case of activated carbon, see below).

(ii) Effect of Shaking.

It was found in initial experiments that slow shaker speeds, of around 0.5Hz, gave rise to large scatter in the results, which was eliminated at higher shaker speeds of about 2Hz. This effect may be due to improper mixing of the solution with the adsorbent, with the result that a proper equilibrium is not reached.

(iii) Effect of Method of Sample Removal.

Experiments were carried out to determine whether or not centrifuging the samples before analysis (the centrifuge chamber being at a different temperature than that of the thermostatic bath) disturbs the established equilibrium, giving rise to error in the final concentration of ethanol as observed by gas chromatography. A set of eight samples, covering a range of

initial ethanol mole fractions ($x_2^{1,0}$) between 0.29 and 0.71 were treated as above, but samples were not immediately removed for centrifuging. Instead, the samples were left for an additional period of roughly three hours at the required temperature but without shaking. This was to allow as much zeolite as possible to settle from the solution before removing for centrifuging and analysis. With significantly less zeolite in the samples being centrifuged, very little shift in equilibrium should be seen compared with the results from those samples centrifuged without settling. In fact, comparison of the two sets of results showed no difference, within experimental error. This would indicate that the original method of centrifuging samples without prior settling does not disturb the established equilibrium significantly.

(iv) Effect of Liquid Evaporation.

Experiments were carried out as outlined above, but without any adsorbent present. Analysis of the solutions after shaking overnight at 40°C showed no significant change in ethanol concentration.

(v) Effect of Equilibration Time.

Eight samples were prepared using approximately the same weight of zeolite in each case and the same ethanol-water solution ($x_2^{1,0} \approx 0.2$). Two samples were removed for analysis immediately after addition of solution and shaking, two after one hour in the shaker bath at 40°C, two after leaving overnight and

two after leaving for two days. Comparison of the results showed very little difference between the latter two sets, indicating that equilibrium has been reached once the sample has been left overnight.

(vi) Use of Rotator Oven.

For experiments run at 40°C, samples were mixed in plastic 25ml screw-top tubes and placed in a rotator oven. This was done in attempt to improve results obtained at 40°C. It was thought that evaporation effects, though small, might be further reduced by using screw-top tubes. However, comparison of results obtained by using these tubes in the rotator oven and the ordinary flasks in the shaker bath showed no significant difference.

In conclusion, from these initial experiments, it was decided that 4-5g of zeolite with 10ml of solution, left overnight in a thermostatic bath with vigorous shaking, followed by removal and centrifuging of samples for analysis, was the optimum method to use. With this final method, errors in the composite isotherm results were less than 2-3%. These are thought to arise from errors in reading ethanol concentrations from the calibration curve and from loss of ethanol by evaporation.

In the case of those experiments carried out on activated carbon, a slightly different procedure was used. The carbon samples were activated at 100°C overnight before use. Approximately 1g of activated carbon was added to each flask in adsorption experiments, since the adsorpton capacity of the activated carbon (as determined by TGA, see p45-46 for ethanol was considerably greater than that of the zeolites used.

As well as the activated carbon isotherm in the range $0.0<x_2^{1,0}<0.2$, the following isotherms were determined:

(i)The 20, 30 and 40°C isotherms of the sample HSIL, having been calcined in air at 550°C, to determine the effect of temperature on adsorption.

(ii)The 30°C isotherm of a sample of HSIL previously used in an adsorption experiment and reactivated at 100°C for four days then at 350°C for 24 hours, to determine the effect of reactivation on the adsorption isotherm.

(iii)The 30°C isotherms for HSILB samples calcined in air at 550, 670 and 700°C, to investigate the effect of calcination temperature of the zeolite on the adsorption isotherm.

(iv)The 30°C isotherms for the samples NaZSM5/1 and NaZSM5/2, calcined at 550°C in air, To determine the effect of varying the aluminium content of the zeolite.

Specific surface excess values were calculated from equation 1, and plotted against the equilibrium mole fraction of ethanol in the liquid phase to give the composite isotherm. From these results, 'single component' isotherms were calculated, as described in Chapter 2 , section 2.2.

Chapter 5. Results and Discussion.

5.1. Thermogravimetric Analysis Results and Discussion.

Temperature programmed desorption (T.P.D.) and weight loss curves for the samples HSIL, HSILB, NaZSM5/1, NaZSM5/2 and activated carbon, saturated with water and with ethanol are shown in Figures 10-18 .

Table 1 shows the maximum temperature at which either water or ethanol is retained, as read from the T.P.D. curve, in comparison with some literature values.

Table 2 displays the calculated adsorption capacities ($(n_i^s)_0$, $mol.g^{-1}$) of these adsorbents for water and ethanol, again in comparison with some values from the literature.

Table 3 shows the adsorption capacities expressed in units of cm^3 of adsorbate g^{-1} of adsorbent, to give an indication of the amount of pore volume filled. the pore volume of silicalite-1 and ZSM5 is taken as being $0.19 cm^3 g^{-1}$.

There are several important points to note about these results. Firstly, for all of the adsorbents, with both ethanol and water, desorption occurs in a single step, as shown by the presence of a single peak in the T.P.D. curves. This suggests that the samples are homogeneous adsorbents.

Secondly, for both ethanol and water, there is an increase in adsorption capacity of the samples HSIL, HSILB, NaZSM5/1 and NaZSM5/2 with decreasing Si/Al ratio. This result agrees qualitatively with results found in the literature[59]. These increases are due to the greater polarity of the zeolite lattice as the aluminium content is increased, resulting in a stronger interaction with the polar -OH groups of both water and

Table 1 . T.P.D. Results.

Sample / Adsorbate	Peak Temperature (K)	Temperature at which desorption ends (K)
HSIL / Water	300	400
HSIL / Ethanol	335	400
HSILB / Water	300	360
HSILB / Ethanol	340	420
NaZSM5/1 / Water	310	400
NaZSM5/1 / Ethanol	340	450
NaZSM5/2 / Water	320	430
NaZSM5/2 / Ethanol	340	560
Act. Carbon / Ethanol	310	420
Silicalite / Ethanol *	—	370
NaZSM5 / Ethanol *	—	490

* – Taken from Ref. [59]
Figure for NaZSM5 is for a sample with Si/Al ≈ 20

Table 2 . Adsorption Capacities of Samples by T.G.A.

Sample	Adsorption Capacity for Ethanol ($mol.g^{-1} \times 10^3$)	Adsorption Capacity for Water ($mol.g^{-1} \times 10^3$)
HSIL	0·6	1·6
HSILB	0·8	2·0
NaZSM5/1	3·2	2·3
NaZSM5/2	3·2	2·1
Activated Carbon	—	11·9
Silicalite*	—	2·4
Na ZSM 5*	—	2·6

* - Taken from Ref. 64

Figure for NaZSM5 is for a sample with Si/Al ≈ 20

Table 3 . Adsorption Capacities of Samples by T.G.A.

Sample	Adsorption Capacity for Ethanol ($cm^3 .g^{-1}$)	Adsorption Capacity for Water ($cm^3 .g^{-1}$)
HSIL	0·035	0·029
HSILB	0·047	0·036
NaZSM5/1	0·189	0·042
NaZSM5/2	0·189	0·038
Silicalite *	—	0·043
NaZSM5 *	—	0·047

* Taken from Ref.64 (see Table 2).

Figure10 .Differential Weight Loss Curve (T.P.D. profile,-o-) and Weight Loss Curve for the Sample HSIL Satd. with Water.(-□-)

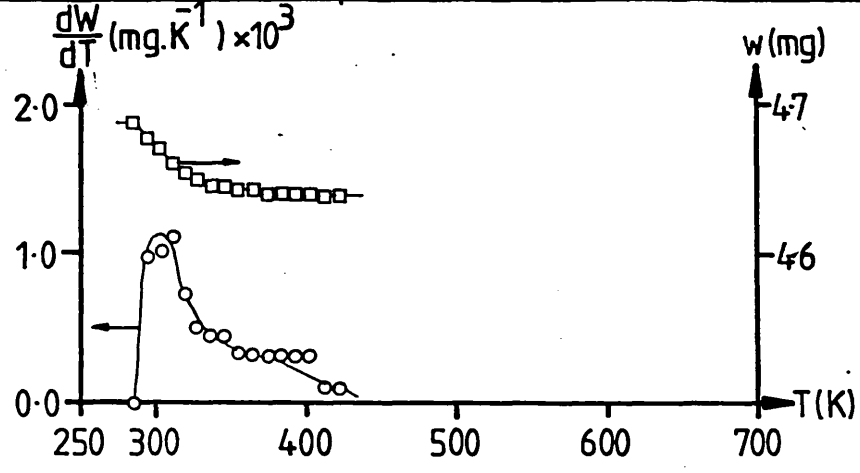

Figure11 .T.P.D. Profile (-o-) and Weight Loss (-□-) Curve for the Sample HSIL Saturated with Ethanol.

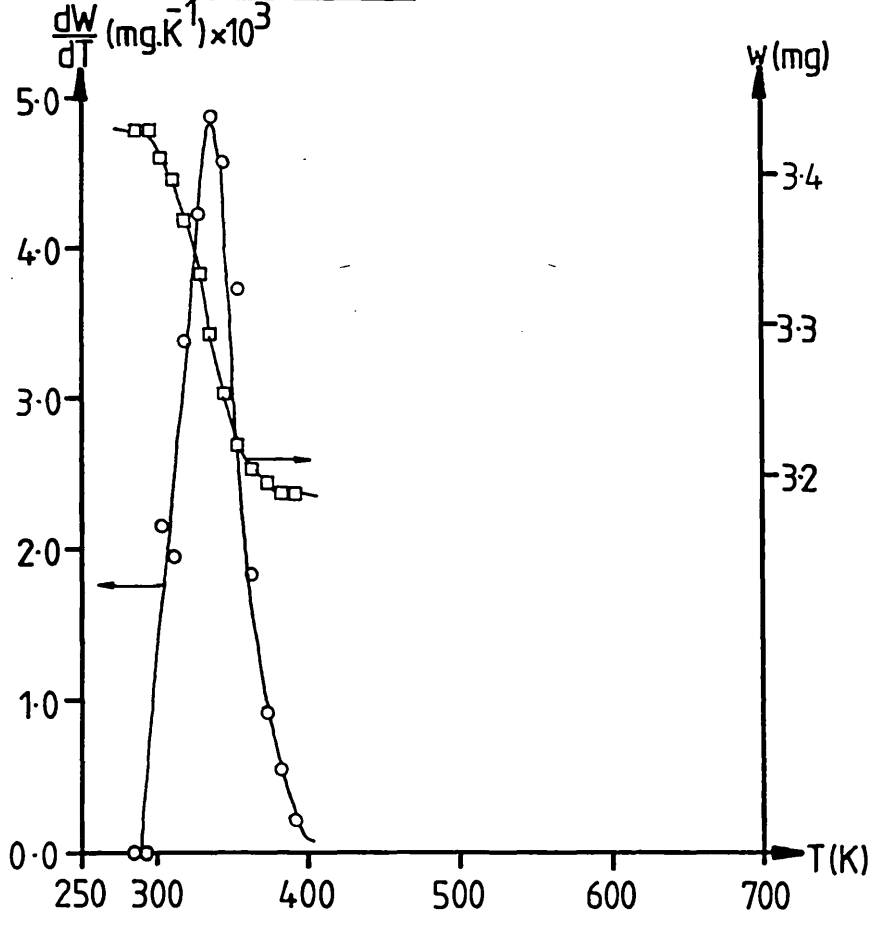

Figures 12 and 13 .T.P.D. profiles(-o-) and Weight Loss Curves(-□-) for Sample HSILB Satd. with Water and Ethanol Respectively.

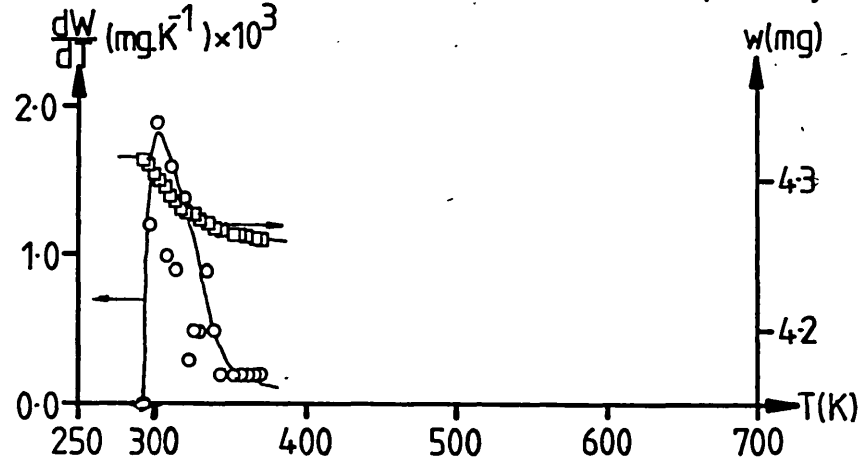

Figure .

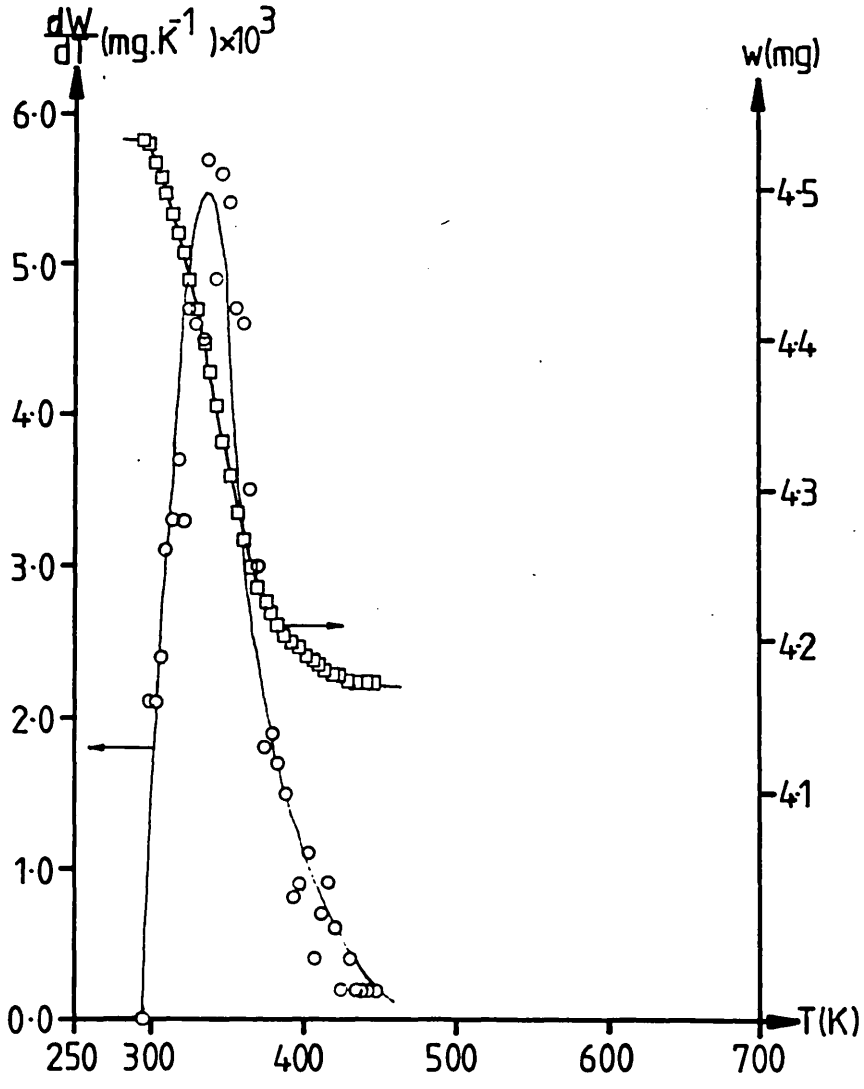

Figures14and15 .TPD. profiles(-o-) and Weight Loss Curves (-□-) for Sample ZSM5/1 Satd. with Water and Ethanol Respectively.

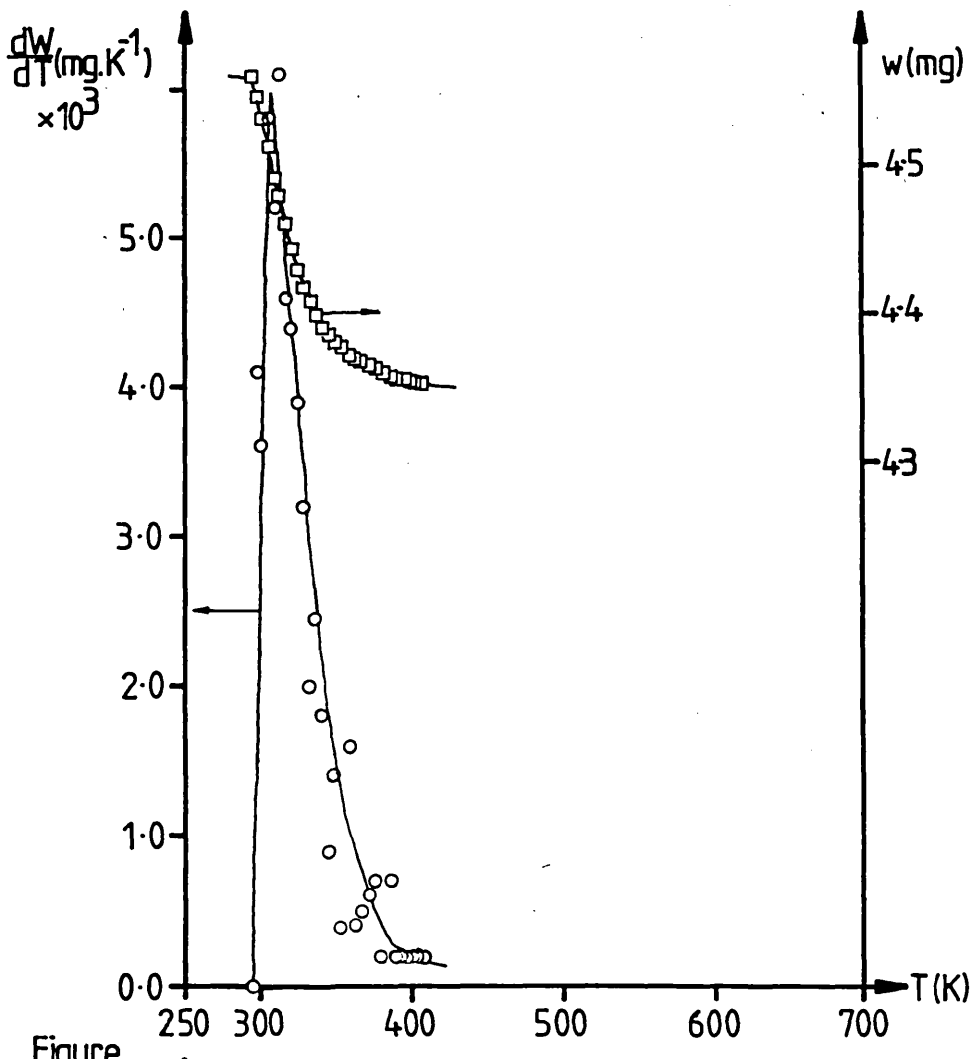

Figure

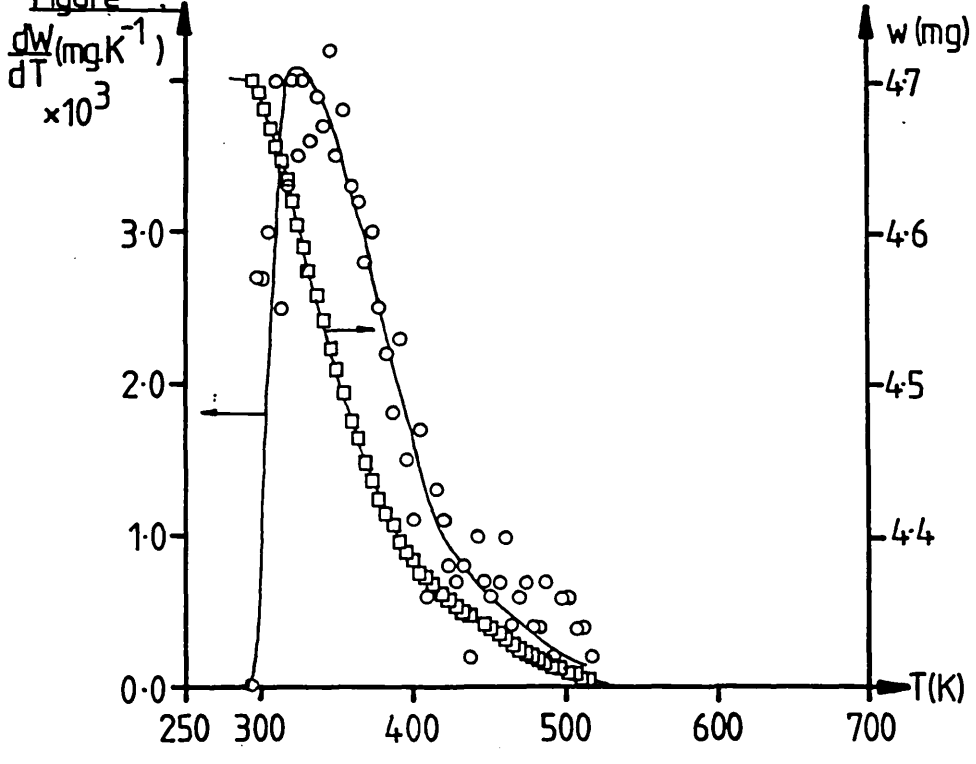

Figures16 and17 . T.P.D. profiles( ) and Weight Loss Curves( ) for Sample ZSM5/2 Satd. with Water and Ethanol Respectively.

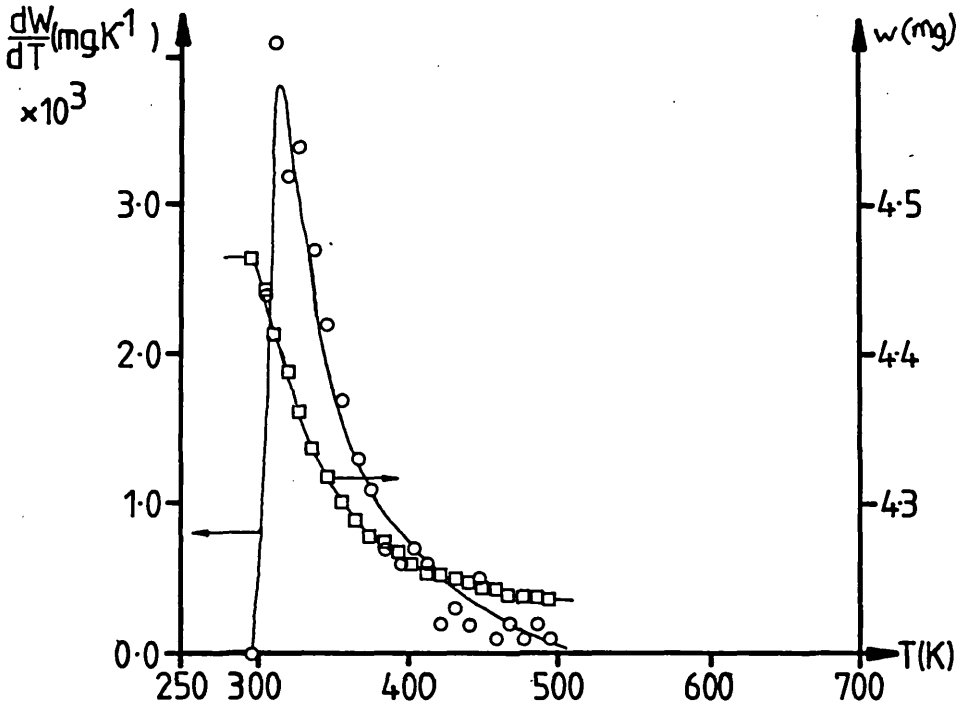

Figure .

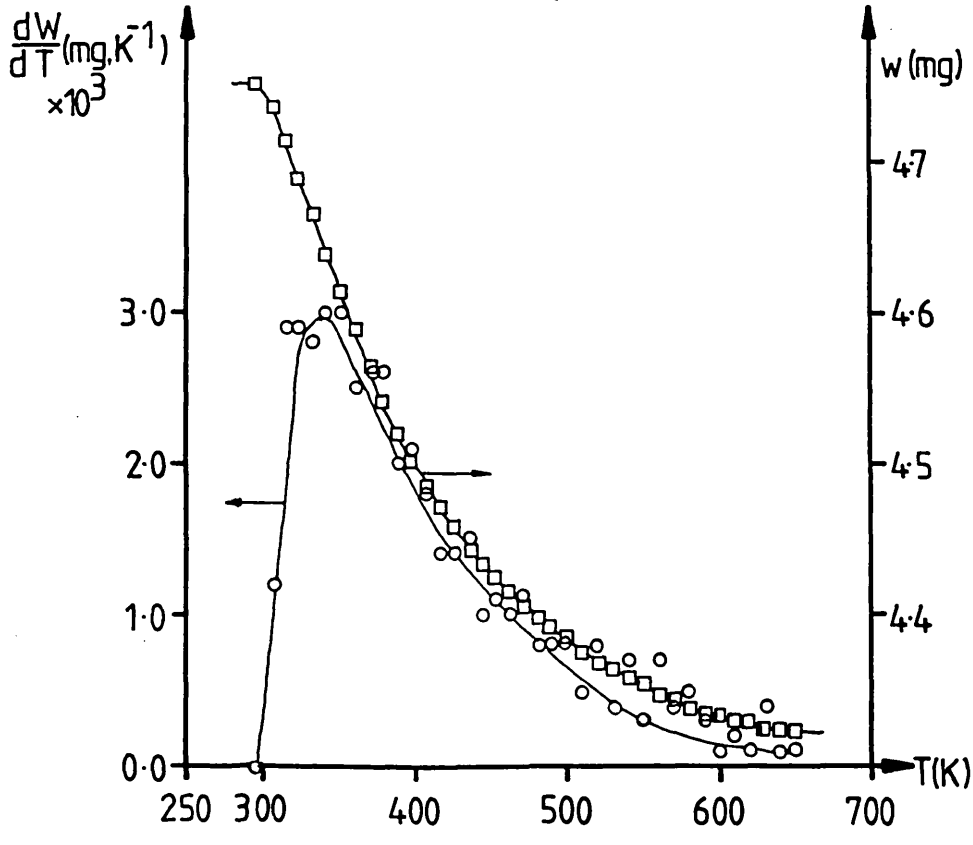

Figure 18 . T.P.D. profile(-o-) and Weight Loss Curve(-□-) for an Activated Carbon Sample Satd. with Ethanol.

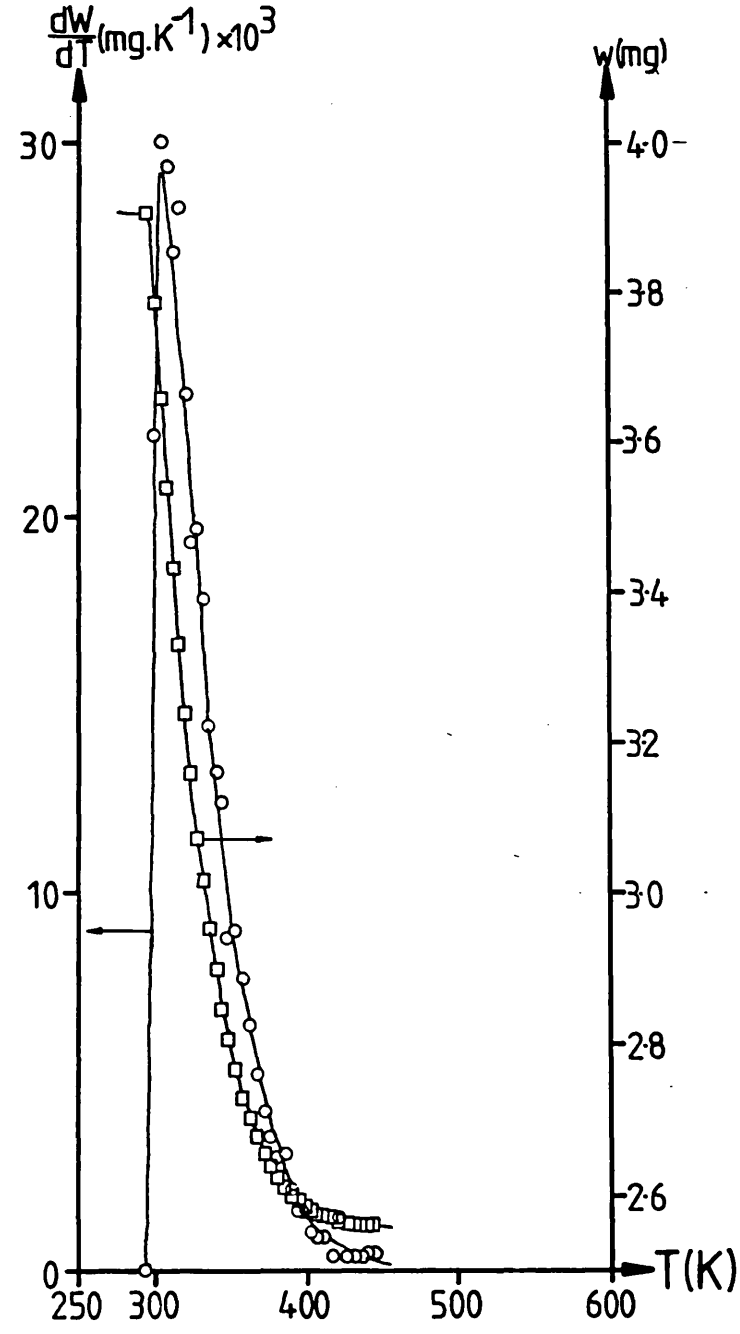

ethanol.This increase in the strength of the zeolite - adsorbate interaction is also reflected in the increase in the maximum temperature at which ethanol and water are retained with lower Si/Al ratio.

The two - step desorption observed by Milestone and Bibby[59] for ethanol on a ZSM5 sample was not seen in this study. This may be due to the fact that these authors were using ZSM5 samples of lower Si/Al ratio, of approximately 20. The catalytic activity which was thought to give rise to this two - step desorption may therefore be less significant in the ZSM5 samples used in this study.

For the samples HSIL, HSILB, NaZSM5/1 and NaZSM5/2, ethanol is retained up to a higher temperature than water. This indicates that these adsorbents interact more strongly with ethanol than with water, which is to be expected since these adsorbents are hydrophobic.

5.2. Calorimetry Results and Discussion.

Heats of immersion of silicalite-1 HSIL in pure water and pure ethanol are shown in table 4 , together with values from the literature. Heats of adsorption of ethanol and water on HSIL are also shown in this table, again in comparison with literature values. Heats of adsorption are calculated from heats of immersion as follows:

$$\text{Heat of adsorption, } \Delta_a H = \frac{\Delta_w \dot{h}}{(n_2^s)_0} + \Delta H_{vap}$$

Where ΔH_{vap}= heat of vaporisation of adsorbate

Heat of vaporisation data are readily obtainable from sources such as the C.R.C. handbook*. Here the heat of vaporisation of water is taken to be 39.8kJ.mol^{-1} and that of ethanol to be 40.5kJ.mol^{-1}

The heats of adsorption obtained by ourselves compare reasonably with those of Klein[61,62] and a value of 51-53 kJ.mol^{-1} for the activation energy for desorption given by Richards[77]. However, the heat of immersion of HSIL in ethanol differs significantly from that of Herden et al.[64] for a silicalite sample. This discrepancy may be due to differences between the samples used. Unfortunately no analysis of the silicalite sample used was presented.

The heat of immersion of HSIL in ethanol is much greater than the heat of immersion in water, demonstrating the hydrophobicity of silicalite-1.

Table 5 shows the heats of immersion of HSIL in aqueous solutions of various ethanol mole fractions. These data are

*e.g.- CRC Handbook, 62nd edn., pp. C694-C698

Tables 4 and 5 .Calorimetry Results.

Table 4 .

Sample/ Liquid	Heat of Immersion ($J.g^{-1}$)	Heat of Adsorption ($kJmol^{-1}$)
HSIL / Water	~1	~41
HSIL/ Ethanol	39·6	~65·5
Silicalite / Ethanol +	54·0	—
Silicalite/ Ethanol *	—	69·7
Silicalite/ Water *	—	39·8

+- Taken from Ref. 64

*- Taken from Ref. 61, 62

Table 5 .

Mole fraction of Ethanol in liquid.	Heat of Immersion of HSIL in liquid ($J.g^{-1}$)
0·0	~1·0
0·0138	4·85
0·0560	20·30
0·3821	37·49
1·0	39·62

Figure 19. Plot of Heat of Immersion $\Delta_w \hat{h}$ ($J.g^{-1}$) against Mole Fraction of Ethanol in Solution x_2^l

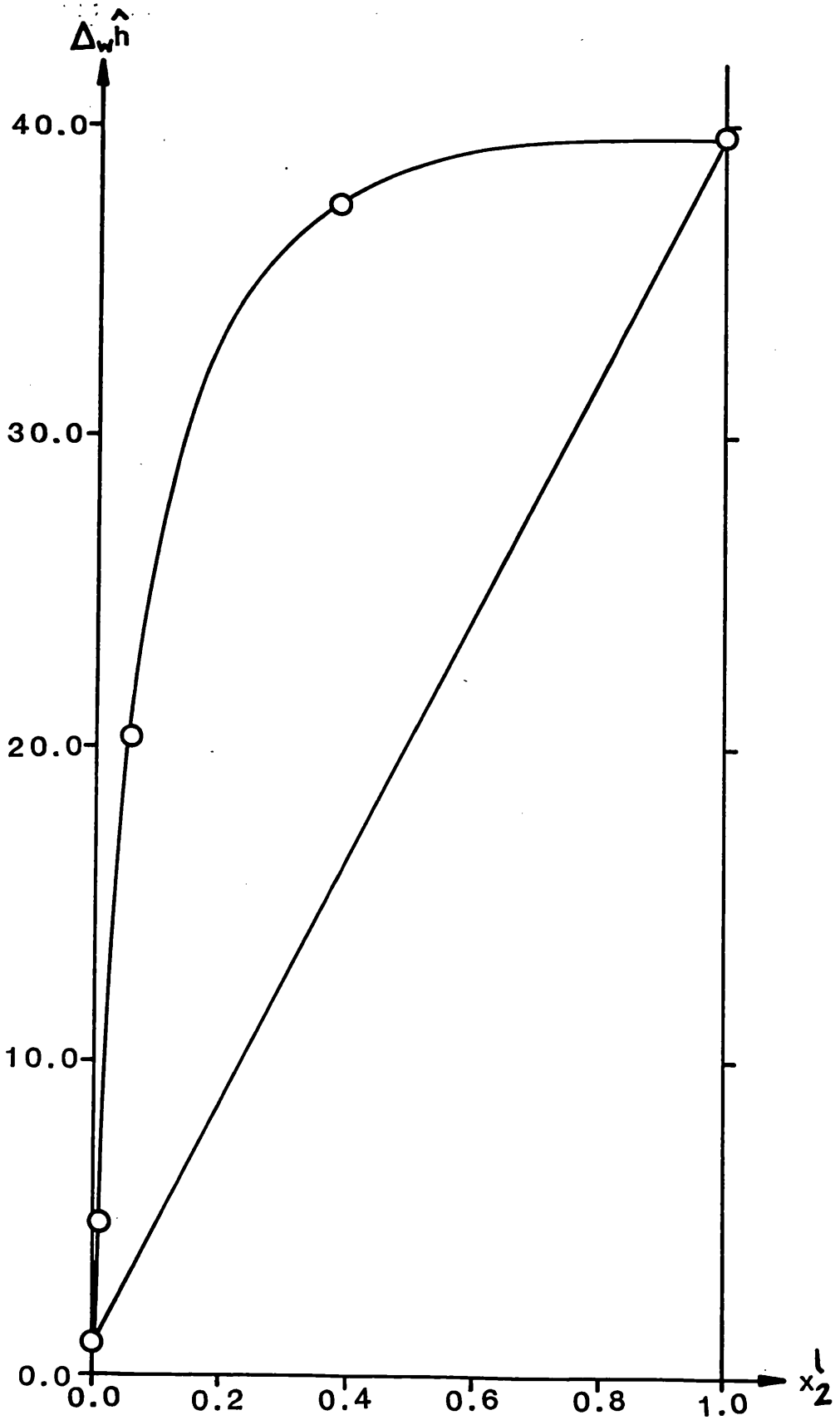

plotted in Figure 19.

As may be seen from Figure 19 , the experimental heats of immersion data lie roughly on a curve. This curve lies above the straight line drawn, which represents the equation:

$$\Delta_w \hat{h} = x_1^1 \Delta_w \dot{h}_1^* + x_2^1 \Delta_w \dot{h}_2^*$$

The equation represents the variation in $\Delta_w \hat{h}$ expected for an ideal system where the adsorbent shows no selectivity for either adsorbate. The fact that the observed heats of immersion lie above this line indicates strong selectivity of the adsorbent for ethanol.

Errors in the $\Delta_w \hat{h}$ values were found to be as much as 20% in the worst cases. This is thought to be due mainly to sticking of the silicalite sample to the inside of the sample bulb on bulb breaking, resulting in incomplete immersion of the sample.

5.3.Composite Isotherm Results and Discussion.

The 20, 30 and 40°C HSIL/ethanol/water composite isotherms are shown in Figures 20, 21 and 22 respectively. All three curves are plotted together in Figure 23 .

The isotherms are basically of the 'U' type, showing selectivity for ethanol over the whole concentration range studied. The silicalite-1 HSIL remains selective for ethanol over the whole temperature range studied also.

The isotherms were formed from the results of several consecutive runs, each run covering wide, overlapping ranges of ethanol concentration. The low experimental scatter in the data and the large number of experimental points give isotherms of high quality and reproducibility.

Examination of Figure 23 reveals that there is only slight variation in the isotherms with increasing temperature, which agrees with the findings of Bui et al.[66].

These isotherms also agree reasonably well with those of Farhadpour et al.[58].Both our results and the results of these authors show a main peak at low concentration followed by a near-linear decreasing region.

However, the isotherms determined in this study display some unusual features, which, as far as is known, have not been observed by other workers.

Firstly, at all three temperatures, the isotherms show a shoulder adjoining to the main peak at very low mole fractions of ethanol, $0.01<x_2^1<0.08$. This shoulder is prominent at 20°C and 30°C, but has decreased significantly at 40°C.

The isotherms also show a second peak in the high concentration

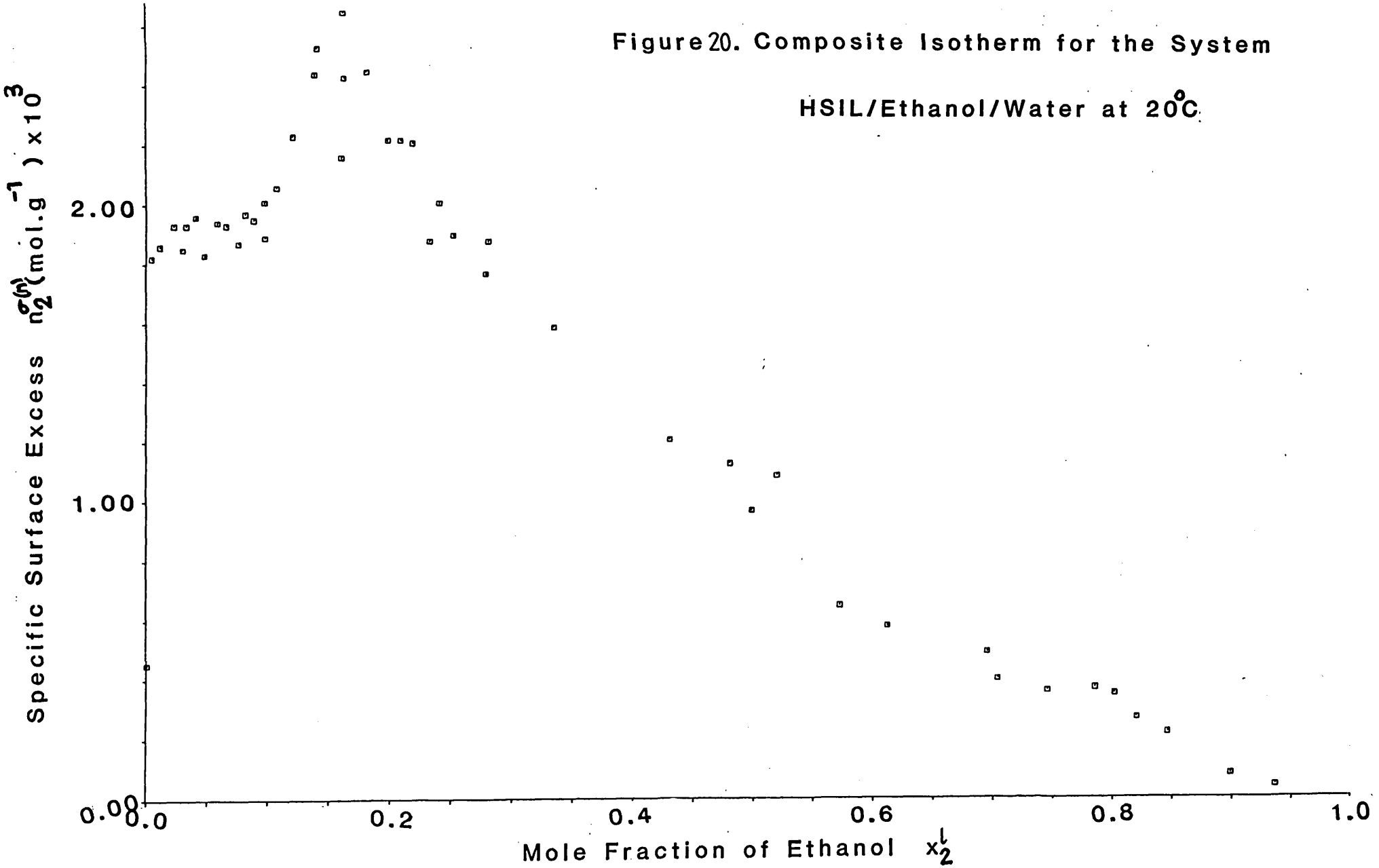

Figure 20. Composite Isotherm for the System HSIL/Ethanol/Water at 20°C

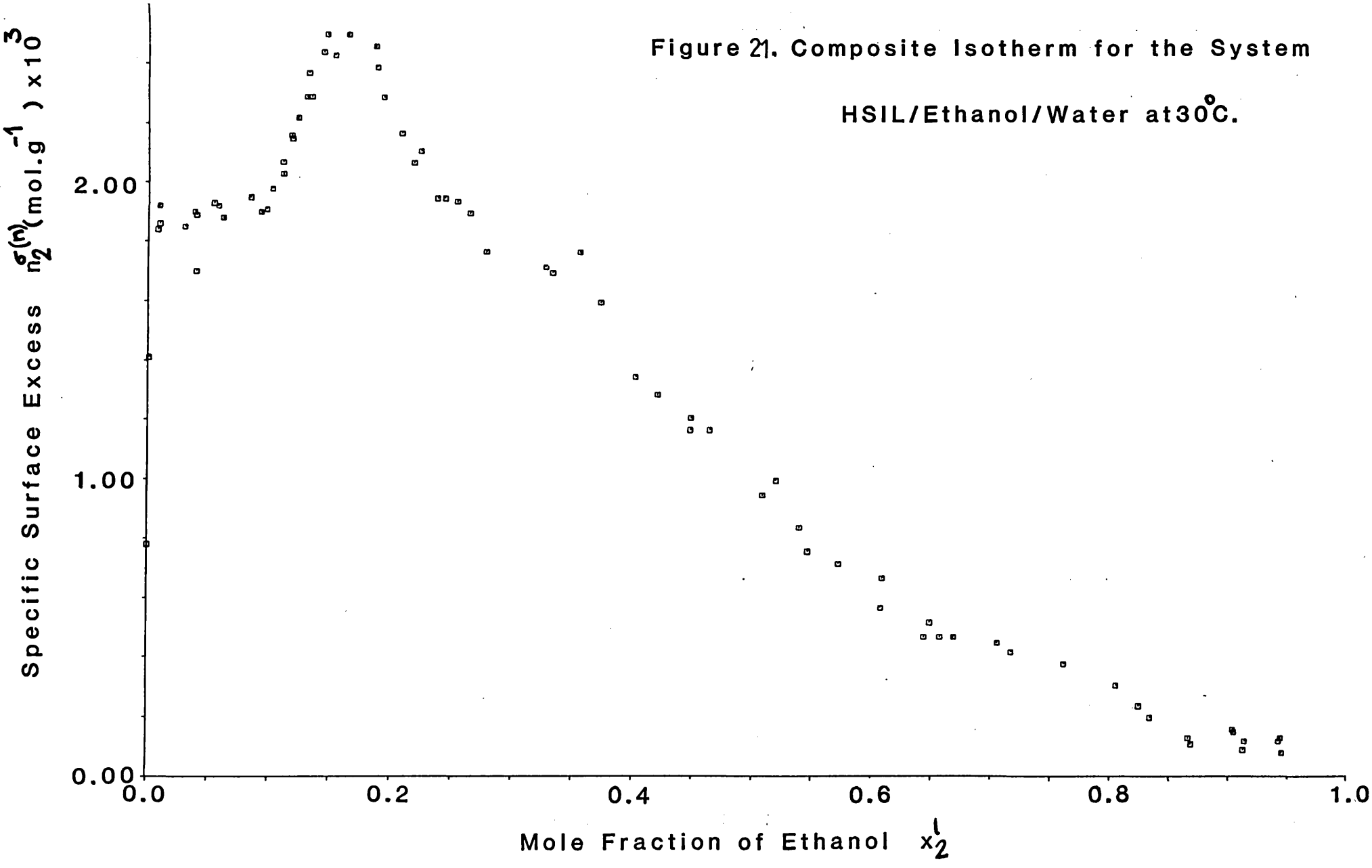

Figure 21. Composite Isotherm for the System HSIL/Ethanol/Water at 30°C.

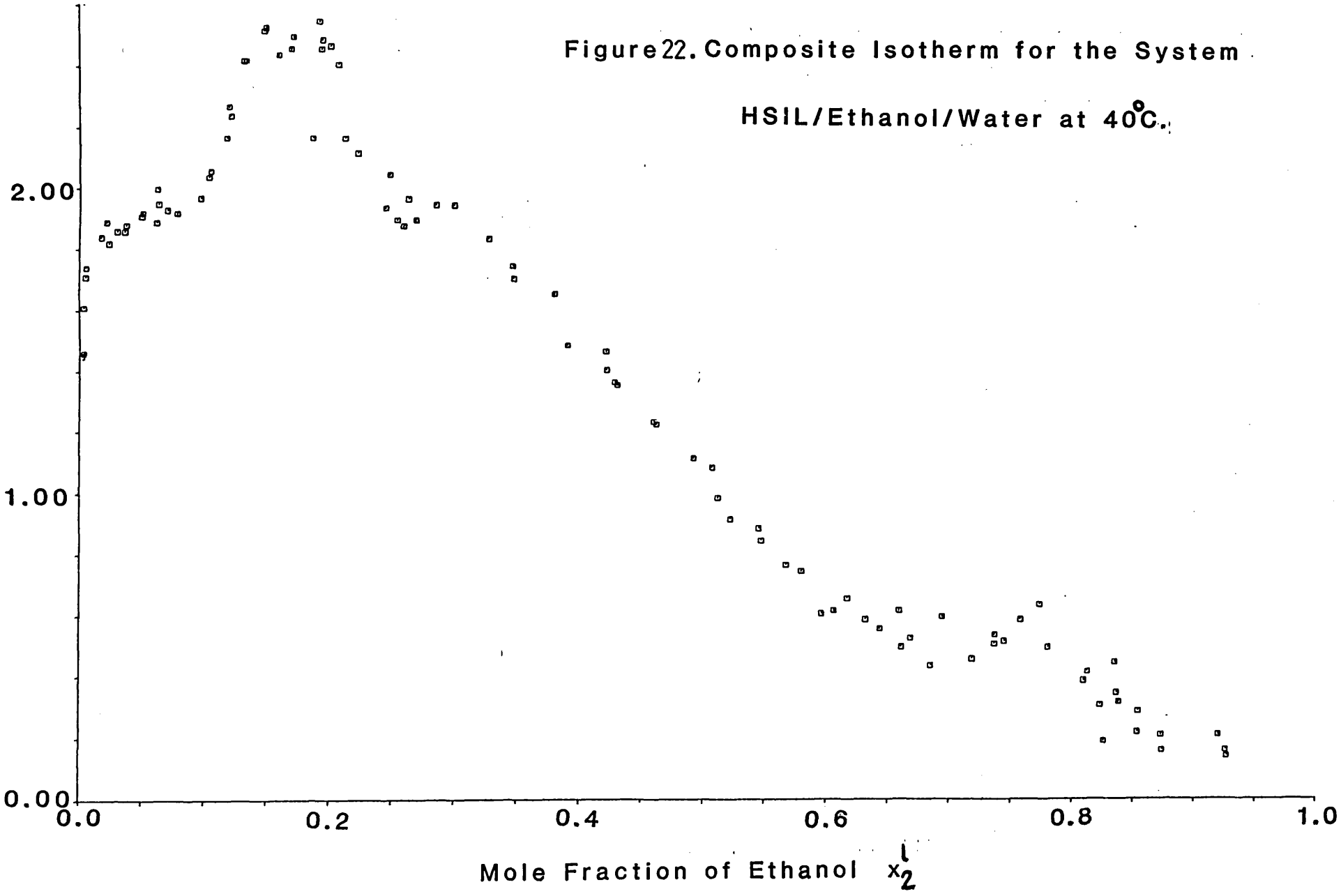

Figure 22. Composite Isotherm for the System HSIL/Ethanol/Water at 40°C.

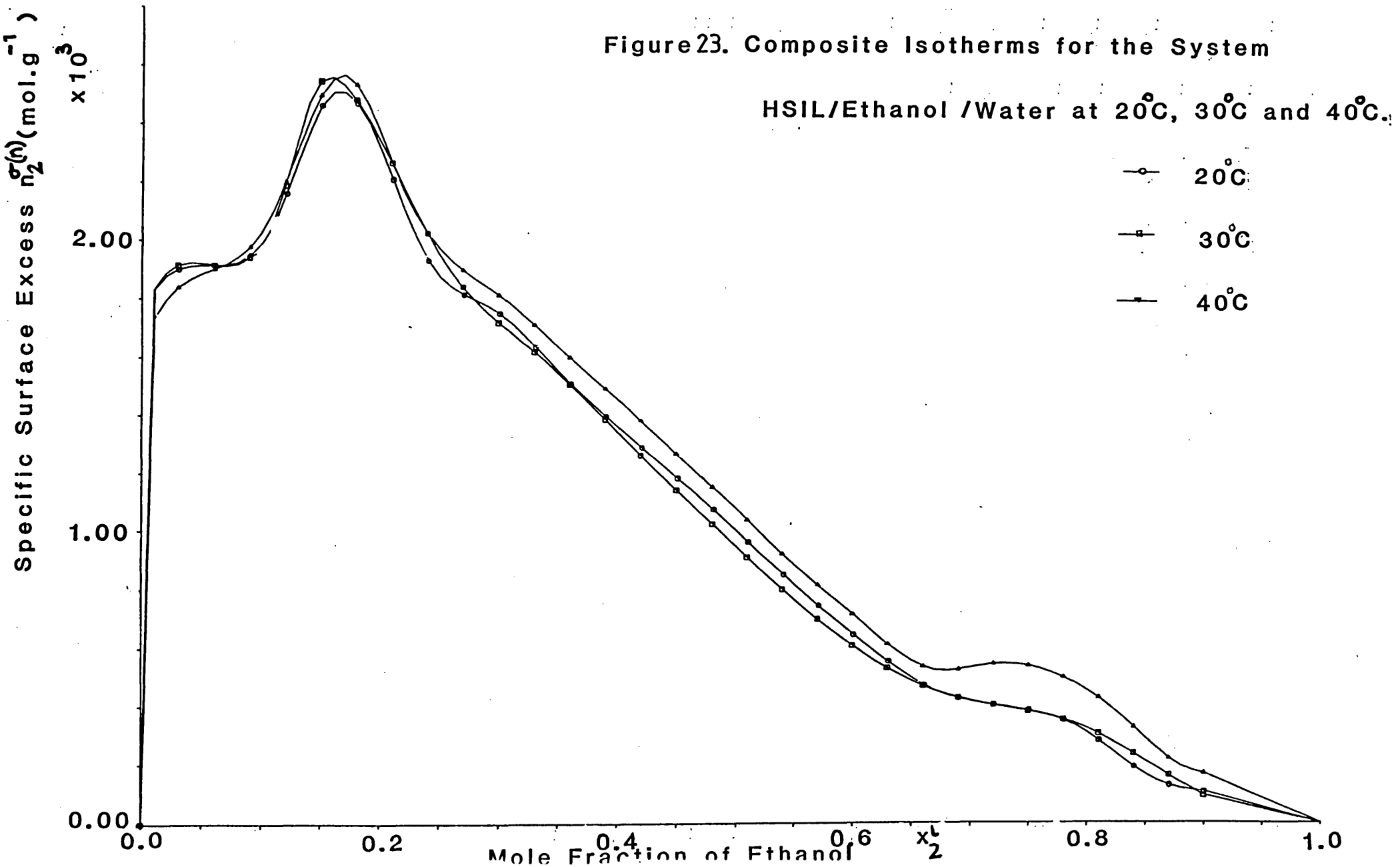

Figure 23. Composite Isotherms for the System HSIL/Ethanol /Water at 20°C, 30°C and 40°C.

region ($x_2^l \approx 0.8$) which becomes more prominent with increasing temperature.

With regard to the shoulder at low mole fractions, there are several possible explanations for this unusual variation in the isotherms:

(i)Sample heterogeneity. The observed isotherm may be thought of as the sum of two 'U' shaped isotherm curves, implying two different types of adsorption.

As discussed in the introduction, there are a number of likely causes of heterogeneity: impurity in the sample, differences between adsorption on the internal and external surfaces of the zeolite, the presence of internal silanol groups and different types of adsorption in different regions of the zeolite channel system.

(ii)Liquid phase interactions between ethanol and water molecules.

(iii)Interactions between adsorbed ethanol and water molecules.

Further experiments were carried out in an attempt to determine which of these factors is the cause of the behaviour seen.

Firstly the 30°C isotherm for a sample of HSIL used in the original isotherm experiments and reactivated was determined. This was done to check the reproducibility of the isotherm with this sample of silicalite-1.

The HSIL was reactivated by filtering it off from the mixture of solution and zeolite and leaving it to dry in air. The filtered HSIL was then kept at 100°C in air for approximately 3 days, before heating at 350°C in air for a further 48 hours to drive

off any remaining adsorbate. Isotherm experiments were then carried out on this reactivated sample in the manner described previously.

The 30°C reactivated HSIL/ethanol/water isotherm data points are shown in Figure 24 in comparison with the original 30°C HSIL isotherm curve. Within experimental error, the reactivated HSIL points lie on the original HSIL curve, showing the reproducibility of the isotherm, with its characteristic features, with the silicalite-1 sample HSIL.

Experiments were performed on a second silicalite-1 sample, designated HSILB, to determine whether the unusual behaviour was due to impurity in the sample HSIL. The sample HSILB was synthesised by a different method to that used in synthesising HSIL, so that it is unlikely that the same impurity, if any, would be present in both. The first batch of experiments were carried out on an HSILB sample calcined at 550°C, as HSIL had been.

The 30°C HSILB/ethanol/water isotherm points are shown in Figure 25, in comparison with the 30°C HSIL isotherm curve. The HSILB isotherm points lie on or very close to the HSIL isotherm curve. The shoulder observed in the case of HSIL is again well defined in the case of HSILB. This demonstrates that the behaviour seen is not due to any impurity in the silicalite-1 sample.

It is also important to note that the crystal sizes of the two samples HSIL and HSILB were considerably different (HSIL average crystal size was ≈5μm ; HSILB average crystal size was ≈20μm). Hence the ratio of surface area to volume for the two samples was significantly different. However, the isotherms were the same

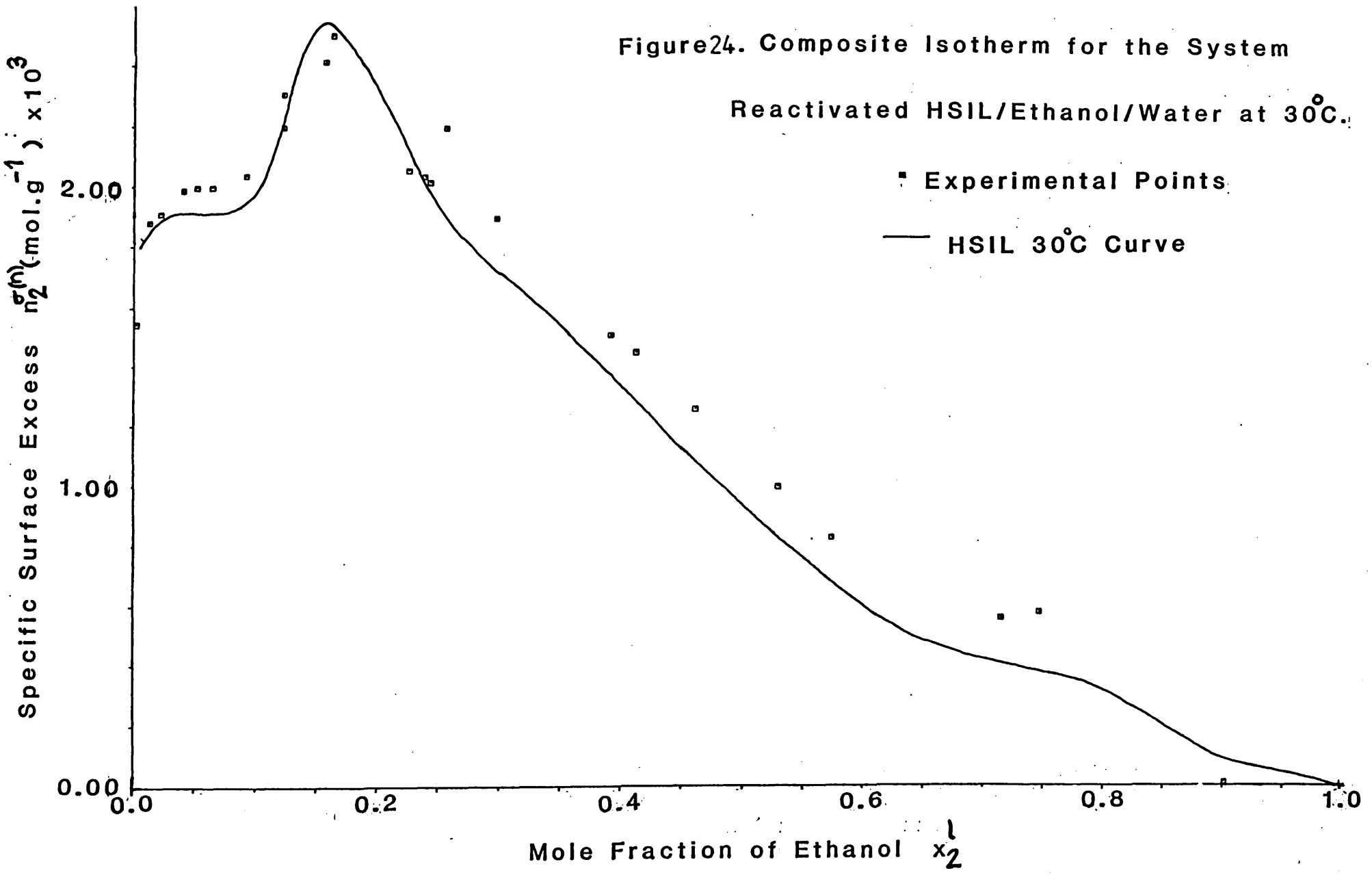

Figure24. Composite Isotherm for the System Reactivated HSIL/Ethanol/Water at 30°C.

▪ Experimental Points

—— HSIL 30°C Curve

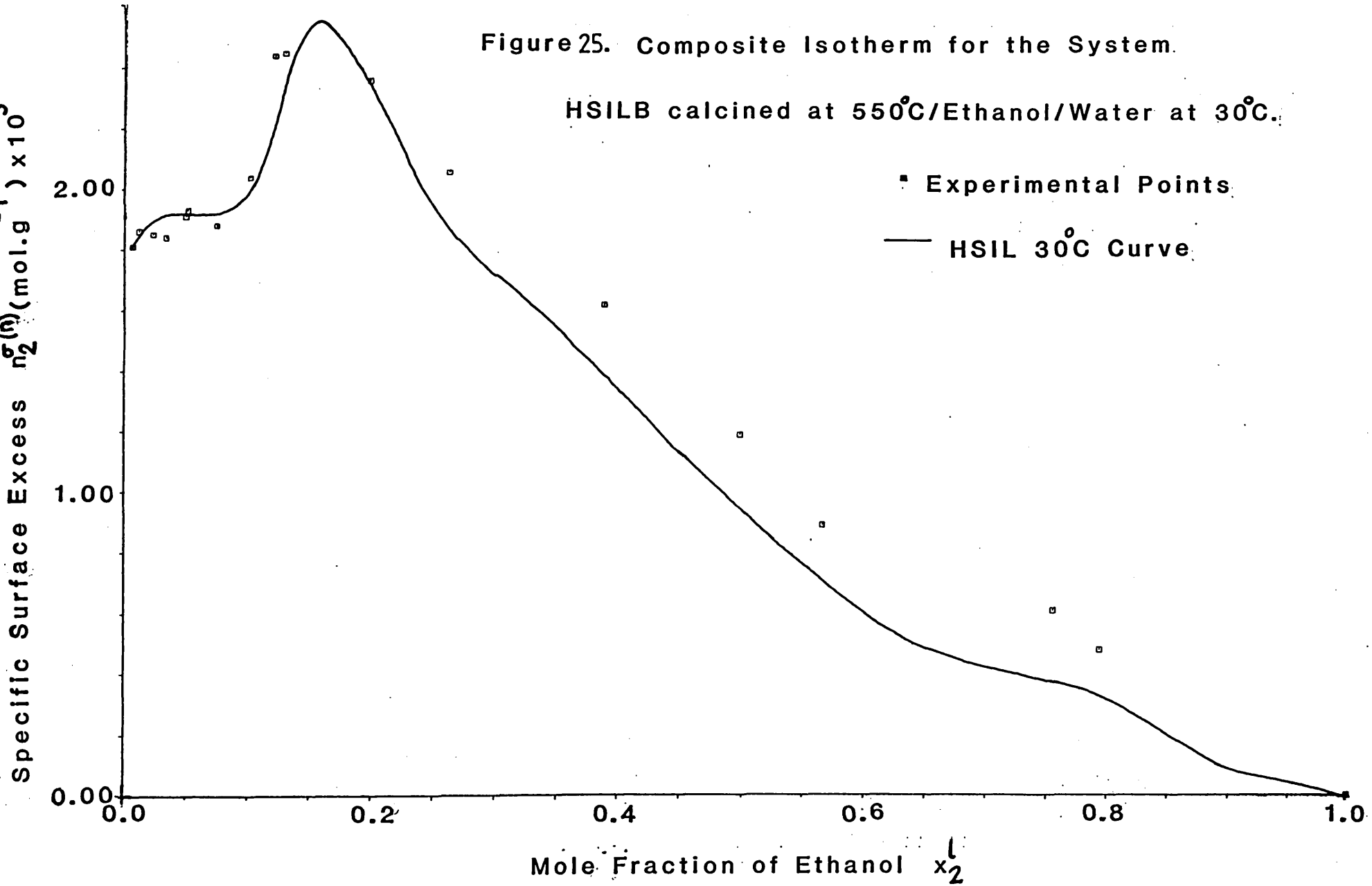

Figure 25. Composite Isotherm for the System HSILB calcined at 550°C/Ethanol/Water at 30°C.

▪ Experimental Points

—— HSIL 30°C Curve

within experimental error. This indicates that the presence of the shoulder in the isotherm is not due to differences between internal and external adsorption.

Isotherms for samples of HSILB calcined at higher temperatures of 670°C and 800°C were then determined. These experiments were performed to investigate whether the internal silanol groups present in silicalite-1 were the cause of the unusual isotherm features obtained. Internal silanol groups are thought to be removed by high temperature treatment[26].

The 30°C isotherm results for HSILB calcined at 670 and 800°C are shown in Figures 26 and 27 respectively, together with the 30°C HSIL isotherm curve.

The isotherms show no significant difference from the results either for the HSILB sample calcined at 550°C or for the HSIL sample. This indicates that the presence of internal silanol groups is not the cause of the behaviour observed.

It may be recalled from the introduction that study of the bulk thermodynamic properties (namely partial molar volume)[33] and n.m.r. studies[34] of ethanol - water solutions show anomalous behaviour in the region $x_2^1 < 0.08$, which coincides exactly with the region where the shoulder is observed in the isotherms obtained. Also, the temperature dependence of the behaviour of ethanol - water mixtures in this region of concentration shows a similar variation to that displayed by the shoulder in the isotherm, in that it is less apparent above 30°C. It seems therefore, in view of this and of the results of the above experiments, that this feature of ethanol - water liquid

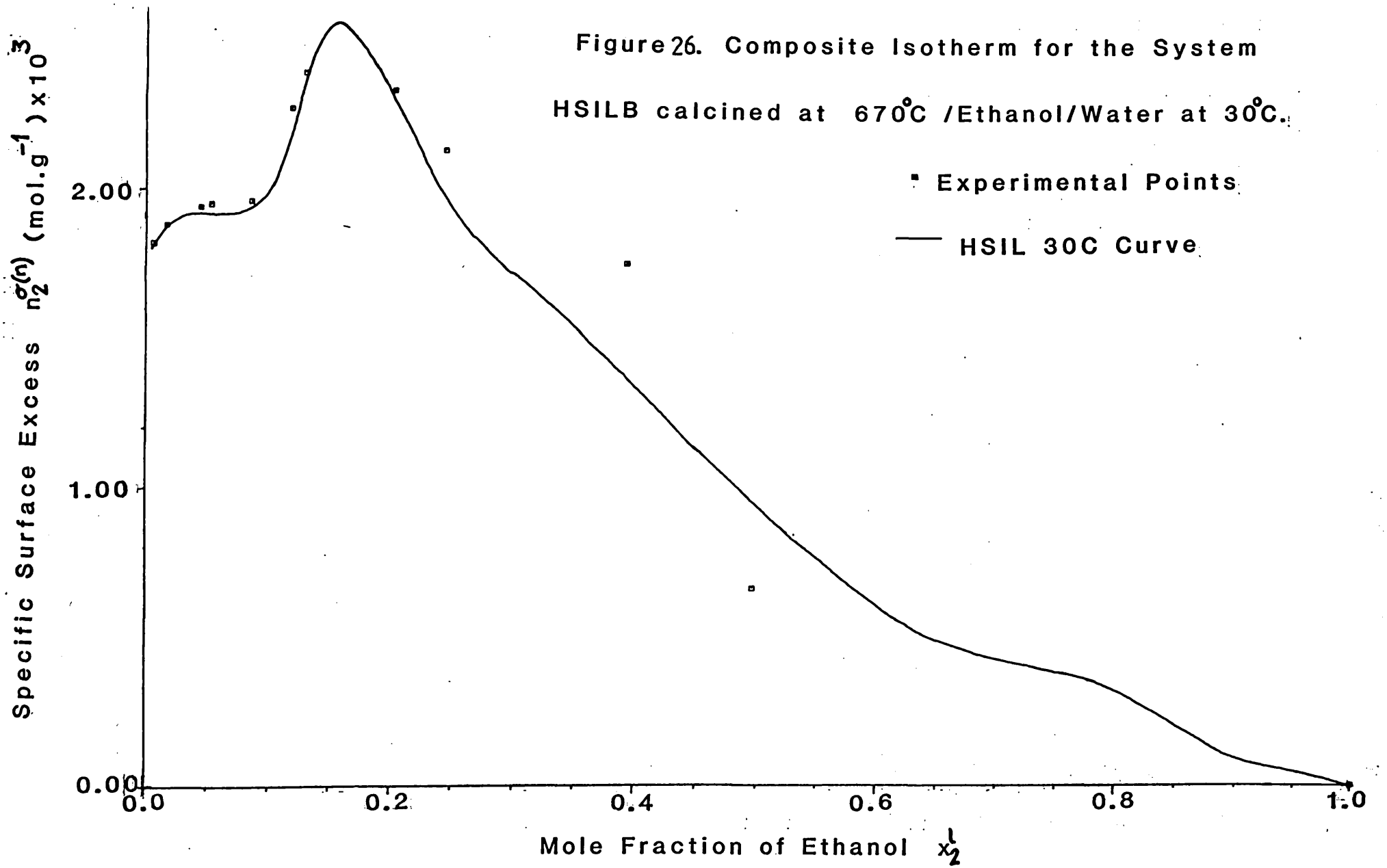

Figure 26. Composite Isotherm for the System HSILB calcined at 670°C /Ethanol/Water at 30°C.

▪ Experimental Points

—— HSIL 30C Curve

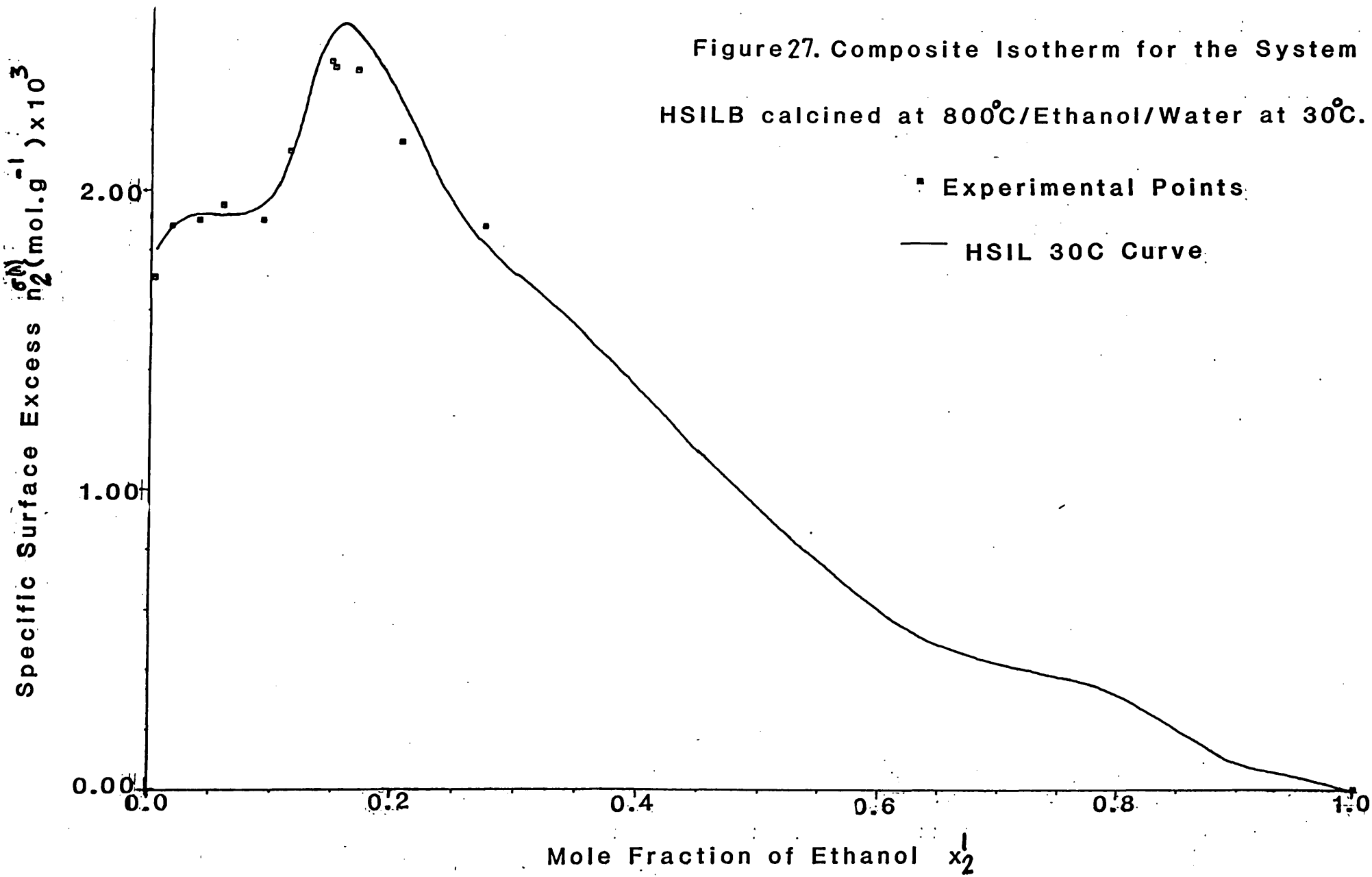

Figure 27. Composite Isotherm for the System HSILB calcined at 800°C/Ethanol/Water at 30°C.

▪ Experimental Points

—— HSIL 30C Curve

structure is responsible for the shoulder observed in the isotherms. If this is the case, then some variation in the isotherm should be detected at low mole fractions of ethanol irrespective of the adsorbent present.

Therefore, isotherm experiments were carried out on an activated carbon sample, concentrating on the low ethanol mole fraction region. The results for this 30°C activated carbon/ethanol/water isotherm are shown in Figure 28. A slight shoulder is observed in the isotherm with a point of inflection at $x_2^1 \approx 0.09$. It is concluded then, that the shoulder observed in the HSIL and HSILB isotherms is due to the structure of the bulk liquid ethanol - water mixture over this concentration range. This is further supported by the fact that most causes of sample heterogeneity, which might also explain the observation, have been dismissed in experiments described above. In addition, it may be recalled that T.G.A. indicated that the samples were homogeneous (see T.G.A. Results and Discussion, Section 5.1).

Models of the liquid structure in this concentration range propose that the ethanol has a structure promoting effect on the water clusters present. Since water molecules are then stabilised in solution, they are less likely to be adsorbed. The selectivity of the adsorbent for ethanol is consequently increased over what might be expected in this region of concentration, shown as a shoulder in the isotherm.

It may be noted that the strength of hydrogen bonds between molecules in the liquid mixture ($\approx$ 20 $kJ.mol^{-1}$) is of the same order of magnitude of the heats of adsorption of these species. Hence an explanation given in terms of the liquid structure is

Figure 28. Composite Isotherm for the System Activated Carbon/Ethanol/Water at 30°C.

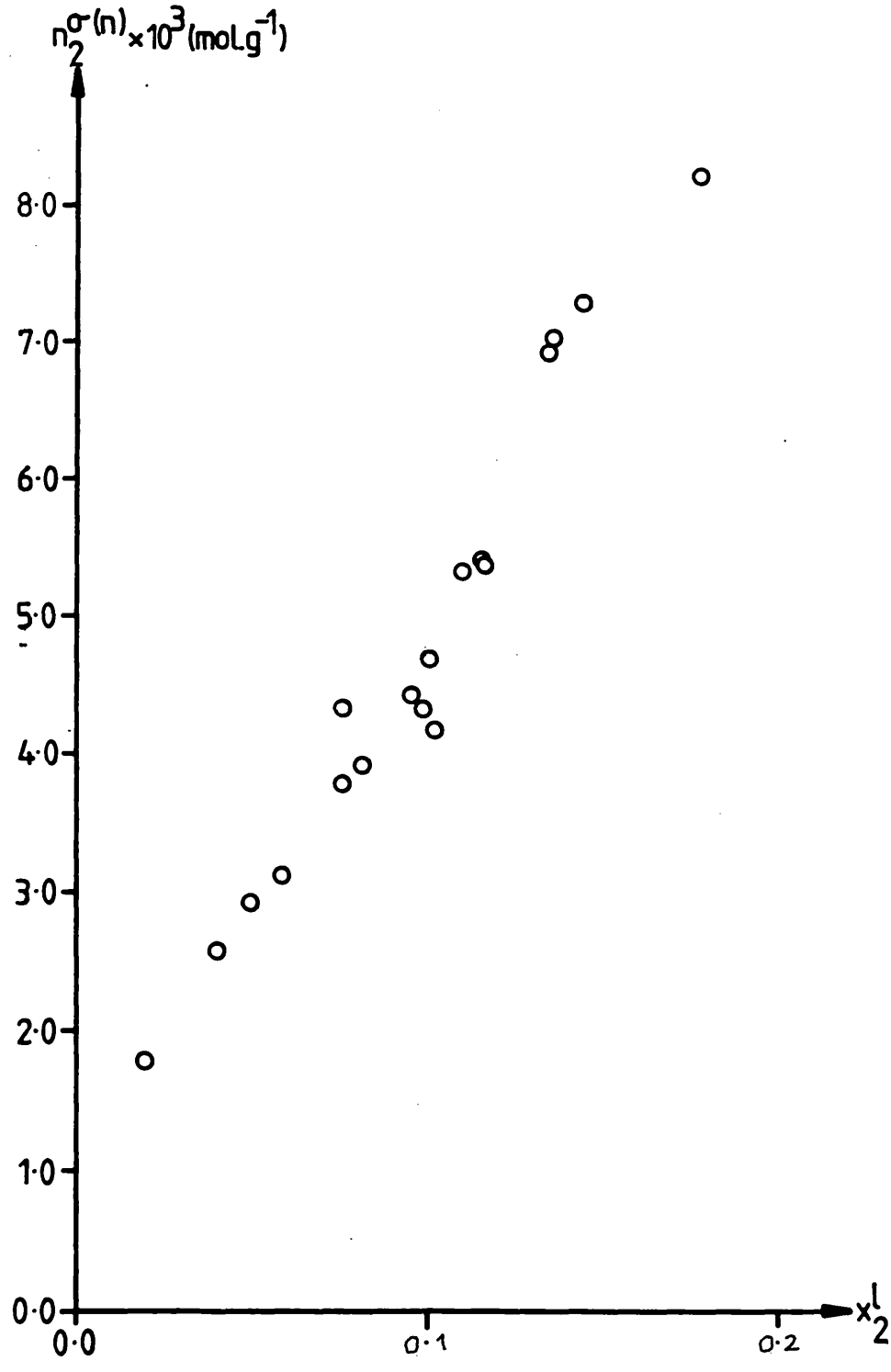

plausible.

It is proposed that this behaviour has gone unnoticed by other workers investigating adsorption from ethanol - water mixtures because the isotherm data produced were insufficiently detailed, especially in the low ethanol mole fraction region, to detect the features observed in this study. Most workers have taken 10-20 points over the whole concentration range to define the isotherm, whereas we have tended to take 7 or more points in the region $x_2^1 < 0.15$ alone, and up to 99 points over the whole concentration range.

It is conceivable that the behaviour observed may be explained in terms of changes in the adsorbate-adsorbate interactions. However, the supporting evidence offered by studies of the liquid mixture structure and by the results for the activated carbon sample make the explanation given above more likely.

Considering the small size of the adsorbate molecules relative to the channel dimensions, it is thought improbable that different types of adsorption in different regions of the channel structure is a plausible explanation of the results obtained.

At the present time we are unable to offer any explanation for the `knee' in the HSIL composite isotherms at high ethanol mole fractions. The same factors as those discussed above must be considered in developing such an explanation.

Experiments were also carried out on the samples NaZSM5/1 and NaZSM5/2 to determine the effect on the adsorption of higher aluminium content in the zeolite lattice. The results of these experiments are displayed in Figures 29 and 30 ,which show the

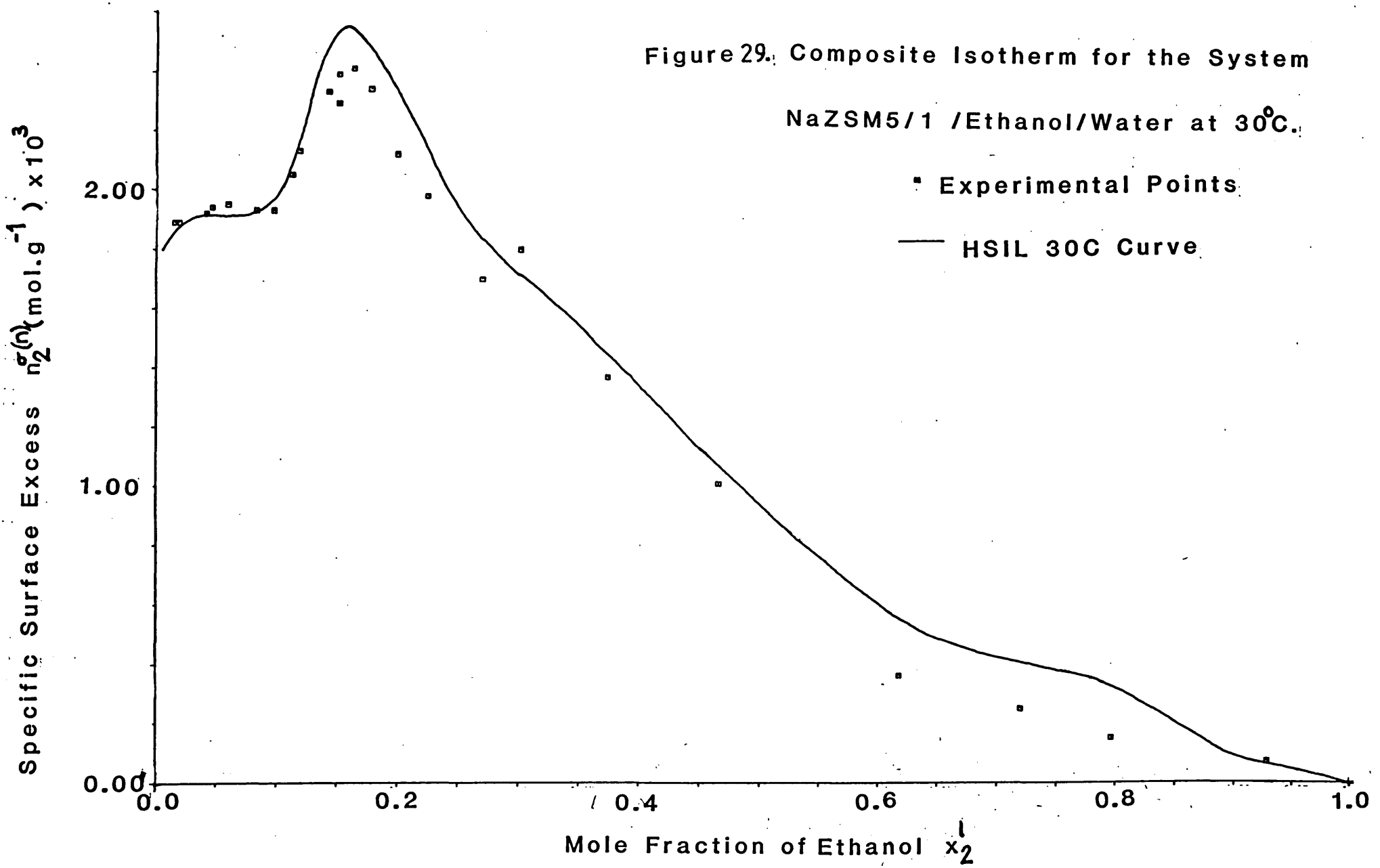

Figure 29. Composite Isotherm for the System NaZSM5/1 /Ethanol/Water at 30°C.

▪ Experimental Points

—— HSIL 30C Curve

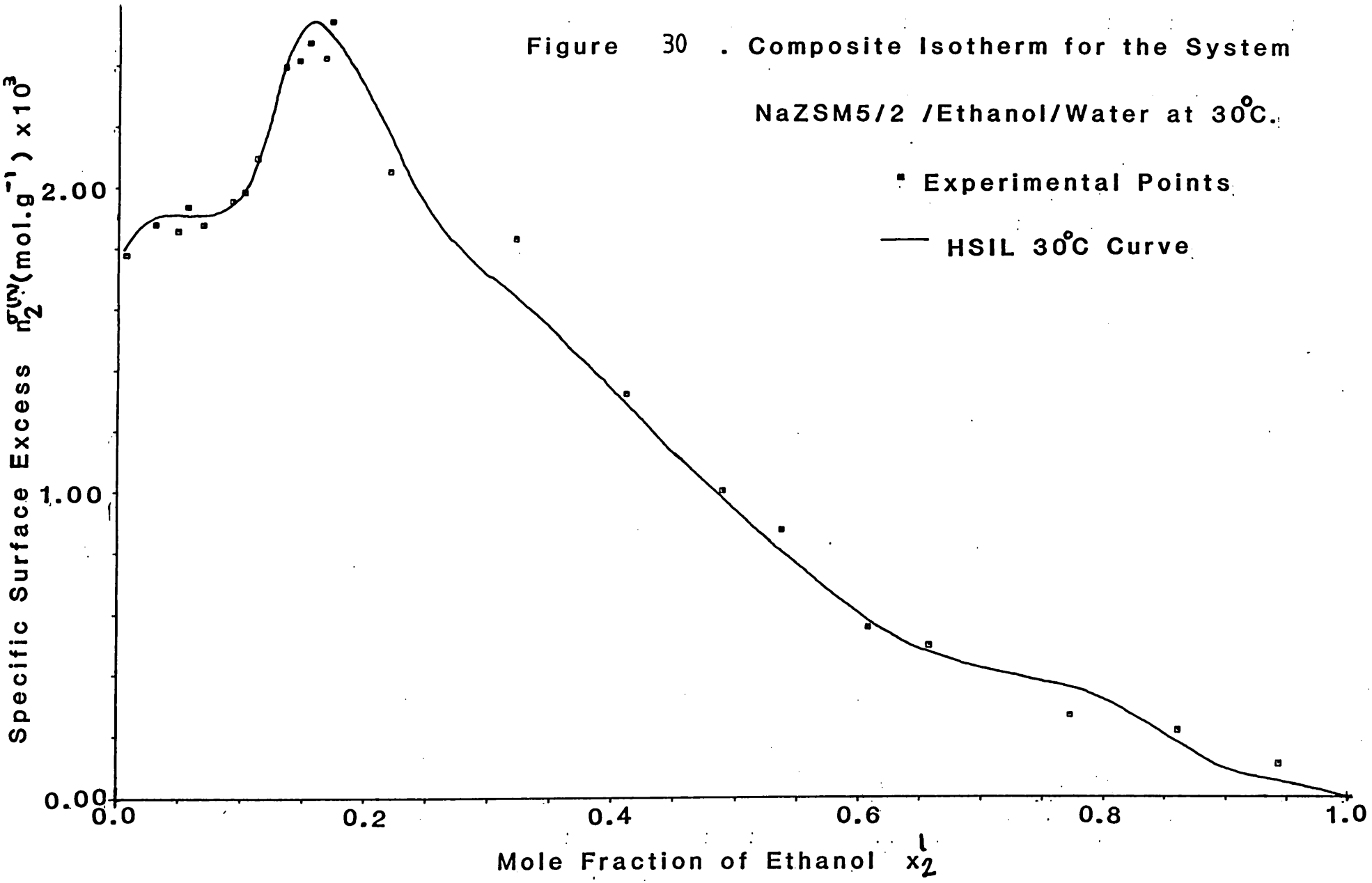

Figure 30 . Composite Isotherm for the System NaZSM5/2 /Ethanol/Water at 30°C.

▪ Experimental Points

—— HSIL 30°C Curve

30°C isotherms for NaZSM5/1 and NaZSM5/2 respectively. Experimental points are plotted with the 30°C HSIL isotherm curve for comparison. As may be seen from Figures 29 and 30 , the presence of small amounts of aluminium and sodium ions in the zeolite make very little difference to the adsorption isotherm. This is because the zeolite is essentially still hydrophobic at lower Si/Al ratios, displaying the same selectivity for ethanol. It is also interesting to note that the shoulder at low ethanol mole fraction observed with the samples HSIL and HSILB is still present in the isotherms of the samples NaZSM5/1 and NaZSM5/2. This seems to reinforce the explanation for this phenomenon given above.

5.4. Single Component Isotherms Results and Discussion.

Single component isotherms were calculated for ethanol and for water from the 20, 30 and 40^{o}C HSIL composite isotherms; from the 30^{o}C HSILB composite isotherm for the sample calcined at 550^{o}C; and from the NaZSM5/1 and NaZSM5/2 30^{o}C composite isotherms. Calculations were carried out according to the method described in the Theory section (Chapter 2 , equations (10), (11) and (12)). Initial calculations gave points where the mole fraction of ethanol in the surface phase exceeded unity, in all of these systems. The isotherms were then 'normalised' by taking the highest value of x_2^s and dividing all x_2^s values by that number. x_1^s was then recalculated. These 'normalised' single component isotherms are shown in Figures 31-36. Table 6 shows the normalisation factor used in each case .

Considering the 20, 30 and 40^{o}C HSIL single component isotherms (Figures 31, 32 and 33 respectively), both sets of isotherms (those for ethanol and those for water) are very similar to those at other temperatures. These similarities are to be expected, since the composite isotherms from which the single component isotherms are calculated are also similar.

Just as the composite isotherms deviate from the usual 'U' shape, so do the single component isotherms deviate from the expected shape (see Figure 5). The ethanol single component isotherms show a shoulder at low concentrations of ethanol in the liquid followed by an increase in x_2^s. However, the isotherms show a peak, then decrease to a minimum. This behaviour cannot be predicted from simple examination of the composite isotherm. It may be an artefact of the method of calculation rather than due

Figure 31 . Single Component Isotherms for the System HSIL/Ethanol/Water at 20°C.

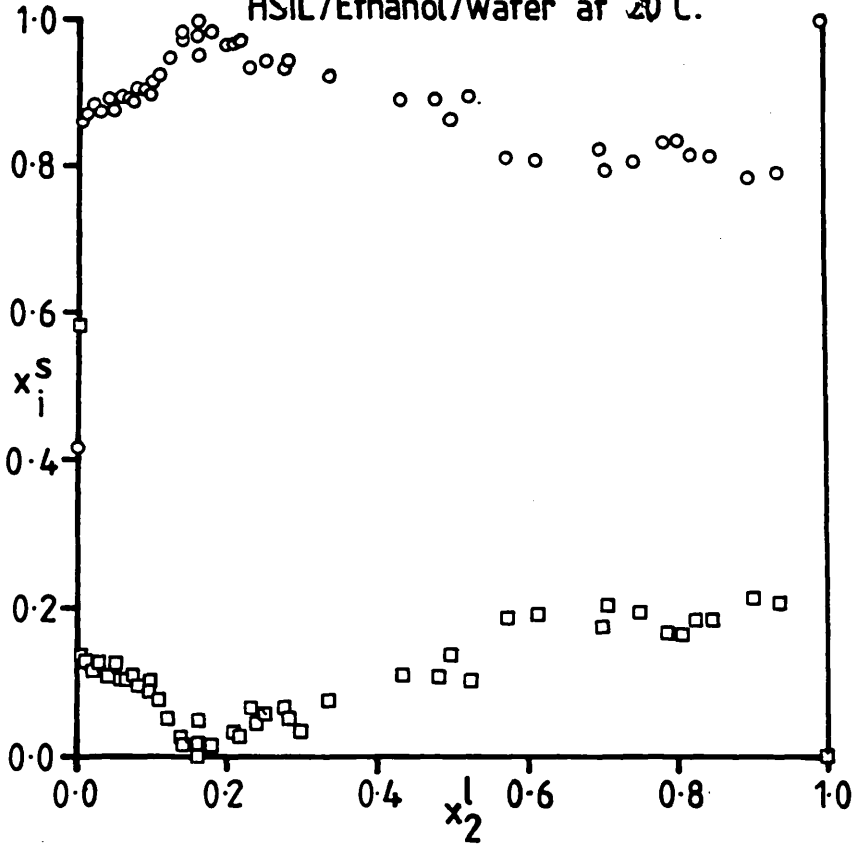

Figure 32. Single Component Isotherms for the System HSIL/Ethanol/Water at 30°C.

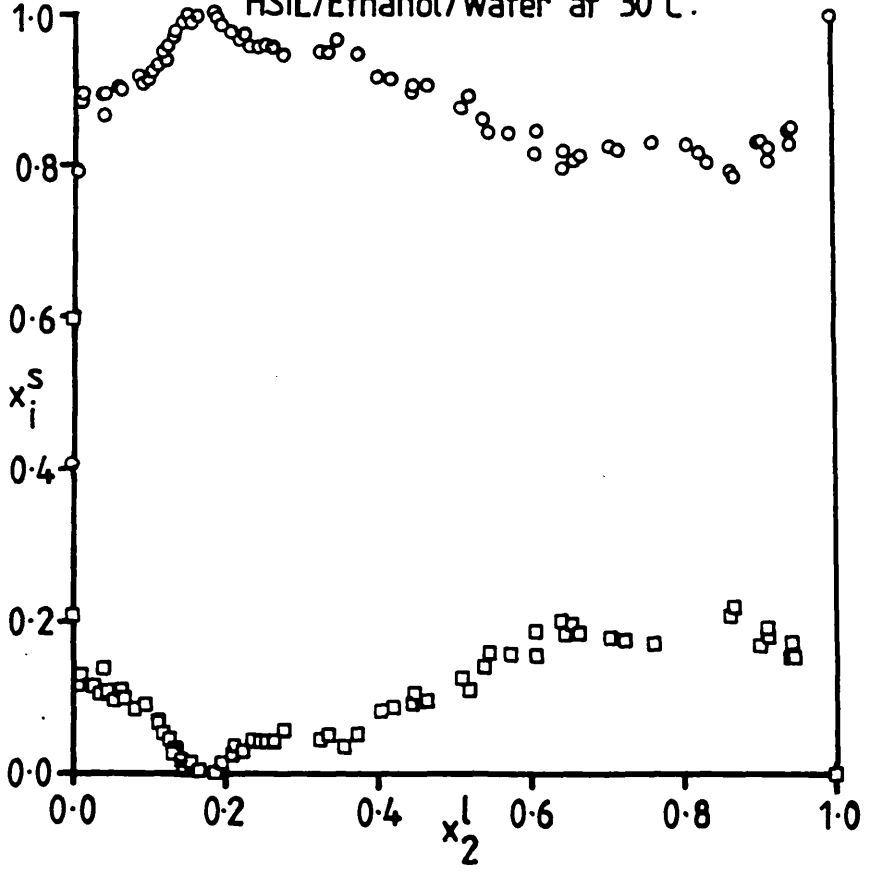

Key: ○ Ethanol , □ Water .

Figure 33. Single Component Isotherms for the System HSIL/Ethanol/Water at 40°C.

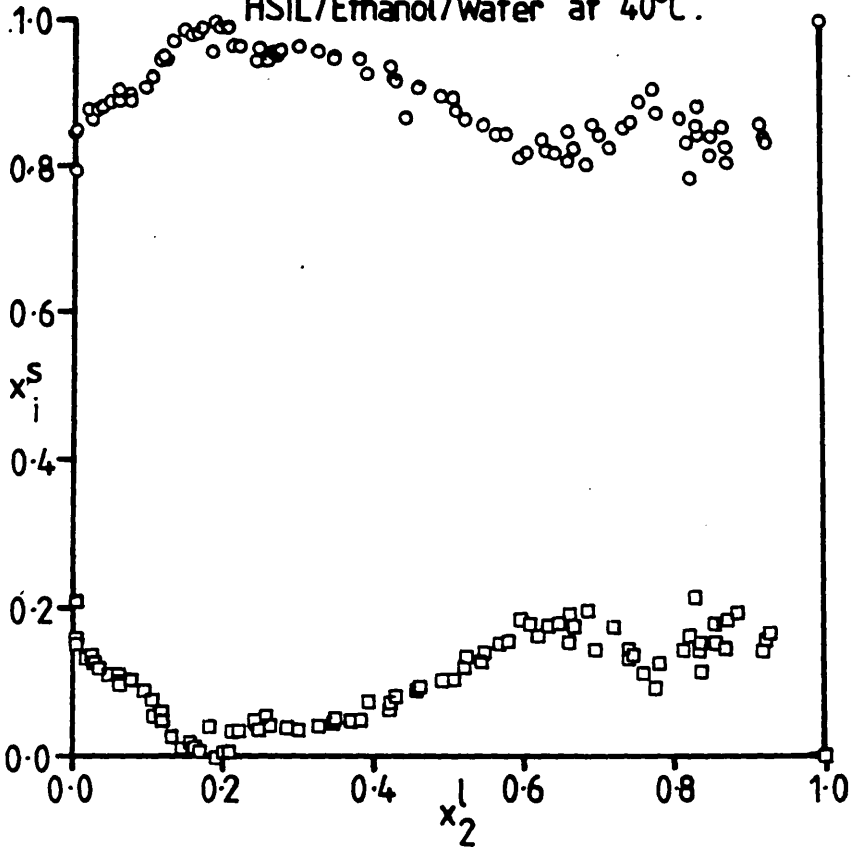

Figure 34. Single Component Isotherms for the System HSILB/Ethanol/Water at 30°C.

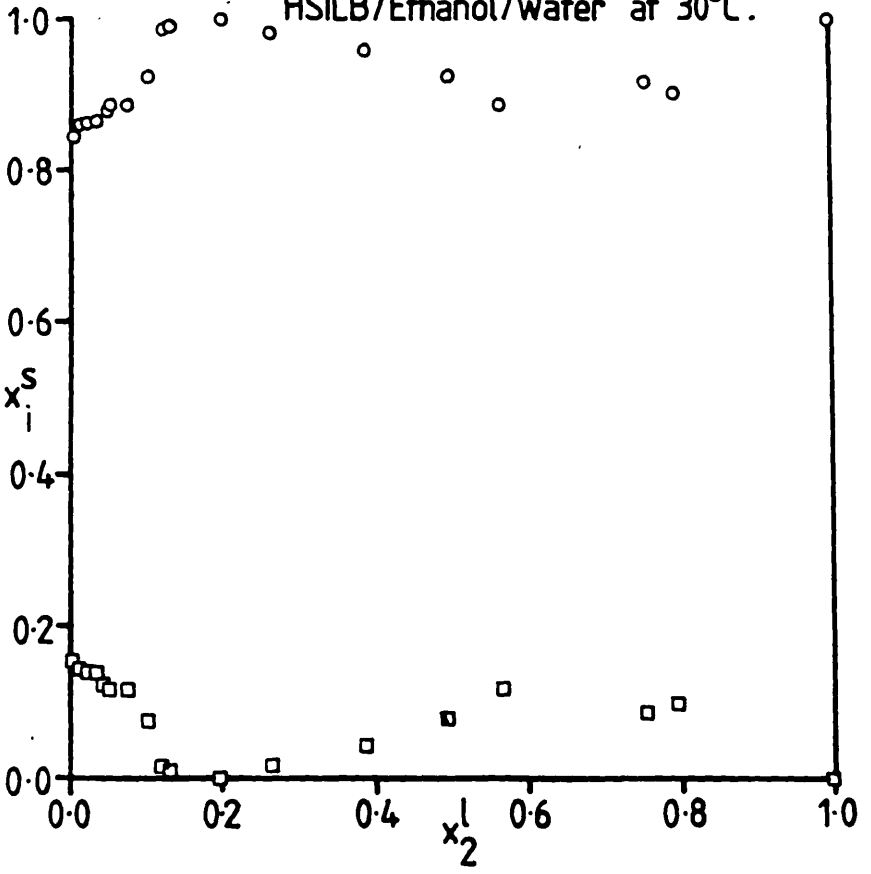

Figure 35. Single Component Isotherms for the System NaZSM5/1/Ethanol/Water at 30°C.

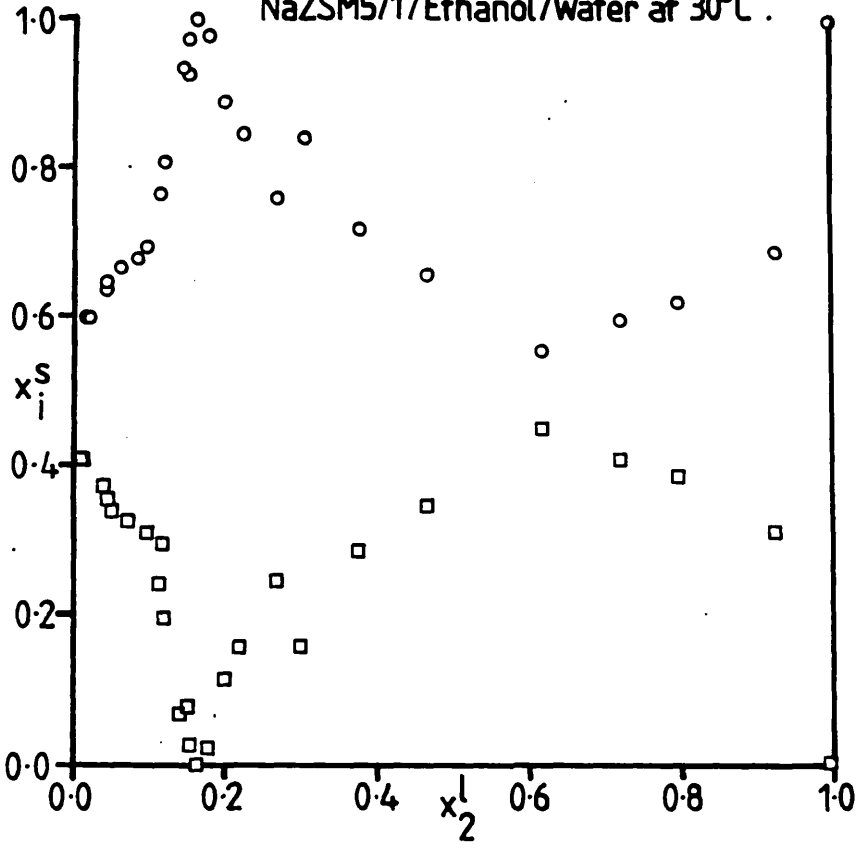

Figure 36. Single Component Isotherms for the System NaZSM5/2/Ethanol/Water at 30°C.

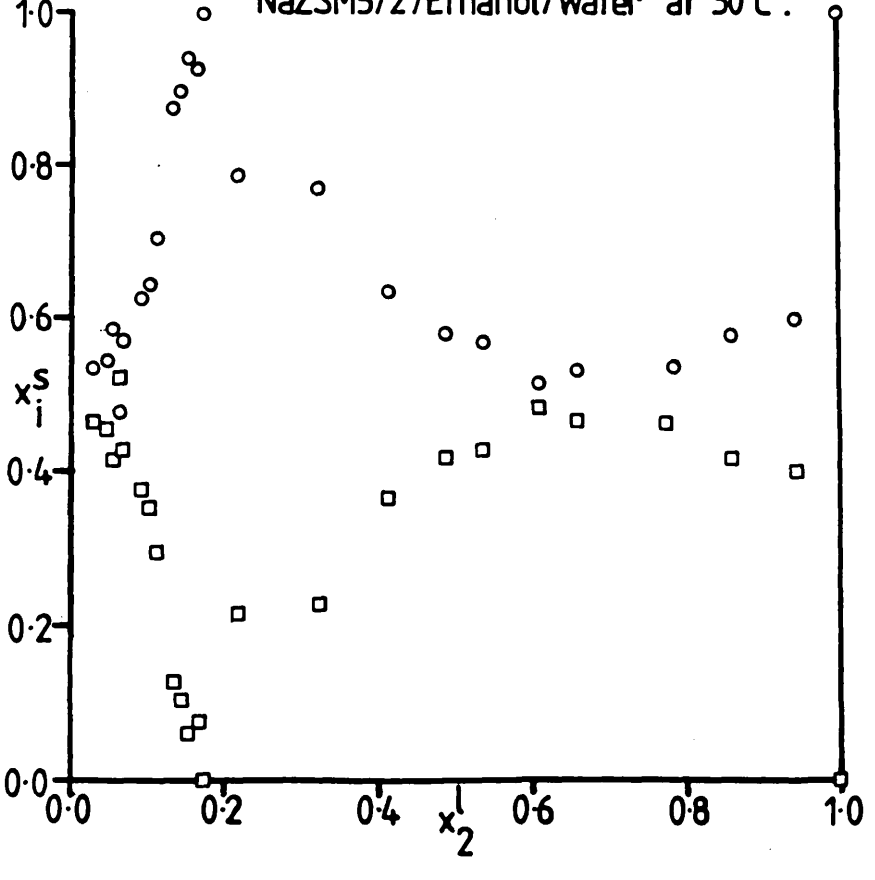

Table 6. Normalisation Factors used in Calculating Single Component Isotherms.

System	Normalisation Factor
HSIL/Ethanol/Water at 20°C	1·2175
HSIL/Ethanol/Water at 30°C	1·2034
HSIL/Ethanol/Water at 40°C	1·2147
HSILB/Ethanol/Water at 30°C	1·1386
NaZSM5/1/Ethanol/Water 30°C	1·3930
NaZSM5/2/Ethanol/Water 30°C	1·6622

to real changes in the system. The fact that the isotherms required normalising also indicates that the method of calculation employed is unreliable. It is possible that assumptions made in the calculation are invalid.

Firstly, it may be that the adsorption capacities calculated from T.G.A., from vapour phase adsorption, differ from the real adsorption capacity when adsorption takes place from the liquid.

Secondly, the assumption that the pore volume of the zeolite occupied by adsorbate remains constant at all concentrations of adsorbate may be invalid.

Therefore, it is difficult to discern whether unusual behaviour in the single component isotherms is due to real changes in the system or to the unsuitability of the treatment applied, where this behaviour does not correspond to behaviour observed in the composite isotherm . Hence no firm conclusions can be drawn from these single component isotherms. It may only be said that the concentration of ethanol in the adsorbed phase appears high, especially at the point corresponding to the peak in the composite isotherm. Here, x_2^s probably exceeds 0.90. This agrees with the observations of other workers[58].

The single component isotherms for the HSILB sample are similar to those for the HSIL sample, which is again to be expected since the composite isotherms are similar and it is difficult to draw any firm conclusions from these isotherms.

For the NaZSM5/1 and NaZSM5/2 samples, the main features seen in the cases of the HSIL and HSILB samples are present, but are more exaggerated. This suggests that either the treatment used is even

less applicable to these systems, or that the presence of aluminium in the structure is having some effect on the shape of the single component isotherms. The ZSM5 zeolites, being more hydrophilic, are likely to adsorb more water than the silicalite-1 samples. This results in a deeper minimum in the ethanol single component isotherm with zeolites of lower Si/Al.

To summarise, then, the single component isotherm results are mostly inconclusive, because the applicability of the treatment used in calculating them is questionable and because of a lack of a means of direct observation of changes in the composition of the surface phase.

It may be recalled from the Theory section, Chapter 2, equation (18), that:

$$K = \frac{x_2^s x_1^l}{x_2^l x_1^s}$$

Values of K were calculated, using the known x_1^l and x_2^l values, and the x_1^s and x_2^s values calculated above. The resulting K values are plotted against x_2^l for each of the systems for which single component isotherms were obtained. These plots are displayed in Figures 37-42. Since the single component isotherms are in doubt, so must the K values calculated from them. Hence it can only be said that, in all of these systems, the value of K is very high (the calculated value being infinite) at the point corresponding to the peak in the composite isotherm. This indicates very strong selectivity for ethanol.

It may also be noted that the K values for the ZSM5 sample are generally lower than those of the silicalite-1 samples,

Figure 37. Graph of $\log_{10}$ of Separation Factor (K) against Mole Fraction of Ethanol in the Liquid (x_2^L) for the System

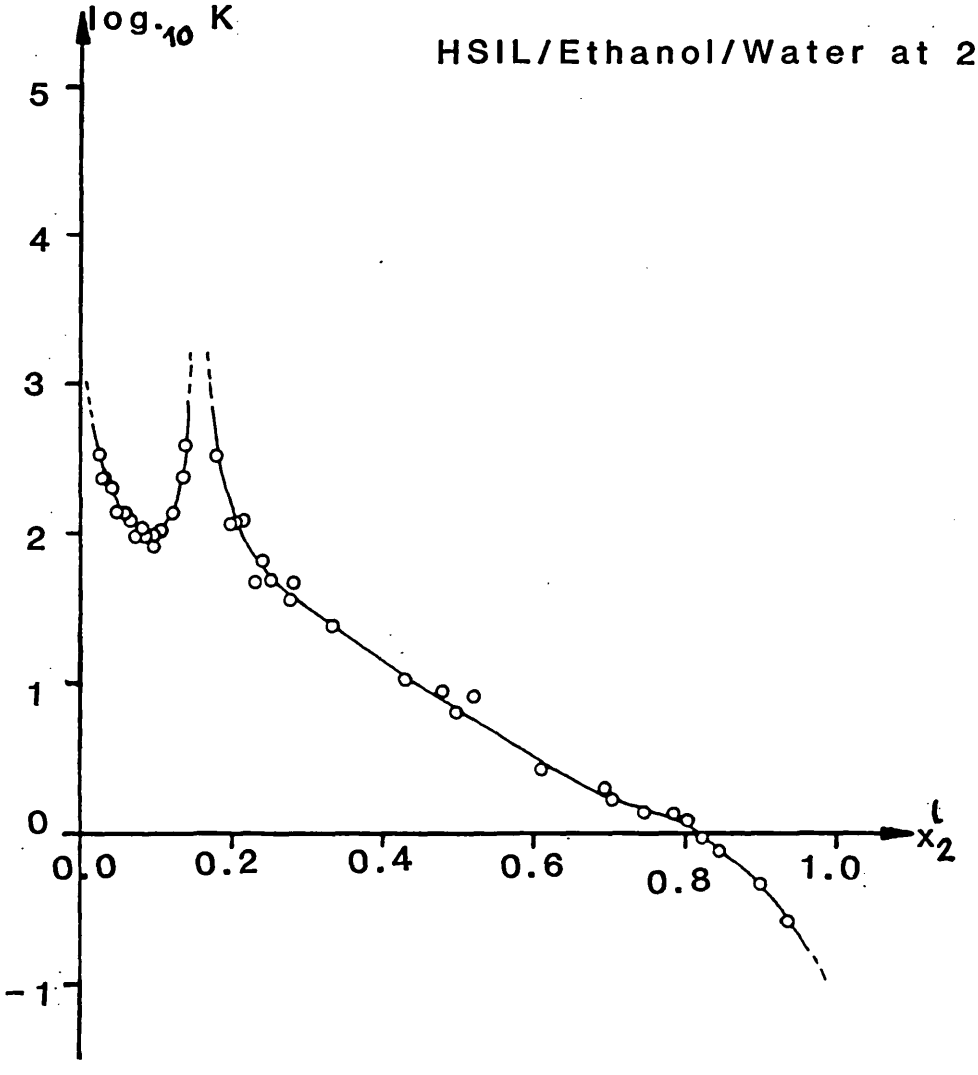

Figure 38. Graph of $\log_{10}$ of Separation Factor (K) against Mole Fraction of Ethanol in the Liquid (x_2^l) for the System

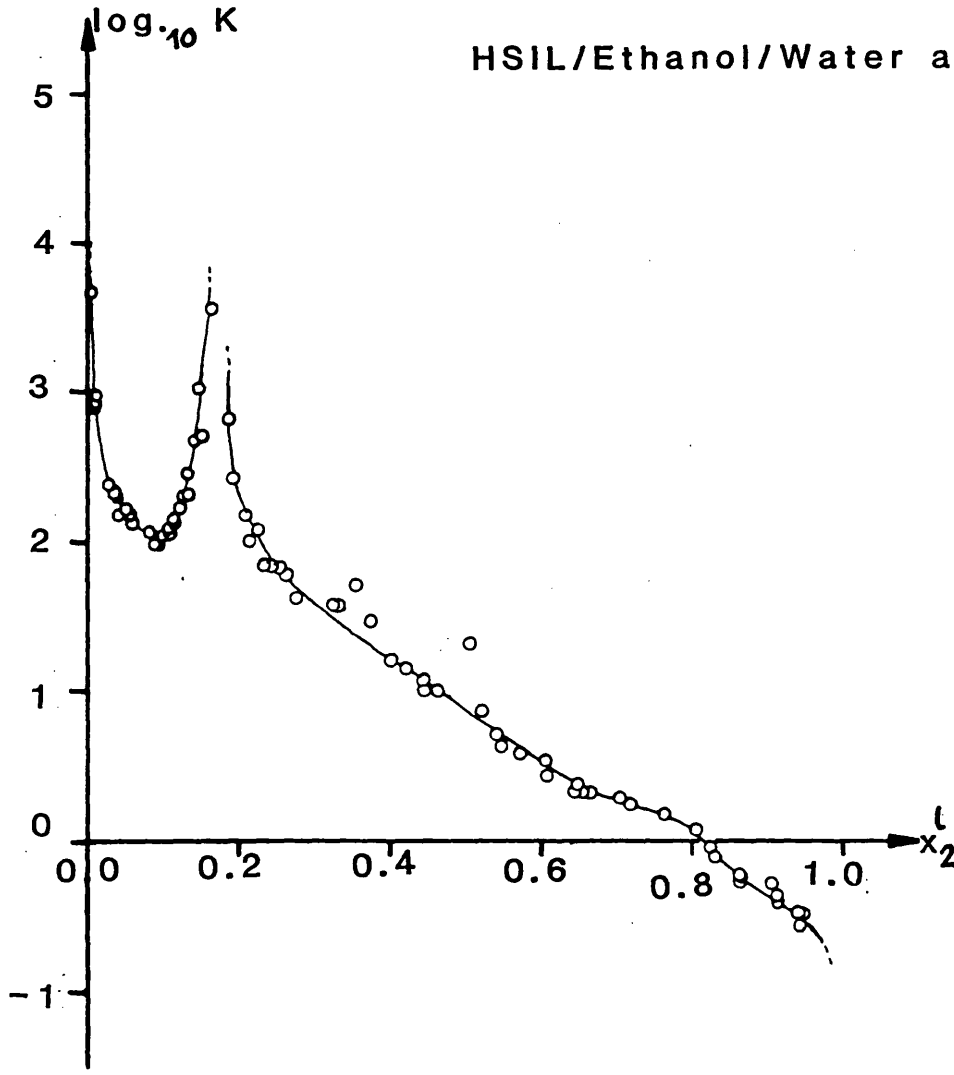

Figure 39. Graph of $\log_{10}$ of Separation Factor (K) against Mole Fraction of Ethanol in the Liquid (x_2^L) for the System

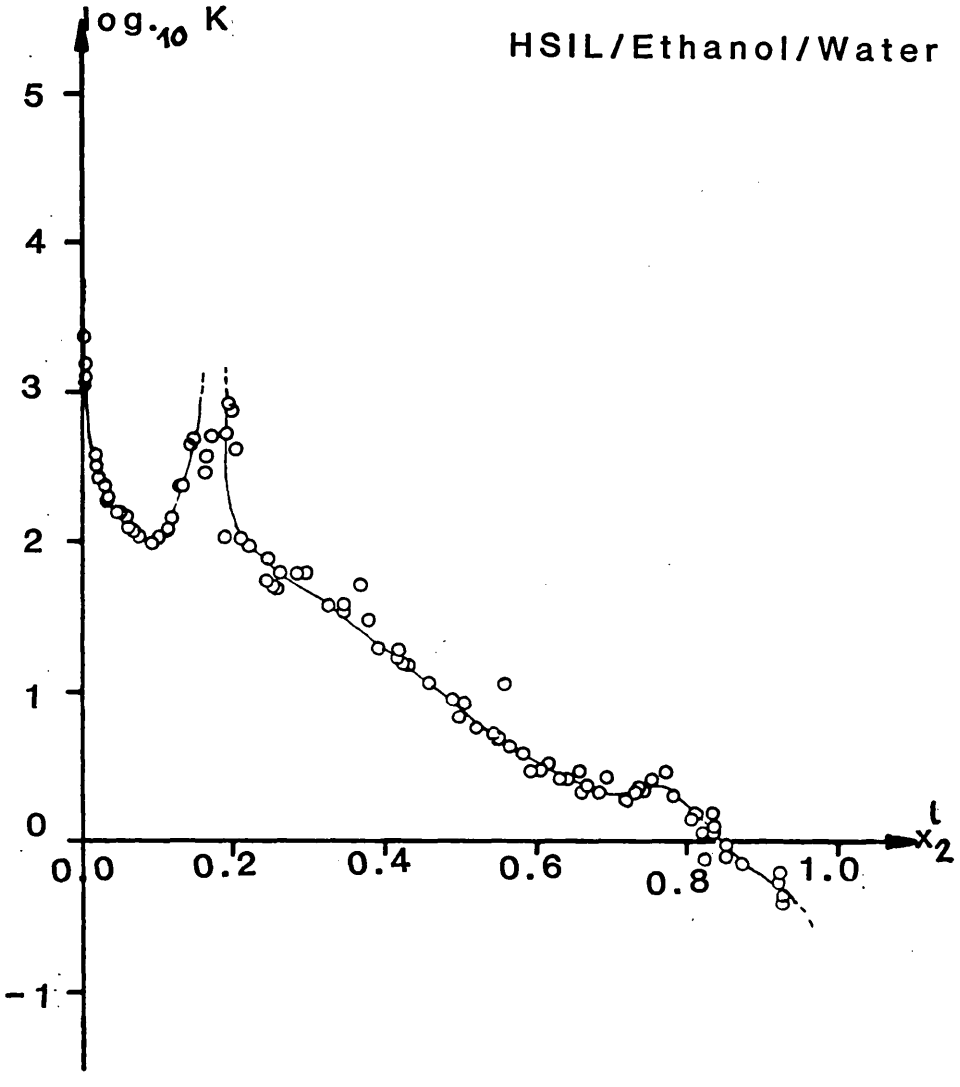

Figure 40. Graph of $\log_{10}$ of Separation Factor (K) against Mole Fraction of Ethanol in the Liquid (x_2^l) for the System

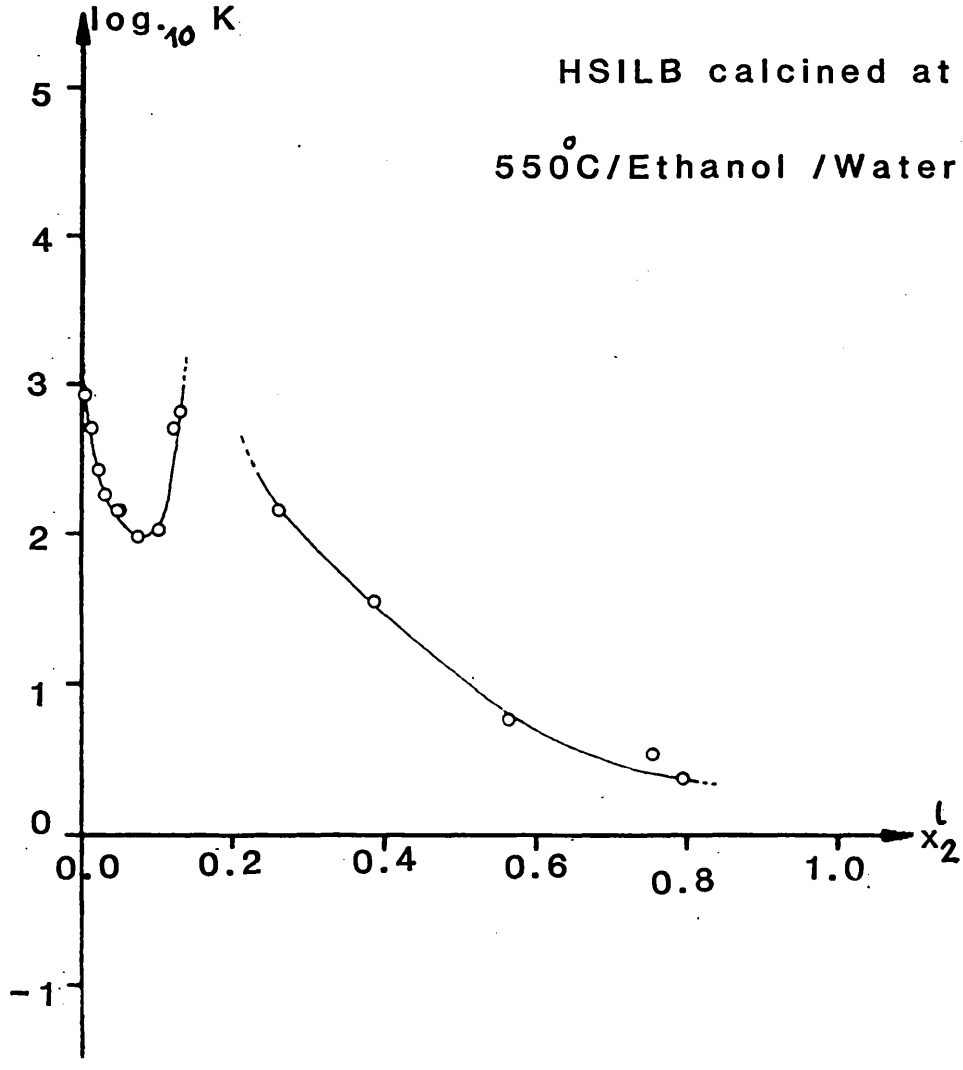

Figure 41 . Graph of $\log_{10}$ of Separation Factor (K) against Mole Fraction of Ethanol in the Liquid (x_2^l) for the System

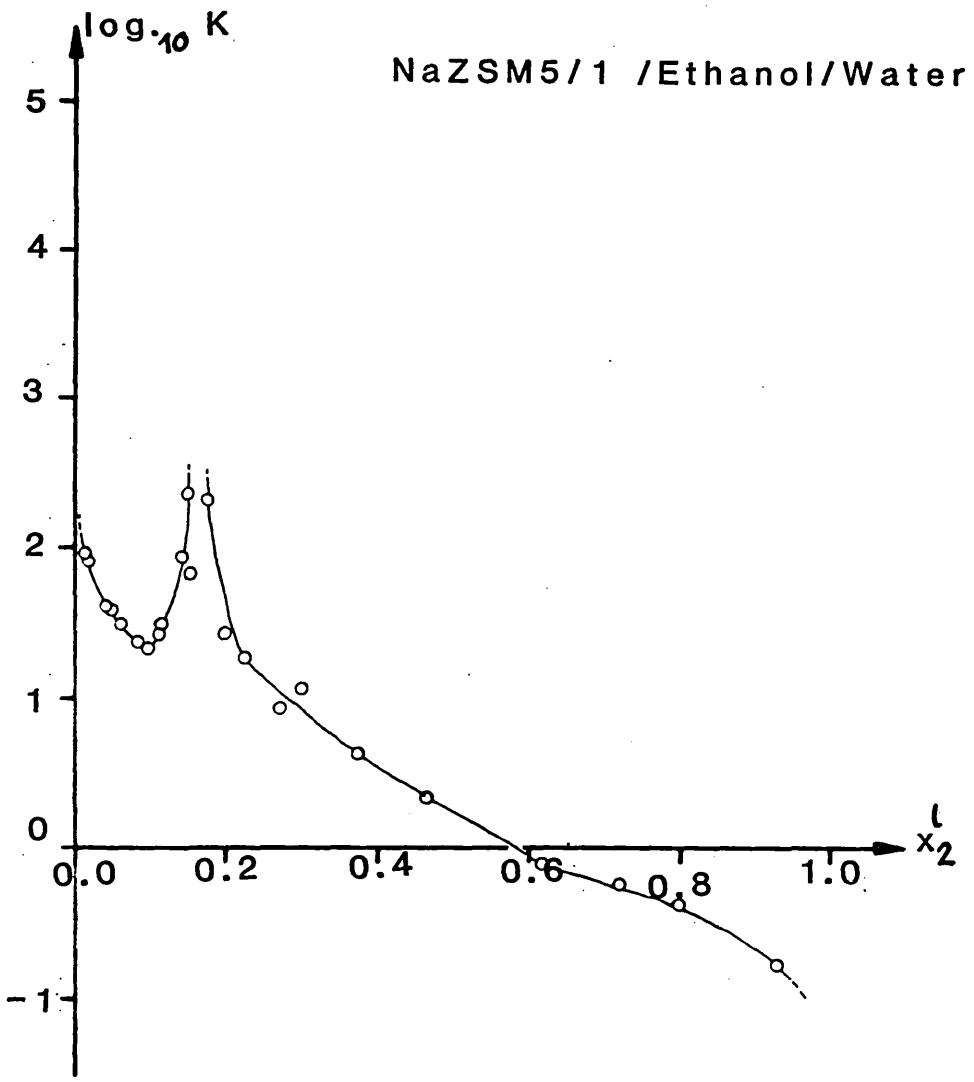

Figure 42. Graph of $\log_{10}$ of Separation Factor (K) against Mole Fraction of Ethanol in the Liquid (x_2^L) for the System

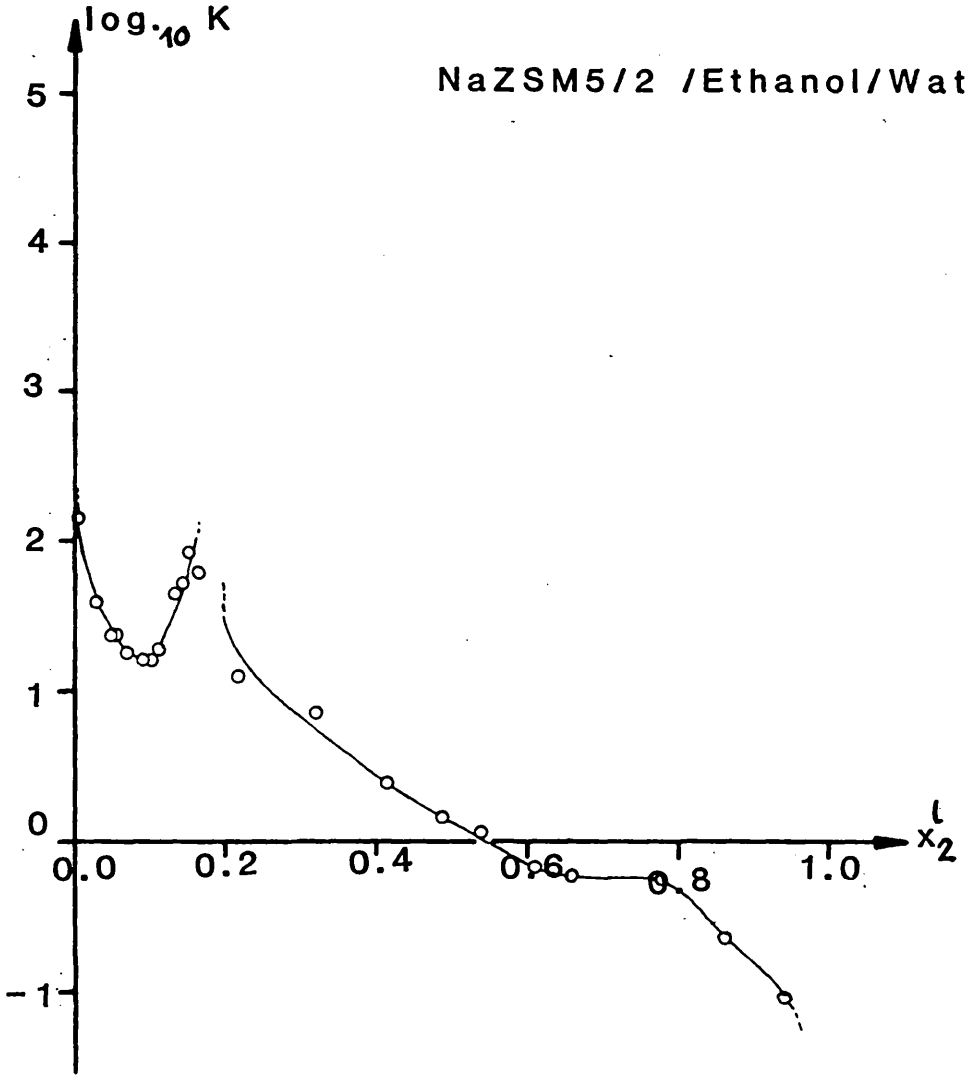

indicating that the increased aluminium content of the ZSM5 samples has reduced their selectivity. This is again explained by the greater hydrophilicity of these zeolites relative to silicalite-1. More water is adsorbed, resulting in a lower selectivity for ethanol.

5.5. Analysis of Linear Isotherm Sections.

The HSIL 20, 30, 40°C isotherms; NaZSM5/1 and NaZSM5/2 30°C isotherms all showed linear sections approximately in the region $0.2<x_2^l<0.6$. In the case of the 30°C isotherm for the HSILB sample calcined at 550°C, there were insufficient points in this region to determine whether the isotherm was linear or not.

A least squares fit was carried out on the points in the linear region, using the computer programme LINREG (see Appendix 3). From the fitted line, the $n_2^{\sigma(n)}$ values at $x_2^l=0$ and at $x_2^l=1$ were calculated. It may be recalled from the theory section (see Chapter 2, section 2.3) that these $n_2^{\sigma(n)}$ values correspond to those of $(n_1^s)_c$ and $(n_2^s)_c$ respectively, according to Schay and Nagy.[48] The mole fraction of ethanol in the surface phase in this region may then be calculated from:

$$x_2^s = \frac{(n_2^s)_c}{(n_1^s)_c + (n_2^s)_c}$$

Table 7 shows the correlation coefficients (R),gradients (a), $(n_1^s)_c$, $(n_2^s)_c$, x_2^s and t values obtained from the fitted lines. For these porous adsorbents, t may be taken to represent the proportion of pore volume occupied by the adsorbates relative to the single component adsorption capacities determined by T.G.A. .

The calculated lines had correlation coefficients of 0.97 or greater, indicating that the experimental points fitted at least fairly well to straight lines.

Considering the linear sections of the HSIL 20, 30 and 40°C isotherms, the lines fitted to the 20 and 30°C points are similar, as indicated by their similar gradients and intercepts.

Table 7. Results of Analysis of Linear Isotherm Sections.

Isotherm	R	$a\,(mol.g^{-1}\times10^{3})$	$(n_1^s)_c$ $(mol.g^{-1}\times10^{3})$	$(n_2^s)_c$ $(mol.g^{-1}\times10^{3})$	x_2^s	t
HSIL 20°C	0·9713	-3·601	0·7880	2·813	0·7812	3·071
HSIL 30°C	0·9849	-3·712	0·8240	2·888	0·7780	3·178
HSIL 40°C	0·9919	-4·728	1·511	3·217	0·6804	4·529
NaZSM5/1 30°C	0·9852	-4·101	1·189	2·912	0·7101	1·638
NaZSM5/2 30°C	0·9857	-3·841	0·8940	2·947	0·7672	1·683

For explanation of symbols please see text.

However, the line fitted to the 40°C points is significantly different. This indicates that change in the system occurs in this region of concentration at temperatures above 30°C.

In all three cases, the value of x_2^s calculated did not agree with x_2^s values taken from the corresponding region on the calculated single component isotherms.

Also, the calculated t values considerably exceeded 1, indicating that the pore volume occupied by the adsorbates in this region is greater than the volume occupied by the single components. However, it may simply be that these systems fail to meet the conditions necessary for the Schay and Nagy treatment to remain valid (see Theory, Chapter 2 , section 2.3). These conditions place great restrictions upon the way in which bulk and surface phase activity coefficients must vary for the treatment to be applicable.

The NaZSM5/1 and NaZSM5/2 lines are reasonably similar to the HSIL 30°C line. However, the ZSM5 samples show markedly different t values to those obtained for HSIL. It is thought that this is due to the greater adsorption capacities of the ZSM5 samples for both water and ethanol.

Since the calculated values of t are so much greater than unity, especially in the case of the HSIL sample, and since, according to Kipling et al. the conditions required for the Schay and Nagy treatment to apply are unlikely to be met in real systems, it seems that the presence of these linear or near-linear isotherm sections is not due to a constant composition of the adsorbed phase. One of the alternative explanations offered by Kipling et al. may then be preferred (see Theory, Chapter 2, section 2.3)

although it is not possible to say which, if any, is correct. These alternatives postulate that the linear region in the composite isotherm is either due to the combination of two linear, parallel single component isotherms, or to the combination of two single component isotherms which are near-linear.

To summarise, the HSIL 20, 30, 40^{o}C and the NaZSM5/1 and NaZSM5/2 30^{o}c isotherms show definite linear sections. However, the presence of these linear regions is not thought to be due to a constant composition of the adsorbed phase.

Incidentally, this conclusion appears to support the results of the single component isotherm calculations. In all of the systems where single component isotherms were obtained, the composition of the surface phase in the region corresponding to the linear sections of the composite isotherms was not found to be constant. In the case of the HSIL 30^{o}C ethanol single component isotherm, for example, a decrease in the mole fraction of ethanol in the surface phase was observed after the peak at $x_2^1 \approx 0.15$. Originally, it was uncertain as to whether this behaviour was real or an artefact. Now, with the support of the conclusion above, the single component isotherms appear more reliable, at least qualitatively. Therefore, some explanation of the unusual shape of the single component isotherms is required. It is proposed that the observation, in all of the ethanol single component isotherms, of a minimum following the initial peak at $x_2^1 \approx 0.16$ may be explained the following way: Once the zeolite has become saturated with ethanol, the -OH groups of the adsorbed

ethanol molecules provide adsorption 'sites' for water molecules. Also, since the ice-like clusters which made it more thermodynamically favourable for water to remain in solution are, in this region of composition, becoming disrupted by the incorporation of ethanol molecules, it is now possible for significant adsorption of water to occur. The concentration of water in the adsorbed phase then increases, decreasing the concentration of ethanol in the adsorbed phase. This accounts for the decrease seen in the single component isotherms after the initial peak. This effect is more marked with the ZSM5 adsorbents (see Figures 35 and 36). Here, the presence of aluminium in the lattice increases the hydrophilicity of the zeolite. Hence water is more likely to be adsorbed in any case.

As the concentration of alcohol in the liquid phase is further increased, it simply becomes more probable that ethanol alone will be adsorbed. Hence the concentration of ethanol in the adsorbed phase rises once more.

It is suggested that the initial peak in the single component isotherms occuring at $x_2^1 \approx 0.16$ is the result of competition between the selectivity of the adsorbent and the increasing significance of the effects described above. At concentrations above $x_2^1 \approx 0.16$, the adsorption of water onto the loaded zeolite begins to dominate. Below $x_2^1 \approx 0.16$ the selectivity of the adsorbent for ethanol dominates.

The linearity of the composite isotherms then arises from the combination of two curved single component isotherms (note that this does not correspond with any of the explanations offered by Schay and Nagy[48] or by Kipling et al.[50]).

5.6. Ideal System Model Results and Discussion.

The suitability of the Ideal System approach to each of the systems 20, 30 and 40°C HSIL, 30°C HSILB, 30°C NaZSM5/1 and NaZSM5/2 with ethanol and water was tested using equation (19) (see Theory, Chapter 2 , section 2.4). The left hand side of this equation,

$$\frac{x_1^1 x_2^1}{n_2^{\sigma(n)}} = \frac{1}{n_s} x_2^1 + \frac{1}{(K-1)}$$

was calculated from experimental data and plotted against x_2^1. The resulting plots are shown in Figures 43-48. According to the Ideal System treatment, these plots should be linear. Examination of Figures 43-48 reveals that, for the systyems studied, this is not the case. The calculated points deviate considerably from linearity, especially at high alcohol concentrations. Hence the unsuitability of this treatment for these systems is demonstrated.

It is proposed that the Ideal System approach fails because in these cases the assumptions underlying the treatment are invalid.

Firstly, the assumption that both ethanol and water occupy the same area on the adsorbent surface is unlikely to be valid.

Secondly, in the case of ethanol - water mixtures, the liquid phase fails to follow ideal behaviour.

In short, the Ideal System treatment fails because the systems studied deviate strongly from ideality.

Figure 43. Graph of $\frac{x_2^l x_1^l}{n_2^{\sigma(n)}}$ against Mole Fraction of Ethanol in the Liquid (x_2^l) for the System

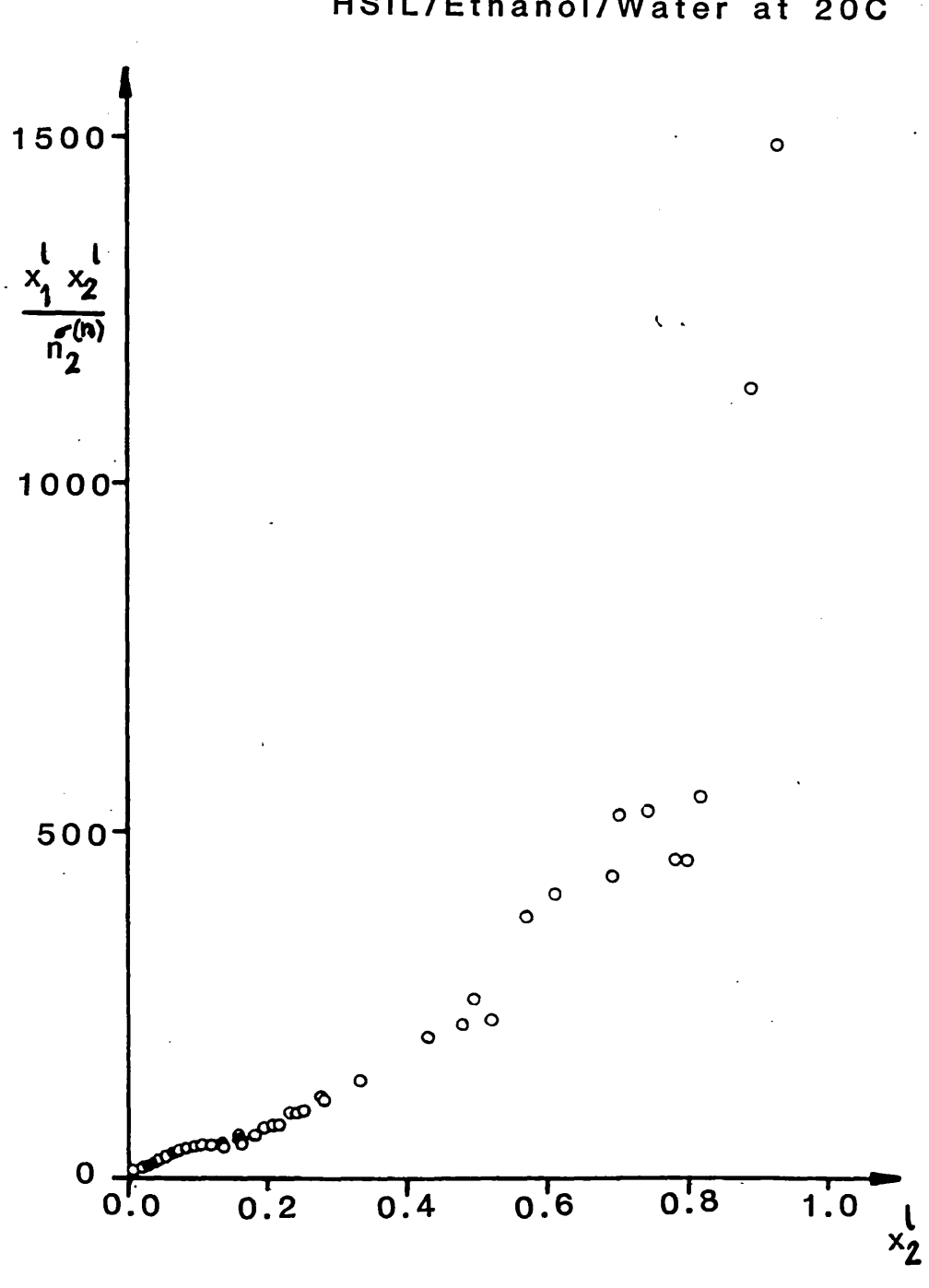

Figure 44. Graph of $\frac{x_2^l x_1^l}{n_2^{\sigma(n)}}$ against Mole Fraction of Ethanol in the Liquid (x_2^l) for the System HSIL/Ethanol/Water at 30°C

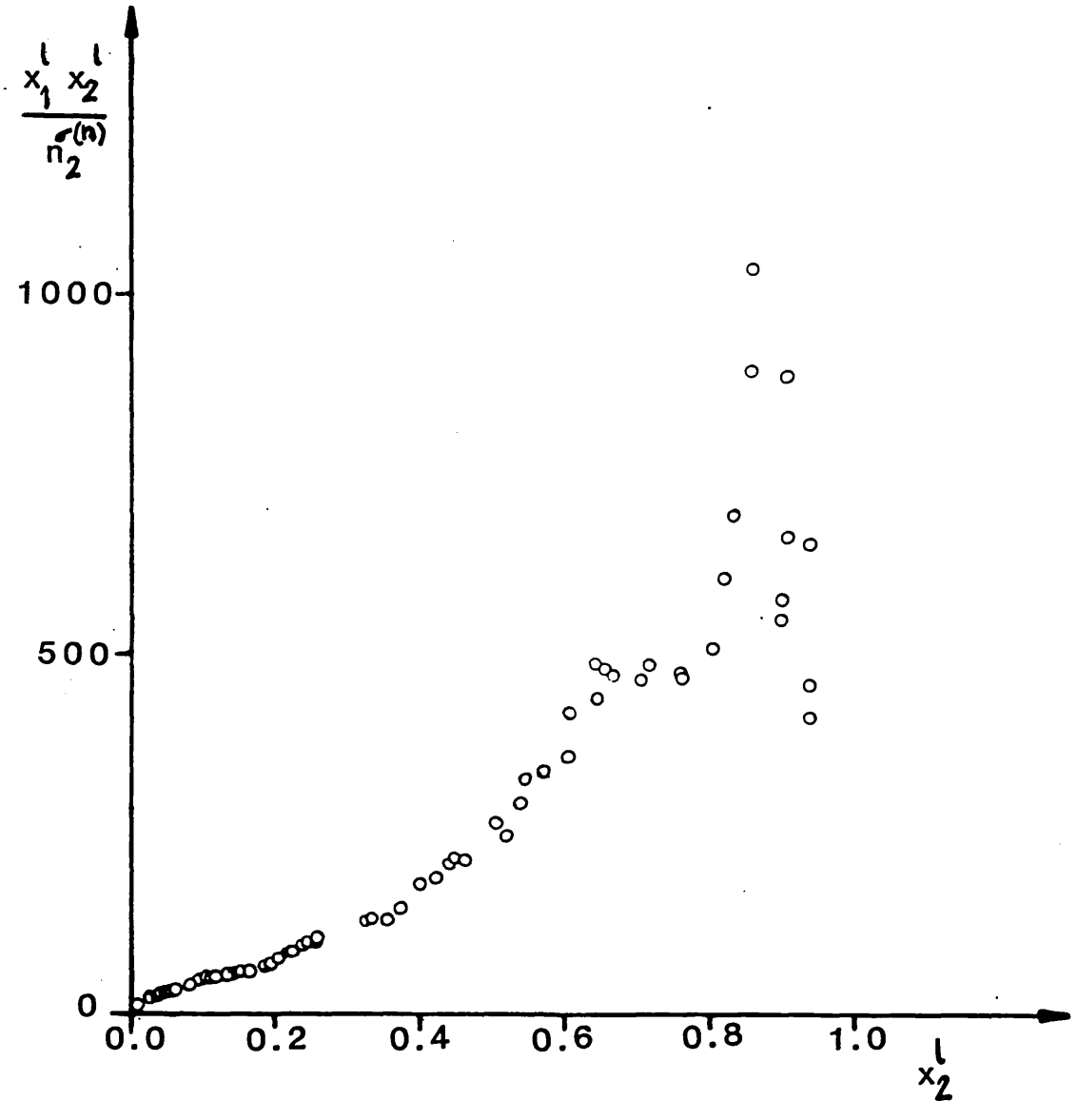

Figure 45. Graph of $\frac{x_2^l x_1^l}{n_2^{\sigma(n)}}$ against Mole Fraction of Ethanol in the Liquid (x_2^l) for the System HSIL/Ethanol Water at 40°C

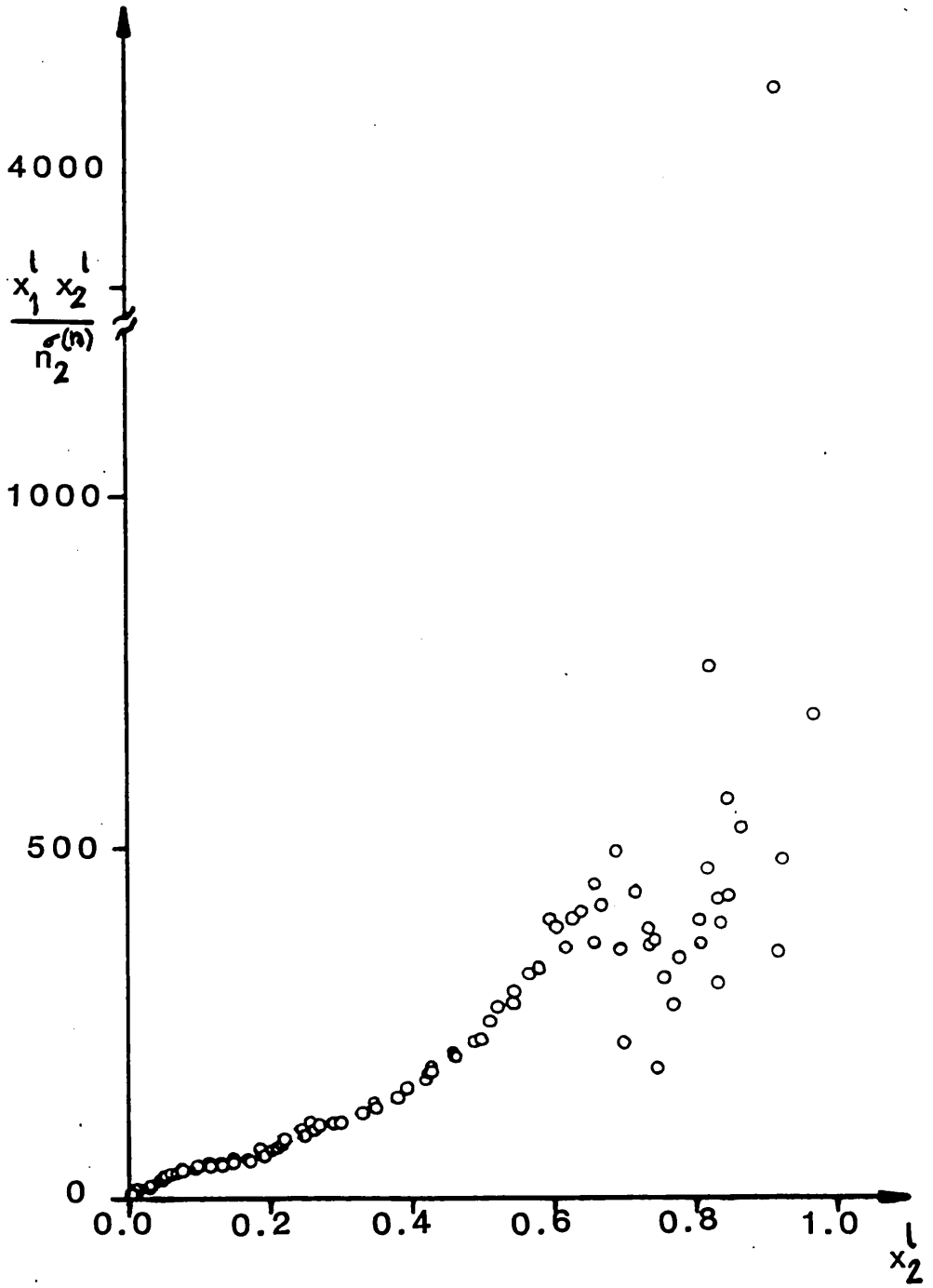

Figure 46. Graph of $\frac{x_1 x_2}{n_2^{\sigma(n)}}$ against Mole Fraction of Ethanol in the Liquid (x_2^l) for the System HSILB calcined at550°C/Ethanol/Water at 30°C

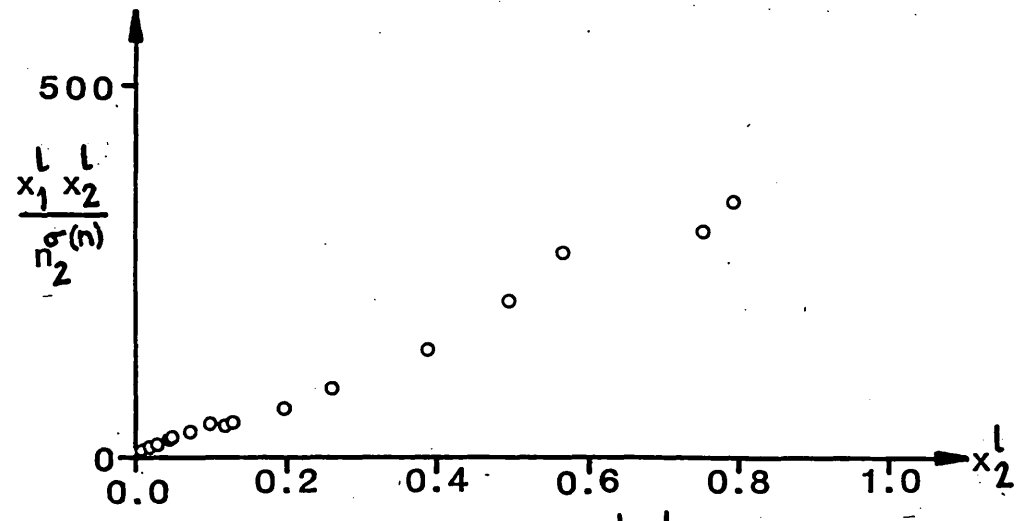

Figure 47. Graph of $\frac{x_1^l x_2^l}{n_2^{\sigma(n)}}$ against Mole Fraction of Ethanol in the Liquid for the System NaZSM5/1 /Ethanol/Water at 30°C

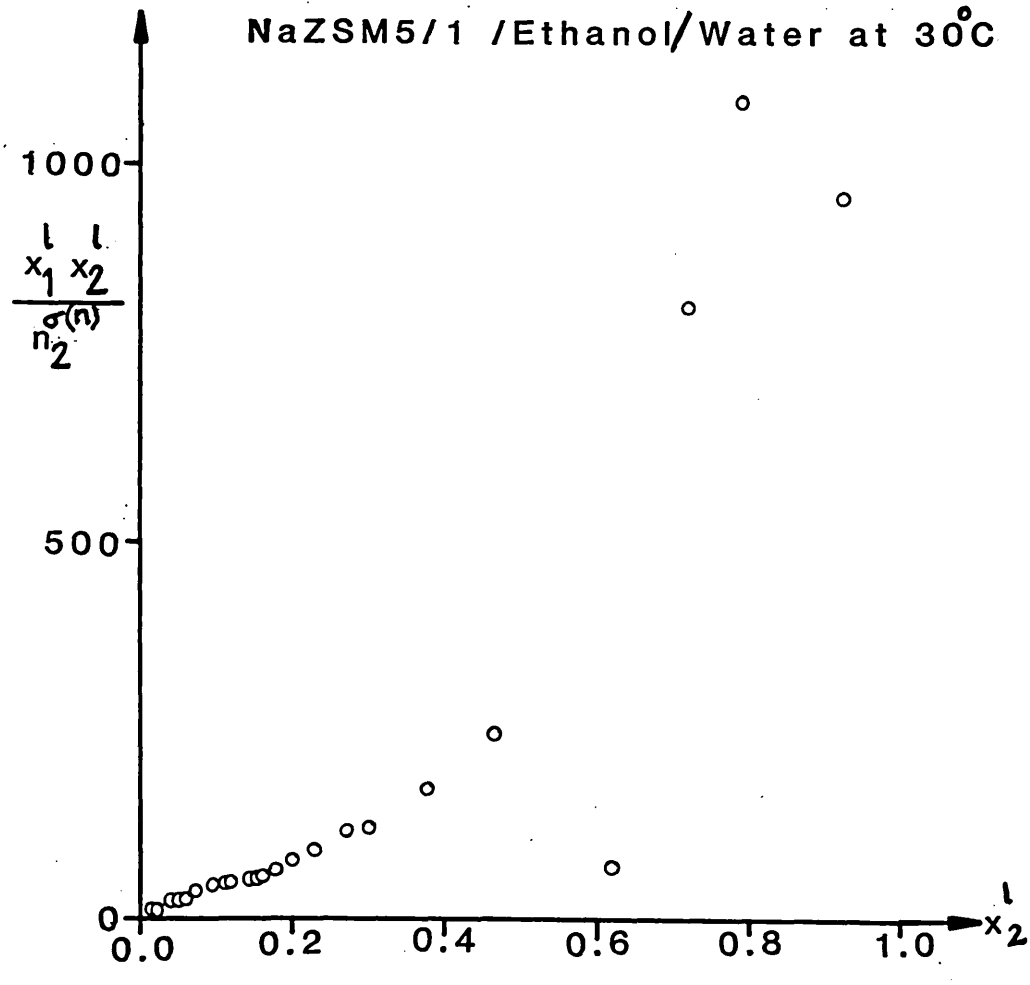

Figure 48. Graph of $\frac{x_2^l x_1^l}{n_2^{\sigma(n)}}$ against Mole Fraction of Ethanol in the Liquid (x_2^l) for the System

NaZSM5/2 /Ethanol/Water at 30°C

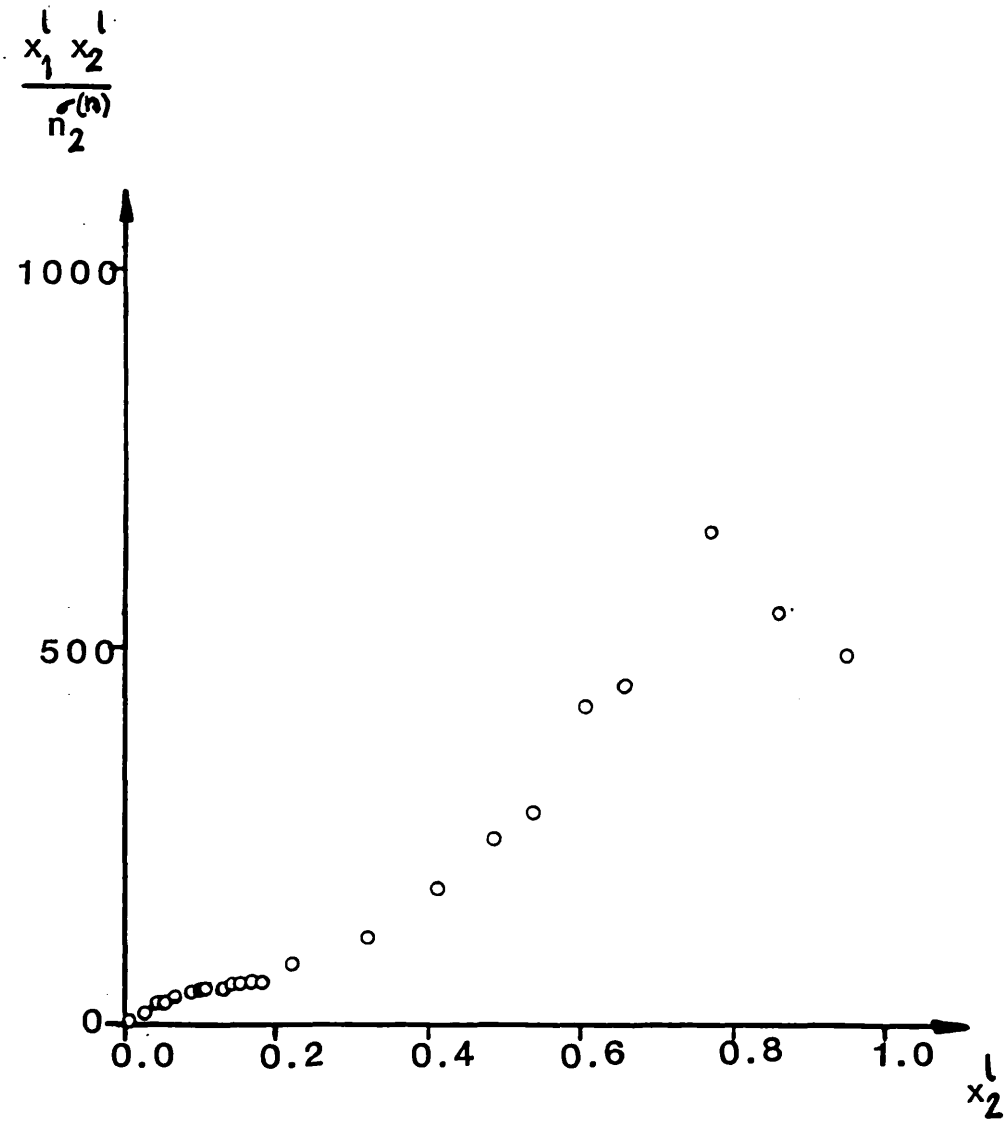

5.7. Thermodynamic Analysis of HSIL Composite Isotherms.

A thermodynamic analysis of the 20, 30 and 40°C HSIL composite isotherms according to the method of Schay[53], Everett[52] and Sircar[54] and as described in the Theory section, was carried out.

The calculated $\Delta_w\hat{h}-\Delta_w\hat{h}_2^*$ values are shown in Table 8, together with those values obtained directly from calorimetry data. Comparison of the two sets of results shows very little agreement. There are several possible reasons for this.

Firstly, there is the fact that only slight variation in the isotherms occurs with temperature, indeed the isotherms overlap in many regions. This makes the the variation of $(\Delta_w\hat{\varepsilon}-\Delta_w\hat{\varepsilon}_2^*)/(1/T)$ with 1/T difficult to determine accurately. It is then difficult to obtain accurate $\Delta_w\hat{h}-\Delta_w\hat{h}_2^*$ values.

Furthermore, accurate integrals of the $n_2^{\sigma(N)}/x_1^l x_2^l \gamma_2^l$ against $x_2^l \gamma_2^l$ are difficult to evaluate curve to give $\Delta_w\hat{\varepsilon}-\Delta_w\hat{\varepsilon}_2^*$ values in the first place. These curves, an example of which is shown in Figure 49, must be extrapolated to $x_2^l\gamma_2^l=0$ and $x_2^l\gamma_2^l=1$ in order to obtain the integral over the entire activity range. Such extrapolation may give rise to error in the calculated integrals, due in particular to the steepness of the curve in the low activity region.

Finally, much of the activity coefficient data used in these calculations had to be extrapolated from data at several other temperatures. This may be a further source of error.

In conclusion, the attempted analysis fails, partly because of the nature of the system studied and partly because of large errors introduced into the calculations.

Table 8 .Comparison of Results of Thermodynamic Analysis of Composite Isotherms with Calorimetry Results.

Mole fraction of Ethanol, x_2^l.	$\Delta_w \hat{h} - \Delta_w \hat{h}_2^*$ from analysis, $J.g^{-1}$.	$\Delta_w \hat{h} - \Delta_w \hat{h}_2^*$ from calorimetry, $J.g^{-1}$.
0·0000	−35·0	+42·00
0·0138		+35·17
0·02	+13·2	
0·0560		+22·70
0·06	+28·4	
0·3821		+2·31
0·40	−12·41	

Figure 49 . Graph of $\frac{n_2}{x_1^l x_2^l y_2^l}$ against $x_2^l y_2^l$ for the System HSIL/Ethanol/Water at 30°C

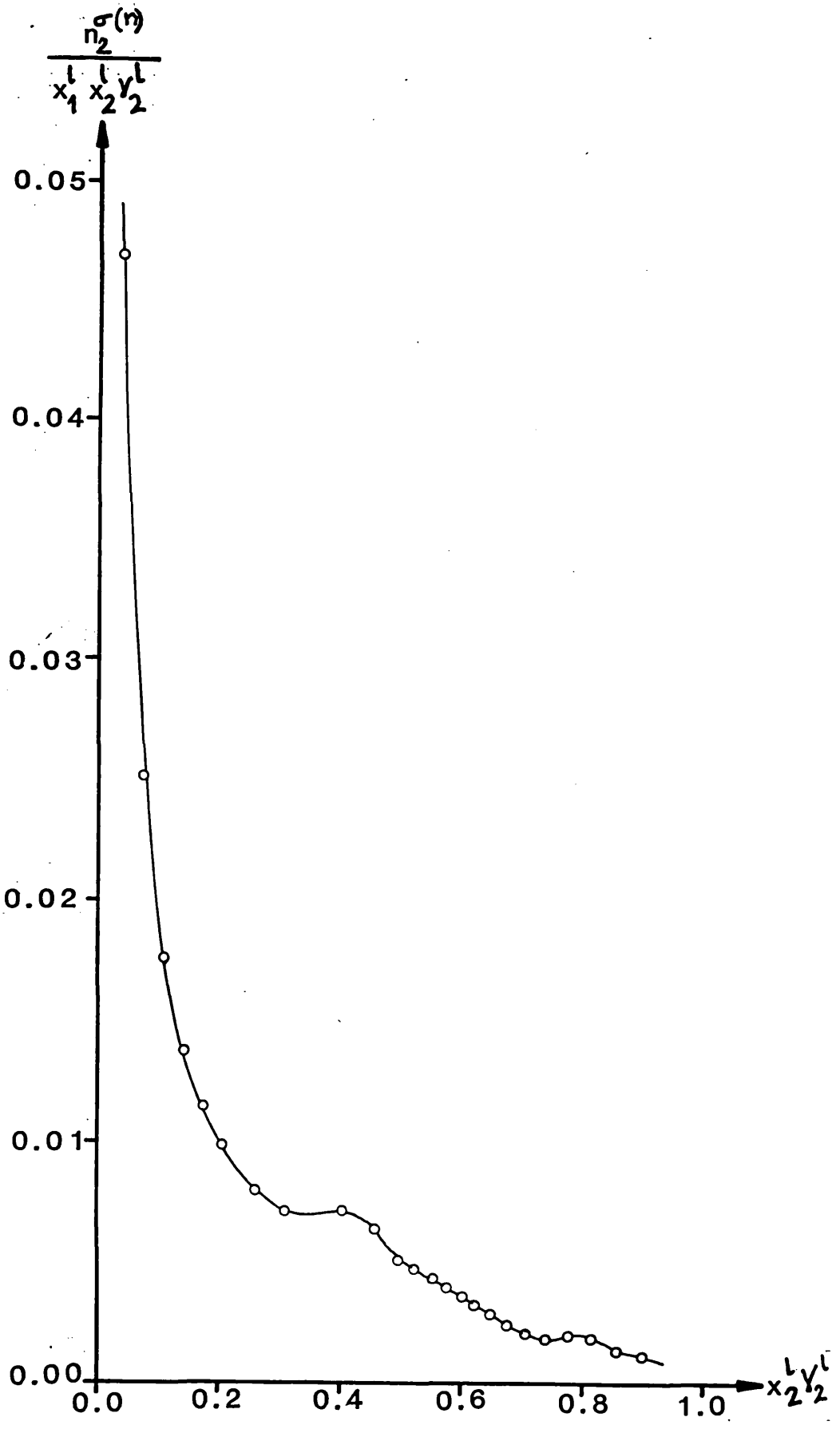

Conclusions.

Silicalite-1 and high-silica ZSM5 zeolites have been shown to be selective adsorbents for the adsorption of ethanol from aqueous solution. The selectivity of the adsorbents, as measured by their respective K values, is very high at the point corresponding to the maximum on the composite isotherm. The concentration of ethanol in the adsorbed phase is also thought to be high ($x_2^1 \approx 0.90$) at this point.

Silicalite-1, after adsorption of ethanol, may be reactivated for use as an adsorbent without significantly impairing its selectivity.

Adsorption at low ($x_2^1 < 0.08$) concentrations is strongly influenced by the structure of the ethanol-water liquid mixture. It is thought that this is the first study of this type on these systems which has observed this phenomenon. It is also proposed that the presence of ethanol molecules in the adsorbate which act as adsorption 'sites' for water molecules and the structure of the liquid phase plays an important part in determining the behaviour of these systems at intermediate ($0.16 < x_2^1 < 0.6$) concentrations of ethanol.

Current theoretical treatments of liquid phase adsorption are unsuitable for application to these systems due to the complex nature of the ethanol-water-adsorbent interactions and to the small variation in the isotherm with temperature.

Concluding Remarks.

This study has provided a valuable body of combined calorimetric and composite isotherm data (scarce in the present literature, as remarked upon by Everett[40]) upon which future developments in the theoretical treatment of liquid phase adsorption may be tested.

A treatment capable of analysing these systems would have to take into account the non-ideality of the bulk and possibly the adsorbed phase, as well as the small change in the isotherms with increasing temperature.

The adsorption of ethanol from aqueous solution on the relatively new molecular sieve type adsorbents such as the aluminium phosphate molecular sieves, may be examined in the future .

Finally, further work is possible on the development of a process where ethanol is selectively adsorbed from a fermentation broth and catalytically converted to gasoline by a ZSM5 type adsorbent.

A process may be envisaged where ethanol produced in a fermentation is removed by a ZSM5 zeolite immersed in the broth. The ethanol-saturated zeolite could then be removed and heated to a suitable temperature in an inert gas stream to produce gasoline. The catalyst would then be reactivated by heating to higher temperature and addition of a small amount of oxygen to the gas stream to remove any coke deposits on the zeolite.

Meanwhile, a batch of activated ZSM5 could be immersed in the fermentation broth to remove more ethanol. Hence the fermentation could be run on an almost continual basis.

Since adsorption of ethanol by ZSM5 appears to be fast, a reasonably high rate of production of gasoline might be acheived.

Appendix 1. Spline Fitting and Integrating Programs.

A smooth curve was drawn through data points obtained. Points were then read from this smooth curve for fitting using PROGRAM SPFIT. PROGRAM SPFIT calls the Numerical Algorithms Group library (NAG library) subroutine E02BAF which performs the fitting. The routine works by fitting sections of the curve to a cubic, such that at the junctions between sections th ecurve is continuous in the function and in its first derivative. The fitted curve is then compared with the original data points to assess goodness of fit. If the fit is unsatisfactory, various parameters may be altered to improve the fit. PROGRAM SPLINT takes the final fitted curve and integrates beneath it numerically between given intervals. PROGRAM SPLINT uses the NAG library routine E02BDF.

The programs are written in FORTRAN 77.

```
      PROGRAM SPLINT
      DIMENSION X(100),Y(100),AK(60),C(60),WORK1(100)
      DIMENSION WORK2(4,60),XB(100),SB(100)
      CHARACTER PFCOM*80,PFERR*40
      K=0
      M=0
      IERR=0
      PFCOM='GET,DATIN.'
      CALL PFREQ(PFCOM,PFERR,IERR)
      REWIND 1
      OPEN(1,FILE='DATIN')
      WRITE(*,10)IERR
 10   FORMAT(I3)
      READ(1,10)M
      DO 20 I=1,M
 20   READ(1,30)X(I),Y(I),W(I)
 30   FORMAT(3F6.4)
      READ(1,10)N
      DO 40 I=5,N+4
 40   READ(1,50)AK(I)
 50   FORMAT(F6.4)
      NCAP7=N+8
      IFAIL=0
      CALL E02BAF(M,NCAP7,X,Y,W,AK,WORK1,WORK2,C,SS,IFAIL)
      WRITE(*,10)IFAIL
      WRITE(*,60)
 60   FORMAT('KNOT POSITIONS ARE')                    /CONTD.
```

```
      DO 70 I=5,N+4
 70   WRITE(*,50)AK(I)
      WRITE(*,80)
 80   FORMAT('SPLINE COEFFICIENTS ARE:')
      DO 90 I=1,N+4
 90   WRITE(*,100)C(I)
100   FORMAT(E10.4)
      WRITE(*,110)SS
110   FORMAT('SUM OF SQUARES OF RESIDUALS =',E10.4)
      IFAIL=0
      OPEN(2,FILE='DATOUT')
      K=90
      WRITE(2,120)K,M
120   FORMAT(2I3)
      DO 130 I=1,90
      X2=I*0.01
      S=0
      IFAIL=0
      CALL E02BBF(NCAP7,AK,C,X2,S,IFAIL)
      WRITE(*,10)IFAIL
      XB(I)=X2
      SB(I)=S
130   WRITE(2,140)X2,S
140   FORMAT(2F6.4)
      WRITE(*,150)
150   FORMAT('EVALUATED SPLINE POINTS ARE:')
      DO 160 I=1,90
160   WRITE(*,170)I,XB(I),SB(I)
170   FORMAT(I3,' ',F6.4,' ',F6.4)
      DO 180 I=1,M
180   WRITE(2,140)X(I),Y(I)
      PFCOM='SAVE,DATOUT.'
      IERR=0
      REWIND 2
      CALL PFREQ(PFCOM,PFERR,IERR)
      WRITE(*,10)IERR
      END


      PROGRAM SPLINT
      DIMENSION X(50),Y(50),W(50),AK(40),C(40),WORK1(50)
      DIMENSION WORK2(4,40)
      CHARACTER PFCOM*80,PFERR*40
      M=0
      IERR=0
      PFCOM='GET,FLIN.'
      CALL PFREQ(PFCOM,PFERR,IERR)
      REWIND 1
      OPEN(1,FILE='FLIN')
      WRITE(*,10)IERR
  10  FORMAT(I3)
      READ(1,10)M
      DO 20 I=1,M
  20  READ(1,30)X(I),Y(I),W(I)
  30  FORMAT(3F7.5)                                    /CONTD.
```

```
      READ(1,10)N
      DO 40 I=5,N+4
   40 READ(1,50)AK(I)
   50 FORMAT(F7.5)
      NCAP7=N+8
      IFAIL=0
      CALL E02BAF(M,NCAP7,X,Y,W,AK,WORK1,WORK2,C,SS,IFAIL)
      WRITE(*,10)IFAIL
      WRITE(*,60)
   60 FORMAT('KNOT POSITIONS ARE:')
      DO 70 I=5,N+4
   70 WRITE(*,50)AK(I)
      WRITE(*,80)
   80 FORMAT('SPLINE COEFFICIENTS ARE:')
      DO 90 I=1,N+4
   90 WRITE(*,100)C(I)
  100 FORMAT(E10.4)
      WRITE(*,110)SS
  110 FORMAT('SUM OF SQUARES OF RESIDUALS= ',E10.4)
      IFAIL=0
      CALL E02BDF(NCAP7,AK,C,DEFINT,IFAIL)
      WRITE(*,10)IFAIL
      WRITE(*,120)DEFINT
  120 FORMAT('INTEGRAL= ',E10.4)
      END
```

Appendix 2.Linear Regression Program.

PROGRAM LINREG performs linear regression on a given set of data points. The program is written in FORTRAN 77.

```
      PROGRAM LINREG
      DIMENSION X(50),Y(50)
      CHARACTER PFCOM*80,PFERR*40
      IERR=0
      PFCOM='GET,LININ.'
      CALL PFREQ(PFCOM,PFERR,IERR)
      REWIND 1
      OPEN(1,FILE='LININ')
      WRITE(*,10)IERR
 10   FORMAT(I3)
      READ(1,10)IN
      SX=0
      SY=0
      SXX=0
      SYY=0
      SXY=0
      DO 30 I=1,IN
      READ(1,*)X(I),Y(I)
      XX=X(I)**2
      YY=Y(I)**2
      XY=X(I)*Y(I)
      SX=SX+X(I)
      SY=SY+Y(I)
      SXY=SXY+XY
      SXX=SXX+XX
      SYY=SYY+YY
      XX=0
      YY=0
 30   XY=0
      D=(IN*SXX)-(SX**2)
      AM=((IN*SXY)-(SX*SY))/D
      C=(SY-(AM*SX))/IN
      SP=SYY+(IN*(C**2))+((AM**2)*SXX)
      SQ=SP-2*((C*SY)+(AM*SXY)-(C*AM*SX))
      SOK=SQ/(IN-2)
      SAA=SOK*(1+(SX**2))/D
      SA=SQRT(SAA)
      SBB=SOK*IN/D
      SB=SQRT(SBB)
      RC=((AM**2)*D)/((IN*SYY)-(SY**2))
      WRITE(*,40)AM
 40   FORMAT('GRADIENT OF LINE IS: 'E10.4)
      WRITE(*,50)C
 50   FORMAT('Y INTERCEPT IS: 'E10.4)
      WRITE(*,60)RC
 60   FORMAT('CORRELATION COEFFICIENT IS: ',E10.4)
      WRITE(*,70)SA
 70   FORMAT('STD. DEVIATION IN INTERCEPT IS: ',E10.4)
      WRITE(*,80)SB                                        /CONTD.
```

```
80   FORMAT('STD DEVIATION IN GRADIENT IS: ',E10.4)
     END
```

References.

(1)Barrer,R.M.; "Zeolites and Clay Minerals as Molecular Sieves", Academic Press 1978.

(2)Dwyer,J.; and Dyer,A.; Chemistry and Industry (7), 237,(1984)

(3)Breck,D.W.; "Zeolite Molecular Sieves", Wiley, 1974.

(4)Lowenstein,W.; Amer. Mineralogist 39, 92,(1954)

(5)Barrer,R.M.;"Hydrothermal Chemistry of Zeolites", Academic Press, 1982.

(6)Meier,W.; et al.; J. Phys. Chem. 85, 2238, (1981).

(7)Flanigen,E.; et al.; Nature (London) 271, 512, (1978).

(8)Kuei-Jung Chao et al.; Zeolites 6, 36, (1986).

(9)Argauer,R.J.; et al.; US Pat. 3,702,886 (1972); also 3,709,979 ; 3,832,449 ; 4,016,245 ; 4,046,859 .

(10)Dwyer,F.G. et al. US Pat.3,941,871 (1976).

(11)Meisel,S.L. et al. Chem. Tech. 6, 86, (1976).

(12)Chang,C.D.; Amer. J. Catal. 47, 249, (1977).

(13)Meisel,S.L. et al. ACS Meeting, Chicago Ill. (1977).

(14)Chen, N.Y. et al. Oil Gas J. 75, 165, (1977)

(15)Lohse,U. et al. Chem. Tech. (Leipzig) 33(7), 370, (1981).

(16)Dyer,A. Sep. Sci. Technol. 13(6), 501, (1978).

(17)Messow,U. et al. Z. Chem. 23(1), 37, (1983).

(18)Kerr,G.T. J. Phys. Chem. 72, 2594, (1968).

(19)Scherzer,J. J. Catal. 54, 285, (1978).

(20)Beyer,H.K. et al. in "Catalysis by Zeolites" ed. B.Imelik et al.

(21)Skeels,G.W. et al. in "Proceedings of the Sixth International Zeolite Conference", p87, Butterworths, 1984.

(22)Khvoschev,S.S.; Izst. Aked. Nauk Gruz SSR, Ser. Khim. 8(1),

26, (1982).

(23)Patzelova,V.; Chem. Zvesti 29(3), 331, (1975).

(24)Chester, A.W. et al. J. Chem. Soc. Chem. Commun. 289, (1985).

(25)Fegan, S.G. and Lowe, B.M. ibid 437, (1984).

(26)Boxhoorn, G. et al. Zeolites 4, 15, (1984).

(27)Elketov, Y.A. et al. "Molecular Sieves", p267, Society of Chemical Industry, London, 1968.

(28)McBain, J.W. "The Sorption of Gases and Vapours by Solids", Rutledge, London, 1932.

(29)Barrer, R.M. J. Chem. Soc. Ind. 64, 130, (1945).

(30)Barrer, R.M. Chem. Abs. 49, 3617, (1955).

(31)Barrer, R.M. Nature 176, 1188,(1955).

(32)Eisenberg, D. et al. "The Structure and Properties of Water", Oxford, 1969.

(33)Franks, F. and Ives, D.J.G. Quarterly Reviews Chem. Soc. 1,(1966).

(34)Coccia, A. et al. Chem. Phys. 7, 30, (1975).

(35)Beddard, G.S. et al. Nature 294, 145, (1981).

(36)Richards, R.E. PhD Thesis, Imperial College, 1985.

(37)"Economic Possibilities for Fuel Alcohol", Chemistry and Industry 12, (1984).

(38)Kipling, J.J. "Adsorption from Solutions of Non-Electrolytes" Academic Press, 1965.

(39)Zettlemoyer, A.C. et al. Croat. Chem. Acta 42, 247, (1970).

(40)Everett, D.H. in "Adsorption from Solution" ed. Ottewill, R.H. et al. , Academic Press, 1983.

(41)Ostwald, W. et al. Kolloid Z. 30, 279, (1922).

(42)Everett, D.H. Trans. Faraday Soc. 60, 1803, (1964).

(43)Williams, A.H.; Medd K. Vetnenskapsakad. 2:No. 27, (1913).

(44)Elton, G.A.H. ; J. Chem. Soc. 2958,(1951).

(45)Kipling, J.J. et al. ibid 4123, (1952).

(46)Hansen, R.S. et al. J. Colloid Sci. 9, 1, (1954).

(47)Jones, D.C. et al. J. Chem. Soc. 213, (1957).

(48)Schay, G. et al. J. Chem. Phys. 58, 149, (1961).

(49)Szekrenyesy, T. Periodica Polytech. 4, 95, (1960).

(50)Kipling, J.J. et al. Trans. Faraday Soc. 58, 1, (1968).

(51)Everett, D.H.; Trans. Faraday Soc. 60, 1803, (1964).

(52)Everett, D.H.; ibid 61, 2478, (1965).

(53)Schay, G.; J. Colloid Interface Sci. 42, 478, (1973).

(54)Sircar, S. et al. I. and E.C. Fundamentals 11, 249, (1972).

(55)Ash, S.G. et al. J.C.S. Faraday I 71, 123, (1975).

(56)Davis, J. PhD Thesis, Bristol, 1983.

(57)Milestone, N.B. et al. J. Chem. Technol. Biotechnol. 31(12), 732, (1981).

(58)Farhadpour, F.A. et al. E.B.C. Symposium on Biotechnology, Nutfield, G.B. , p203, 1983.

(59)Milestone, N.B. et al. J. Chem. Technol. Biotechnol. 34A(2), 73, (1984).

(60)Costa, E. et al. Ind. Eng. Chem. Process Des. Dev. 24, 239, (1985).

(61)Klein, S.M. ; Report (1982) IS-T-1020, Order No. DE 83004981 Avail. NTIS from Energy Res. Abstr. 8(6), (1983), Abstr. 12061.

(62)Klein, S.M. et al. A.I.Ch.E. Symp. Ser. 70(230), 53, (1983).

(63)Chriswell, C.D.; "Ethanol Purification by Adsorption", Executive Summary, Ames Lab. Report, D.O.E. , Iowa State Univ.

Ames, Iowa, 1981.

(64)Herden,H. et al. Zeolites (4), 255, (1984).

(65)Ake, T.P.; MSc Thesis 1984. Report, 1984, IS-T-1171 Order No. DE 85004874 , Avail. NTIS from Energy Res. Abstr. (10)7, (1985), Abstr. 11021.

(66)Bui, S. et al. Ind. Eng. Chem. Process Des. Dev. 24, 1209, (1985).

(67)Dessau, R.M. et al. US Pat. 4,442,210 (1984).

(68)Nai, Y.C. et al. Braz. Perdido PI BR 8 200,547 (1982).

(69)Garg, D.R. et al. Can. CA 1,195,258 (1985).

(70)Groszek, A.J.; Eur. Pat. Appl. EP 101254 A2 (1984), GB Appl. 82/22621 (1982).

(71)Kulprathipanja, S. et al. US Appl. 202,048 (1983).

(72)Akhmadeev, V. Ya. et al. Khim. Technol. Vody. 3(6), 535, (1981).

(73)Pitt, W.W.Jr. et al. Proc. Intersoc. Energy Convers. Eng. Conf. 1980, 15^{th}(3), 2363.

(74)Feldman,J. ; US Appl. 325,450 (1982).

(75)Dearborn, R.J.; Report 1982, D.O.E. IRS/10297-T2 , Order No. DE 83005040. Avail. NTIS from Energy Res. Abstr. 8(8), (1983), Abstr. 18193.

(76)Pirzada et al. Analyst (London) 108(1290), 1096, (1983).

(77)Richards, R.E. and Rees, L.V.C. Zeolites 6, 17, (1986).